RR 241

Ontario
Ministry of
Transportation and
Communications

Research and
Development
Branch

Thermal Characteristics of Rock Aggregate Materials

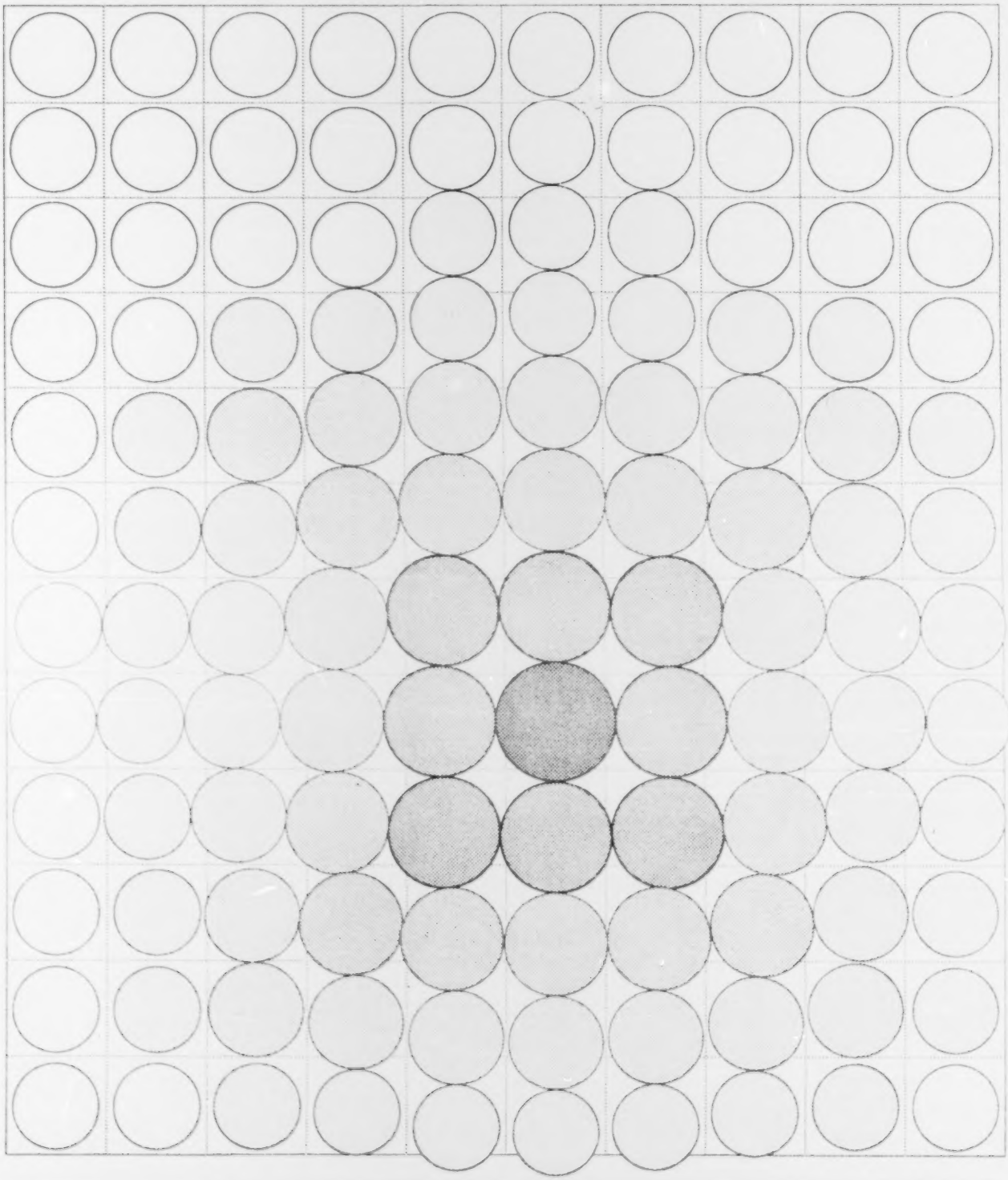

ISSN 0228-7048

ISBN 0-7729-2852-5

88-05246/

Technical Report Documentation Page

Thermal Characteristics of Rock Aggregate Materials

Author:	S.A. Senior, Principal Researcher J.A. Franklin, Project Director
MTC No.:	RR 241
Date:	October, 1987
Other Nos.:	ISSN: 0228-7048 ISBN: 0-7729-2852-5
Published by:	The Research and Development Branch Ontario Ministry of Transportation and Communications
Participating Agencies/-Client:	Division of Geological Engineering Department of Earth Sciences University of Waterloo
Abstract:	Thermal cyclic testing was completed on 53 specimens, including 11 different rock types, cement mortar, and a variety of calibration materials. The objective was to measure the thermal expansion characteristics of common aggregates and to identify possible mechanisms of concrete deterioration caused by thermal incompatibility of the mortar and aggregate. Rock cubes were instrumented with electrical resistance strain gauges to measure thermally induced expansions and contractions. The specimens were automatically monitored during 56 daily cycles of temperature in the range -20°C to +70°C. The results were checked against known standards and found to be reliable. Low, and in some cases negative, coefficients of thermal expansion were measured for certain of the rock types tested. Furthermore, many of the rocks showed a non-linear relationship, such that expansion coefficients were much lower at sub-freezing temperatures. Some rock types also expanded anisotropically. Irreversible "growth" of some rocks, and shrinkage of mortar were recorded. The thermal expansion mechanisms were shown to be little affected by moisture content at low levels of saturation and are therefore divorced from the deleterious effects of ice formation. Three thermal mechanisms have been hypothesized — aggregate-mortar thermal incompatibility; anisotropic aggregate expansion; and aggregate "growth". In some cases, these may act in combination to cause cracking in the mortar matrix, thus accelerating mechanical breakdown and the more severe effects of freeze-thaw deterioration. These hypotheses should be checked by testing the suspect aggregates in concrete.
Key words:	aggregates, thermal expansion, strain gauges, thermal cycles, anisotropic thermal expansion, residual thermal strain, aggregate mortar incompatibility
Comments:	This research was funded under Ontario Joint Transportation and Communications Research Programme, Project No. 22327.
Distribution:	Regional geotechnical staff and recipients of the geotechnical mailing list.
Copyright Status:	Crown copyright

RR 241

Thermal Characterictics of Rock Aggregate Materials

S.A. Senior
Principal Researcher

J.A. Franklin
Project Director

Division of Geological Engineering
Department of Earth Sciences
University of Waterloo

Prepared for:

J.E. Gruspier
Research Engineer
Materials Research Office, MTC

C.A. Rogers
Petrographer
Engineering Materials Office, MTC

Published by
The Research and Development Branch
Ontario Ministry of Transportation and Communications
Hon. Ed Fulton, Minister
D.G. Hobbs, Deputy Minister

Published without prejudice as to the application of the findings. Crown copyright reserved; however, this document may be reproduced for non-commercial purposes with attribution to the Ministry.

For additional copies, write:
The Editor, Technical Publications
Room 320, Central Building
1201 Wilson Avenue
Downsview, Ontario
Canada M3M 1J8

Telephone: (416) 235-4704
CNCP Dialcom Electronic Mail: 23:MIN006

October, 1987

Contents

1/ Introduction 1
1.1/ Research Objectives & Terms of Reference 1
1.2/ Review of Earlier Investigations 1

2/ Test Methods 3
2.1/ Selection of Test Techniques 3
2.2/ Heating and Cooling Equipment 3
2.3/ Data Acquisition System 4

3/ Sample Selection and Specimen Preparation 5
3.1/ Rock Samples 5
3.2/ Control Specimens 5
3.3/ Strain Gauging 5
3.4/ Moisture Conditioning and Sealing 6

4/ Trials and Calibrations 7
4.1/ Proving Trials Using Aluminum and Rock 7
4.2/ Calibration of Aluminum Strains versus Temperature 7
4.3/ Correction for Apparent Thermal Strain 7
4.4/ Proving Trials on Various Materials 8

5/ Full-Scale Testing Program 8
5.1/ Initial Slow Cycle 8
5.2/ Automatic Cycling 8

6/ Calculation Procedures 9

7/ Discussion of Results 10
7.1/ Comments on the Testing Procedure 10
7.2/ Temperature-Strain Graphs 10
7.3/ Behaviour of Standard Specimens 11
7.4/ Linear and Curvilinear Rock Behaviour 11
7.5/ Anisotropic Rock Behaviour 11
7.6/ Hysteresis, Growth and Shrinkage 12
7.7/ Moisture Effects 12
7.8/ Concrete Deterioration Hypotheses 13

8/ Conclusions 14

References 15

Figures 17

Appendices

A/ Sample Designations, Locations and Thin Section Descriptions 53

B/ Thermal Coefficients of Expansion 61

List of Figures

1/ Wiring Connections of System Apparatus 17

2/ Specimen Box and Specimens 18

3/ Data Logger 19

4/ Freezer and Strain Gauge Leads 19

5/ Strain Gauged Specimens 20

6/ Humidity Control Box 21

7/ Epoxy Coating of "Dry" Specimens 21

8/ Calibration Specimens 22

9 to 23/ Graphs -- Strain vs Temperature 23

24 to 29/ Graphs -- Residual Strain vs Cycle 48

Appendices

A1 to A3/ Photomicrographs of Rock Specimens 56

A4/ Rock Mineralogy and Grain Size 59

A5/ Rock Index Test Data 60

B1/ Published Coefficients (Standard Specimens) 68

1/ Introduction

1.1/ Research Objectives and Terms of Reference

The research described in this report was completed by the Geological Engineering Division, Department of Earth Sciences, University of Waterloo, under contract to the Ontario Ministry of Transportation and Communications (MTC).

The Ministry's requirements and our recommended techniques and program were addressed in a proposal entitled "Coefficient of Thermal Expansion of Rocks in Various Temperature Ranges" submitted on January 19, 1984. Terms of reference were finalized in a Memorandum of Agreement dated May 1, 1984.

The general objective of the research was to investigate the thermal behaviour of certain aggregate-making rock types. Of particular interest was a dolostone aggregate from Manitoulin Island which, when used in a concrete, has shown excessive expansion in the freeze-thaw test ASTM C666. This aggregate was suspected to have an anomalous (low) thermal expansion coefficient and thus to be incompatible with cement paste. The consequent differential thermal expansion had been tentatively identified as a cause of concrete cracking.

The terms of reference as specified in Schedule A of the Memorandum were to measure and report dimensional changes that occur in cubes of rock when the temperature is cycled in the range -20°C to +60°C. The dimensional changes were to be measured as a function of the following variables:

- rock type
- temperature within the range
- rock anisotropy
- repeated cycles
- variations in water content

1.2/ Review of Earlier Investigations

The earliest known publication on the effects of temperature changes on rock is a study by Bartlett (1832) who measured the thermal expansion coefficients of granite, marble, and limestone in the range -14°C to +39°C. Adie (1836) measured the expansion coefficients of two granites, marble, sandstone, and greenstone in the range +10°C to +98°C and reported permanent expansion of the greenstone after successive heating cycles. Hallock (1891) found that the thermal properties of various rocks altered most significantly when subjected to sub-freezing temperatures. A report by Souder and Hidnert (1919) on the thermal expansion of nine marble samples cycled within the range +24°C to 100°C identified increasing permanent expansion with each cycle. Griffith (1936) studied 106 samples of various lithologies over a single temperature cycle in the range 0°C to 260°C. In a study by Hockman and Kesslar (1950), differential expansion rates were observed for 48 moist and dry granite samples. A single cycle in the range -20°C to +60°C was performed using interferometry measurements of expansion. No permanent expansion was recorded.

Studies at higher temperatures include one by Baldwin-Wiseman and Griffith (1909) who measured expansion in the range +20°C to +300°C. They found that permanent expansion could be caused by a single heating event for several samples of sandstone, limestone, marble, and granite. Wheeler (1910) exposed diabase, marble, and granite to six repeated thermal cycles between +19°C and +1000°C. Each of the rock types was found to expand permanently after the first cycle, with successively decreasing amounts of expansion in subsequent cycles. No further changes were noted after the fifth cycle.

It is apparent that physico-chemical changes such as those resulting from freeze-thaw or alkali-aggregate reaction may not be the only cause of concrete deterioration. The thermal expansion of hardened Portland cement has been investigated by Davis (1930) and Meyers (1940) who determined that factors such as water saturation, composition, and age can influence the behaviour of the material. Koenitzer (1936), in a pioneer study of cement mortar and aggregate thermal interaction, established that the thermal expansion of concretes was influenced by the properties of the component materials used. His initial results showed that expansion characteristics of a concrete mix could not be determined from the sum of the properties of individual component materials. Later work by Walker, Bloem, and Mullen (1952) showed that thermal coefficients of concrete vary proportionately to the quantity and character of aggregate in the mixture.

The response of concretes exposed to environmental temperature cycling has been noted in several previous cases. Pearson (1941, 1943) attributed the rapid failure of a concrete to a dolomite marble aggregate with a low thermal expansion coefficient. Callan

(1952) reported decreased concrete durability resulting from large differences in thermal coefficients between coarse aggregate and mortar. Further studies by Mather *et al.* (1953) statistically identified the thermal expansion coefficient, among various other physical properties of limestone aggregates, as being significant in the durability of concrete to freeze-thaw cycles. Recrystallized limestone aggregate (marble) was reported to have been used in concrete pavement exhibiting permanent "growth" in Maryland, USA (Shah, 1974).

Thermal stresses produced by differential heating of concrete can lead to failure. Thomlinson (1940) developed a theory for calculating such thermal stress conditions in concrete slabs.

Differential thermal expansion of aggregates and mortar may be a contributing factor in some cases. A theoretical analysis of the type of such stresses is outlined by Smith (1956). Typical cement mortar has an expansion coefficient of 8 to 13 microstrain per °C (Cook, 1966) whereas the average value for carbonate aggregates lies between 2 and 11 microstrain per °C (Harvey, 1967). Thermal cycling of a concrete containing such materials might be expected to generate high local stresses at the mortar/aggregate interface. If restrained deformations are allowed to take place, these stresses might be relieved by the generation of microfractures through the weaker cement paste. The resulting dilation and increase in permeability of the concrete would hasten mechanical and chemical weathering and lead to a shorter useful life span.

Typically, coefficients of thermal expansion are reported as constant values, at least within a restricted range of temperatures, implying an approximately linear expansion as a function of temperature. Although such behaviour is typical for most metals, it is not for rocks. Willis and DeReus (1939) identified non-linear behaviour over the temperature range +3°C to +60°C for certain limestones, with decreased rates of expansion at lower temperature. Harvey (1967, 1968) reported non-linear expansion coefficients and grain size effects. He demonstrated that coarse-grained limestones are more apt to show non-linear behaviour than fine-grained ones in the temperature range -20°C to +80°C.

Moisture content has also been shown to affect thermal expansion. Expansion curves published by Hockman and Kessler (1950) indicate a decrease in thermal expansion coefficient with the expulsion of moisture from several granite samples tested. More recent work by Hudec (1980) and Hudec and Sitar (1975) has indicated that the thermal expansion coefficient of carbonate rocks is greater for dry rocks than for those in a moisture-saturated condition. Moisture adsorption at constant temperature is considered responsible for the reduction of thermal strain.

2/ Test Methods

2.1/ Selection of Test Technique

Freeze-thaw tests such as ASTM C666, and C671, used for routine measurement of the durability of concrete, were rejected as unsuitable for purposes of this research. They measure the combined effects of freeze-thaw behaviour and thermal expansion and contraction within the mass concrete, but they do not isolate these individual effects, nor do they discriminate between behaviour of the aggregate and that of the mortar matrix. In addition, the freeze-thaw tests do not sufficiently investigate behaviour at sub-freezing temperatures.

The standard tests for thermal expansion measurement were also rejected. They require complex and expensive measuring apparatus such as dilatometers, interferometers, or X-ray diffraction methods. Coefficients of thermal expansion using dilatometers (Valentich, 1981), which determine changes in material size from mechanical measurements, are only capable of measuring one direction of expansion on a single specimen (Loubser and Bryden, 1972). Specimens prepared for dilatometer instruments are typically much larger than coarse aggregate particles and take much longer to reach thermal equilibrium.

Interferometers are high precision instruments usually required for the measurement of standard reference materials (Hahn, 1970). They require that specimens be prepared into complex shapes with exact dimensions. The measurements are made over a length much smaller than the typical size of a coarse aggregate particle. The results, therefore, may not be indicative of average thermal behaviour, especially in coarse-grained rocks (Johnson and Parsons, 1944). As when using dilatometers, only single specimens may be studied at one time.

Another limitation of standard equipment is that temperature ranges are usually confined to those easily reached — typically room temperature to 100°C. Modifications are required if this temperature range is to be extended. Measurements are usually infrequent, such as at the start and end of a cycle, and may involve periodic removal from the temperature environment. In contrast, this study required a test that would allow the simultaneous evaluation of many rock types over many cycles, with continuous monitoring and graphical recording of temperature and strain.

A method was selected that made use of electrical resistance strain gauges (ERSGs) bonded to the faces of rock cubes. It was modelled on earlier work by Callan (1950, 1952) who used ERSGs for the determination of mean expansion coefficients of several coarse aggregate source rocks. ERSGs have several advantages:

- They are inexpensive and small enough to be mounted on a cube specimen the size of a large aggregate particle.
- They permit the measurement of anisotropic expansion when bonded in different directions to different cube faces of the same specimen.
- Strains can be monitored easily using a data logger that scans many channels in quick succession.

2.2/ Heating and Cooling Equipment

Figure 1 shows a schematic outline of the test apparatus and the wiring connections of the system.

An insulated plywood box was constructed to hold the specimens. Its exterior was cooled throughout the test program by keeping the box in a walk-in freezer at an ambient temperature of -26°C. The interior was heated, during the heating half-cycle only, by two Minco Products Inc. HR8723 30 x 45 cm thermofoil heating elements. Output from the heaters, power rated at 0.23 W/cm^2 (320 W maximum), was controlled by a Variac voltage regulator. A wire mesh tray above the heaters was used to hold the specimens and to anchor the ERSG lead wires (Figure 2).

Moisture conditions within the box (Section 3.4) resulted in some problems that were corrected only with difficulty. Erratic readings were diagnosed as caused by electromagnetic (inductive) pickup of alternating currents by the ERSGs. A high level of electrical noise resulted from the proximity of the heaters and fan, particularly when the air within the box was saturated. Filters in the data logger proved insufficient to remove this noise. The problems were solved by grounding the wire mesh screen on which the specimens rested, and the interior foil lining.

Voltage regulation to the heating pads and also the thickness of fibreglass insulation, contained between the plywood exterior and the masonite interior of the box, were adjusted by trial and error to give approximately equal durations of heating and cooling. The base was lined with an extra layer of polystyrene foam and the interior with aluminum foil for better heat transfer and dissipation. The heaters lay directly on asbestos board. They were covered by aluminum foil-

wrapped masonite to further dissipate the heat.

A small fan attached to the lid of the box provided continuous air circulation for more uniform heat distribution. The fan motor, a source of heat, was installed on the outside to allow the box interior to reach the required sub-freezing temperatures.

Temperature cycling was controlled by a Beede MR4-207 dual set point relay activated by a type-T thermocouple (constantan:copper-constantan) inserted in a dummy rock specimen within the insulated box. The relay unit switched the heaters ON at the lowest required temperature of cycling, and OFF again at the maximum required temperature.

Rates of heating and cooling were limited to a maximum of 1.5°C per minute at the beginning of each cycle, to minimize thermal gradients within specimens, and to avoid resulting thermal stresses between the individual component minerals. Richter and Simmons (1974) determined that a heating rate kept below 2°C/min is sufficient to eliminate the effects of minerals with significantly differing expansion coefficients. Temperature change was non-linear throughout each phase, increasing or diminishing exponentially until the required temperature had been reached. The heating cycle lasted an average of ten hours and the cooling cycle nine hours.

2.3/ Data Acquisition System

Up to 100 channels of data were available using the B & F Instruments Inc. SY256-17 data loggers (Figure 3). There were two such units, each with its own independent power supply for energizing the strain gauge bridges and with amplifiers and balance potentiometers to condition the signals. The main unit housed the system's internal clock and channel-scanning instrumentation, a voltage-to-frequency converter, and a paper tape printer for backup. A teletype output was also available for data transfer. Lead wires from the ERSGs were taken from the specimen box to terminal units on the exterior of the freezer, and from there to the data logger (Figures 1, 4).

Alternative scanning rates were available, of either 20 channels per second with resolution to 1 microstrain, or 4 channels per second with resolution to 0.1 microstrain. Other options included the number of consecutive continuous scans (1 to 15), the number of readings per scan (1 to 15), and the time interval between scans (0.1 to 10.0 hours).

The data logger teletype output was modified to allow it to communicate directly with a Hyperion (Bytec-Comterm) microcomputer through a signal modulator. This was connected permanently to the logger so that all data could be stored and processed using diskettes. Ninety-four channels were accessed during each hourly scan (24 scans per day), at a resolution of 0.1 microstrain. Each scan required more time (70 seconds) as a result of the microcomputer and the data logger being linked together.

3/ Sample Selection and Specimen Preparation

3.1/ Rock Samples

A total of 53 specimens were subjected to the full temperature cycling program. These included 45 specimens of 11 different rock types and eight of metals, cement mortar, and titanium silicate glass for purposes of calibration and test reliability assessment.

The 11 rock types were selected by MTC to represent a range of Ontario aggregate making materials, including some with mineralogy similar to the USA sample whose thermal behaviour had been questioned, and including a sample from the quarry used in the Maryland concrete pavements (Section 1.2).

The carbonate samples included a coarse and a fine grained limestone; three of dolostone from two different formations and a dolomite cemented sandstone; two of calcitic marble; and one of dolomitic marble. Non-carbonate samples included one of meta-arkose and another of diabase. Petrographic descriptions are given in Appendix A.

Cubic, 25 mm specimens were chosen to ensure a minimum temperature differential between the outside and centre of the specimen while at the same time providing sufficient area for the application of strain gauges. It was also important to ensure sufficient (at least 10) mineral grains beneath each gauge so that results would be little affected by individual grain and grain boundary movements.

The 10 to 20 kg quarry block samples were cut into slabs and then into prisms and cubes using a slow speed diamond saw. Anisotropic samples had cubes cut with faces aligned parallel and perpendicular to the fabric (bedding planes or foliation). Strain gauges were applied parallel and perpendicular to the rock fabric, mounted on two cube faces oriented perpendicular to the fabric. No gauge could be applied in the plane of the fabric because of the limited number of available data channels. A minimum of eight cubes were prepared for each rock type, four for the thermal testing program and the remainder for preliminary tests of moisture content, coating materials and index properties. The unused portions of the block samples will be returned to MTC who plan to prepare aggregates and make concretes from them for further thermal testing.

Surface preparation prior to the fixing of strain gauges consisted of grinding on a slow speed lapping wheel using 320-grit silicon carbide abrasive powder.

3.2/ Control Specimens

The following are details of standard specimens for control and calibration that were prepared and tested alongside the rock cubes:
- carbon steel (1018-20, 0.25% carbon)
- aluminum (6061-T6, 97% Al)
- copper ("tough pitch", 99.9% Cu)
- brass (61.5% Cu, 35.0% Zn, 3.25% Pb)
- quartz crystal (gauged perpendicular to {001})
- titanium silicate glass (ULE 7971)

The metal specimens were cut from 25 x 9 mm bars. The quartz specimen was a hexagonal slice cut perpendicular to the C-axis of a large crystal (35 mm diameter) supplied by the Earth Sciences Department of the University. The titanium silicate was a 30 mm cube supplied by the Corning Glass Works, Corning, New York.

A mortar sample was also tested. This was prepared by MTC using a standard 30 MPa 28-day strength mix made with normal Portland cement and standard sand (source: Guelph Sand & Gravel). Cubic specimens were sawn from two cast cylinders, one containing an air-entraining agent.

3.3/ Strain Gauging

High quality strain gauges, bonding adhesives, and coating materials were needed. Applications of ERSGs to moist rock and cement surfaces can lead to erratic results (Kohlbeck and Scheidegger, 1984). Extreme care must also be taken in preparing and cleaning the surfaces to which the gauges are to be bonded, and in protecting the completed gauges against subsequent ingress of moisture.

CEA series strain gauges were selected, manufactured by the Micro-Measurement Division of Measurements Group Inc. These are general purpose gauges fabricated from a constantan-alloy grid on a polyamide backing. They are further protected by encapsulation of the gauge grid with a thin polyamide film, and have large integral copper-coated terminals for ease of soldering. The selected gauge had overall dimensions of 20.3 x 6.9 mm and an active grid area of 12.7 x 4.6 mm. Gauges from three different "lots" of identical type were used. Each lot of gauges was of

slightly different alloy composition. Comprehensive gauge property data were supplied with each lot.

The selected adhesive was M-bond AE-15, also by Micro Measurement Division. This was a two-component, 100% solids epoxy resin for general purpose stress analysis and transducer gauging.

All faces of the specimen cube, except those to receive the gauges, were carefully masked to keep them clean. The surfaces to be gauged were de-greased using a spray of chlorothene-based solvent, and then "conditioned" with a dilute acid cleaning solution directly followed by a neutralizing agent. Carbonate rocks were slightly etched by the acid to give a rougher surface and improved bonding. The conditioned surface was scrubbed with cotton-tipped applicators and wiped clean and dry with a gauze sponge.

The adhesive had a pot life of about one hour but was used only during the first 30 min after mixing. Twenty gauges were applied using a single 20 mL mix of prepackaged adhesive. Gauges were carefully aligned parallel and perpendicular to the rock fabric on opposite cube faces, and held in position using mylar adhesive tape. To apply an even pressure to the gauge and to produce an even, thin glue line, small stainless steel pressure plates with teflon and rubber underpads were secured to the cube using rubber bands.

To cure the adhesive, the specimens were placed in an oven and the temperature raised to 65°C. This temperature was held for two hours. The specimens were removed and allowed to stand for 24 hours before removing the pressure plates and exposing the gauges for connection of the lead wires (Figure 5). This procedure was used to allow gradual degassing of the gauge adhesive. A more rapid cure may result in trapping air pockets beneath the gauge grid.

The gauges were sealed with a preliminary coating of M-Coat D applied to the exposed lead wires and solder tabs. This toluene-thinned acrylic acts as a moisture barrier and an electrical insulator. It also works as a primer for the second coating of M-Coat G, a two-component, 100% solids, polysulfide-modified epoxy which was applied over the entire gauge area and surrounding rock surface. This final coating was to protect the gauges against moisture penetration and physical damage.

3.4/ Moisture Conditioning and Sealing

The specimens were moisture-conditioned for 21 days prior to testing. For each type, two specimens were to be tested "dry", and two "moist". The "dry" specimens were placed in a desiccator, and the "moist" ones in a humidity box above a saturated solution of copper sulphate to give a controlled environment of 98% relative humidity at a constant temperature of 24°C (Figure 6). Control specimens were used to measure weight gains and losses and to determine water contents at the end of this period. Low levels of saturation (15 to 20%) were achieved.

The specimens were to be sealed to maintain their moisture contents during thermal cycling. Several sealing materials, including silicone and urethane rubbers and filled and unfilled epoxy resins, were considered. The rubbers were rejected on the advice of chemists who recommended epoxies as having superior moisture barrier characteristics. Several epoxies were tested through ten thermal cycles using dummy specimens. A West Systems epoxy formulation was selected as the most efficient, but even this proved ineffective, allowing moisture losses of 21 to 25% for particular limestones and 10% for mortar samples.

A compromise decision was made to seal the "dry" specimens with epoxy (Fig. 7) and to maintain the "moist" ones in a humid atmosphere by including dishes of copper sulphate solution in the specimen box. Solution was added during the test, by injection of water through tubes passing through the corners of the box.

4/ Trials and Calibrations

4.1/ Proving Trials Using Aluminum and Rock

Initial trials were run to check and adjust the heating and cooling rates; to determine uniformity of temperature within the specimen box; and to determine the temperature gradient between the interior and exterior of a specimen rock cube. For these trials, four type-T thermocouples were installed in the box. Three were attached to specimens of aluminum. A fourth "control" thermocouple, sealed in a hole drilled in a meta-arkose cube, was attached to the meter relay (Section 2.2).

The temperatures measured by the four thermocouples were found to differ by a maximum of 1.5°C throughout the range to be used in testing. This showed that thermal gradients in the box and specimen were sufficiently small.

4.2/ Calibration of Aluminum Strains versus Temperature

In the full-scale testing program, aluminum strain readings were to be used in place of thermocouple readings as the standard measure of temperature. Thermocouple output could not be scanned or recorded by the data logging equipment. The three aluminum strain-gauged "thermometers" were positioned to allow averaging of temperature throughout the box and were monitored at quarter points in the scan to obtain an average temperature for the scan. Each of the three aluminum specimens used in the proving trials was instrumented with an ERSG from a different lot from the three used in the full-scale experiment.

A calibration was therefore needed between aluminum strain and temperature within a rock cube, as measured by the "control" thermocouple. Strain readings were taken at 5°C intervals during the heating and cooling half-cycles. An equation relating aluminum strain output to "control" thermocouple temperature was obtained for each of the three aluminum specimens using a fourth-order polynominal curve-fitting routine. Individual temperature calibrations for each of the aluminum specimens were averaged. The averaged calibration was used as the standard measure of temperature from this point on in the testing program.

Calibration was started only after five cycles of temperature had been completed. During the initial five cycles there was found to be a slight drift in ERSG readings, probably caused by further curing of the strain gauge adhesive and, possibly, by zero shift of the data logger.

4.3/ Correction for Apparent Thermal Strain

The electrical resistance of strain gauges varies significantly as a function of temperature. The change in resistance results in an "apparent" strain that requires a correction to the raw data.

Titanium silicate glass has unusual characteristics of dimensional stability in the temperature range -20°C to +70°C, having a mean temperature coefficient of expansion of 0.3 microstrain/°C. This material, as well as fused silica which has similar thermal stability, has frequently been used in applications requiring minimal thermal expansion. Finke and Heberling (1978), for example, have used titanium silicate to apply temperature corrections in their determinations of thermal expansion coefficients of metals over large temperature ranges. Fused silica has been used similarly by Poore and Kesterson (1978).

Three ERSGs, one from each lot, were fixed to three faces of the titanium silicate cube which was placed in the box along with the rock specimens. Relationships between temperature and ERSG outputs from the titanium silicate specimen ("apparent strain") were separately determined for each ERSG lot from average readings over the first 100 scans, using a polynomial curve-fitting procedure. Corrected rock strains were obtained for each scan by subtracting the calculated titanium silicate strain, for the appropriate ERSG lot and temperature, from the rock gauge reading.

The reason for averaging the first 100 scans rather than using the actual titanium silicate reading for the scan in question was long-term drift in strain readings from the gauges mounted on this specimen (Fig. 23). The cause of this apparent 80 microstrain expansion is not understood by us, nor has it been explained by personnel from Corning Glass. It may have been caused by inadequate annealing of the glass specimen, by creep of the strain gauge cement, or by instrument drift.

4.4/ Proving Trials on Various Materials

The calibration specimens of metal and quartz crystal (Fig. 8), along with two trial rock specimens, were initially subjected to thermal cycling for the purpose of evaluating the reliability and resolution of the test method. Measured temperature coefficients of expansion were found to be within 2% of values published for these materials (Appendix B).

5/ Full-Scale Test Program

5.1/ Initial Slow Cycle

The 53 specimens to be used in the full-scale experiment were first tested through one cycle in which temperature was raised and lowered slowly. This was to allow comparison with later automatic and faster cycles in order to evaluate possible thermal lag effects and drift caused by further curing of the strain gauge adhesive. The gauge outputs were zeroed at a reference temperature of 15°C.

During the heating cycle, temperature was raised in increments to a maximum of 50°C by adjusting the voltage supply to the heaters. Time was allowed for the temperature to reach equilibrium at each increment and then strain readings were recorded for all channels. During the cooling cycle, the temperature was lowered in increments to -20°C. At the end of each half-cycle, the temperature was allowed to return to the reference temperature in one step. A value for the temperature coefficient of expansion was calculated corresponding to each of the incremental steps (Appendix B).

5.2/ Automatic Cycling

Automatic thermal cycling was started after the slow cycle. Testing was stopped after 56 complete cooling and heating cycles through the temperature range -20°C to +70°C. Raw data from the strain gauges were scanned hourly and stored, together with the time record, on floppy diskettes. The paper tape record from the data logger was kept as a hard copy backup in case of system failure. The paper tape had to be replaced every five days whereas the diskettes were capable of storing more than ten days of continuous data. Five diskettes were needed to collect and store all raw data for the 56 temperature cycles. Copies were used for data processing.

6/ Calculation Procedures

Data on the diskettes were processed using an IBM Personal Computer. Programs were written in BASIC to perform all functions other than graph plotting, which employed the off-the-shelf program "GRAFIT" by Golden Software Inc. The sequence of data processing was as follows:

- "Cleaning" of the data by removal of extraneous information such as channel number, date, etc.
- Computation of centre-cube temperature for each scan from the average of the three aluminum strain readings, using results of the calibration described in Section 4.2.
- Computation of corrected strain readings for each scan using results of the titanium silicate measurements of apparent thermal strain described in Section 4.3.
- Subdivision of the data set into individual files, one per strain gauge.
- Creation of a parallel set of files containing only odd numbered cycles, so that plotting would take less time and could be done using GRAFIT (which can only handle a limited number of data points).
- Plotting of temperature versus strain for odd numbered cycles (Figures 9 to 23).
- Linear interpolation of strains at 20°C for each cycle, from the individual files, using data points at temperatures immediately above and below 20°C.
- Calculation of residual strain at 20°C by subtraction of the interpolated value for the first cycle.
- Plotting of residual strain versus cycle number (Figures 24 to 29)
- Calculation of "alpha", the coefficient of linear thermal expansion, for the initial slow cycle and for subsequent cycles 2 and 48 (slow cycle results in Appendix B).

The coefficient of linear thermal expansion (alpha) is strictly defined as an infinitesimal change in strain for a corresponding infinitesimal change in temperature (Skinner, 1966), and therefore is the "tangent" value equal to the slope of the temperature-strain curve.

More commonly, a "mean coefficient" or "chord" value is reported, calculated as $(\Delta L/L)/\Delta T$ (Roy *et al.*, 1981) where $\Delta L/L$ and ΔT are incremental measurements of strain and temperature. The "chord" value is the slope of the line between two successive measurements and is reported at the corresponding mid-point temperature. Temperature coefficients given in this report are chord values.

Because strains are usually small, alpha is more often expressed in terms of microstrain, as "x 10^{-6}/°C".

To convert from Imperial units, use 1.0 x 10^{-6}/°F = 1.8 x 10^{-6}/°C.

7/ Discussion of Results

7.1/ Comments on the Testing Procedure

Results of the testing program are regarded as reliable. An overall measuring accuracy of within 10 microstrain (generally much better) was achieved in spite of the aggressive testing environment and the long duration of testing (7 weeks of continuous cycling).

The procedure employed in this test series was found to have important advantages over alternatives, which may be summarized as follows:

- The small specimens were simple to prepare. Variations in size and shape were unimportant and did not affect the results. Being small, of a size similar to a coarse aggregate particle, the specimens suffered from minimal thermal lag and were free from the defects that are often present in larger sizes. On the other hand, the cubes were large enough to contain a sufficient number of grains to give satisfactory results even for the coarser grained rock types.

- The cubic shape of the specimens allowed strain gauging in directions parallel and perpendicular to the rock fabric. Thermal anisotropy could thus be measured using a single specimen.

- The use of ERSGs allowed automatic scanning with data logging equipment, and therefore simultaneous testing of a large number of specimens at moderate cost over a prolonged test period — an essential in most practical testing applications.

- The automatic and more-or-less continuous scanning of strains coupled with graph plotting allowed detailed examination of the complete record of strain versus temperature within the hysteresis and permanent strains — as opposed to making the simplistic and, for many rocks, incorrect assumption that strain is proportional to temperature.

The following limitations of the testing equipment and procedure became apparent. Few of these are inherent, and most can readily be corrected for future testing programs:

- Large freezers are not often available. A small freezer, but one with adequate thermal capacity, would be more suitable for routine testing. The large walk-in freezer was used as a last resort when a smaller freezer was found incapable of lowering the ambient temperature to the required -20°C.

- Heating and cooling rates were non-linear. Similar cycling would be difficult to reproduce. The rates depended on insulating characteristics and materials of the box and on the number of specimens it contained, and were governed by "ON/OFF" control of the heaters. Programmed linear temperature cycling would be preferable as standard.

- The procedure for testing specimens at a constant "moist" or "dry" condition was less than satisfactory. Of the many coating materials tried, none was found that would maintain moisture in the specimen for extended cycles of heating and cooling. Furthermore, the expedient of maintaining a high humidity in the specimen box gave rise to electrical induction problems. Further research is needed into humidity control, and into measurement of volumetric changes that occur as a result of humidity changes even at constant temperature.

- Larger specimens will be needed if concretes containing these or other aggregates are to be tested. The size of a concrete specimen will need to be at least ten times that of the largest aggregate particle. Direct strain gauging of such large specimens is likely to be impractical. One solution, allowing the use of ERSGs to keep costs low and maintain the important scanning capability, would be to construct simple demountable ERSG transducers of the spring/cantilever type.

7.2/ Temperature-Strain Graphs

Each of the temperature-strain graphs (Figures 9-23) contains 500 data points linked by straight-line segments. Only odd-numbered cycles between 1 and 49 have been plotted. Occasional spurious data points are evident which have probably been caused by pulses of ambient electrical noise. Clearly, all gauges continued to perform well throughout the test program, except one gauge on Specimen I2 (Figure 17(a)). A bonding or wiring failure is suspected in this case.

Each graph relates to a single strain gauge. Heading captions give the rock name followed in parentheses by a sample letter designation, specimen/moisture designation, and gauge orientation. Rock names and sample letter designations correspond to detailed petrographic descriptions in Appendix A. Specimens

1 and 2 were "moist" (conditioned in a humid environment, Section 3.4) whereas specimens 3 and 4 were air-dried. Gauge orientations are designated as PL (parallel) or PP (perpendicular) to the rock fabric. This designation has been omitted for isotropic rock types, which were instrumented with one gauge only. Note that the scales are different for Figures15, 19, 21, 22 and 23.

7.3/ Behaviour of Standard Specimens

Specimens of aluminum, copper, brass and steel, and the quartz crystal specimen (Figures 21 and 22) showed linear reversible behaviour. The gradients of these graphs were all within 5%, and usually within 1%, of established values of alpha for these materials (Appendix B), which confirms the reliability and precision of the test method.

The calibration standards of metals and quartz showed slight drift to a maximum of ±20 microstrain (Figure 24). The drifts were non-systematic and may have been due to any number of causes. Drifts of this order are to be expected for strain-guaged systems subjected to extremes of thermal cycling and moisture. They appear to have had an insignificant effect on the results as a whole.

Surprisingly erratic behaviour was recorded for the titanium silicate glass (Figure 23). The slope of each heating half-cycle was, as expected, approximately 30 microstrain of expansion per 90°C temperature rise. However, an apparent permanent expansion of some 80 microstrain developed during repeated cycling. This might be real, caused by insufficient annealing of the glass, or apparent, caused by some deficiency in the strain gauge bonding. The latter is, perhaps, unlikely in view of there being three gauges on this specimen, rather than one, and all three gauges recorded similar behaviour.

7.4/ Linear and Curvilinear Rock Behaviour

Linear behaviour was rarely exhibited by the rock specimens. The sample of Bertie-Akron dolostone (Figure 14) gave linear temperature-strain curves closest to those typical for metal specimens.

Most other rock types, however, showed curvilinear behaviour and a corresponding increase of slope and alpha values at higher temperatures. A typical example was the meta-arkose, which had alpha values increasing from about 3 to 6 microstrain per °C as the temperature rose from -20°C to +50°C. The most curvature occurred for the two calcite marble samples (Figs. 17 and 19). For these, alpha typically varied from -5 microstrain per °C at -20°C to +10 microstrain per °C at +50°C. The dolomites and dolomitic sandstone, in contrast, behaved in a more linear fashion.

Non-linear thermal coefficients have been previously reported for various rock types (Willis and DeReus, 1939; Johnson and Parson, 1944; Hockman and Kessler, 1950; Harvey, 1967, 1968). The data presented here confirm this behaviour. Non-linear thermal expansion is exhibited not only by rocks but also by most rock-forming minerals (Skinner, Table 6.1, 1966). Alpha coefficients increase with temperature.

7.5/ Anisotropic Rock Behaviour

Anisotropic thermal expansion was recorded for most of the rock types with identifiable fabrics. Expansion was observed to be greater perpendicular to the fabric direction in most cases.

Degrees of anisotropy of thermal expansion can be examined in terms of the ratio of alpha perpendicular to fabric divided by alpha parallel to fabric. This ratio proved to be typically 1.4 to 2.0 for most of the rock specimens designated "anisotropic" from visual inspection. The ratio was greatest (as high as 10.1) for the USA calcite marble (Figure 17). Thermal anisotropy appeared also to increase at lower temperatures.

Exceptionally, there was a tendency for greater expansion parallel with the rock fabric. This effect was most pronounced for the meta-arkose)sample (Figure 11) which had thermal anisotropy ratios in the range 0.6 to 0.8.

Observed thermal expansion anisotropy might be explained either by the preferred orientation of mineral grains which themselves are thermally anisotropic, or by concentrations of thermally different mineral types along bedding or foliation planes. Results of the present study are inconclusive in this regard.

Not only are most rocks thermally anisotropic, but so are the common rock forming minerals such as quartz, calcite, and the feldspars. They have a high degree of differential expansion depending on crystallographic orientation. Calcite crystals, for example, have a negative coefficient of expansion (-5 microstrain per °C) in the direction perpendicular to their C-axis, compared with +18 microstrain per °C in the orthogonal direction. Dolomite crystals are also anisotropic but, unlike calcite, all expansion coefficients are positive (Bayer, 1971, Table 1).

7.6/ Hysteresis, Growth and Shrinkage

All standards and rock specimens showed some degree of hysteresis; the temperature-strain path described a hysteresis loop. At higher temperatures, alpha values were greater during cooling than during heating, whereas at lower temperatures, the reverse was true. Typical differences in alpha measured during cooling and heating half-cycles were in the order of 0.2% for metals, 1.5 to 6% for most rocks tested, and up to 50% for the calcite marbles.

"Growth" of some specimens occurred, defined as a permanent expansion (residual strain) that increased with each successive thermal cycle. This is best observed in graphs of strain versus cycle number, Figures 24 to 29. Growth was particularly marked for the calcite marbles, the calcarenite limestone, and the Manitoulin dolostone (Figures 28, 29, 24 and 26). The Ontario calcite marble (Figure 29) had expanded permanently by 500 microstrain (0.05%) after 56 cycles.

Growth was most pronounced during the initial ten to twenty cycles, after which specimens usually stabilized in their expanded configuration. This is clearly illustrated by the behaviour of the calcarenite limestone (Figure 24).

"Shrinkage" occurred in the cement mortar and also in the "moist" specimens of Logan diabase (Figure 25). Mortar shrinkage may have been caused by ongoing moisture loss. Contraction of cement pastes is caused by curing and varies with temperature, initial moisture content, and time (Zoldners, 1971). Moisture loss may also be produced at sub-freezing temperatures by the expulsion of moisture as a result of freeze-drying (Litvan, 1973).

Shrinkage of the Logan diabase may also have been the result of moisture loss. Clay minerals in the form of plagioclase alteration products absorbed water during moisture conditioning and are likely to have dried and contracted during thermal cycling. Shrinkage did not occur for the air-dried specimens of the same rock.

Shrinkage also occurred during initial temperature-cyling of the unsealed "moist" specimens of Nelson dolostone and dolomitic sandstone (Figures 26, 29). These rock types are highly susceptible to short-term moisture expansion (Section 7.7) so that the shrinkage may have resulted from subsequent loss of absorbed moisture.

Specimen growth and shrinkage were accompanied by changes in the temperature coefficient, alpha. An arbitrary comparison between cycles 2 and 48 showed alpha for most specimens to increase by about 0.5 to 1.1 microstrain per °C at temperatures below freezing, whereas alpha at higher temperatures was much less affected. Thus, temperature-strain characteristics that showed an initial pronounced curvature tended to straighten out with increasing numbers of thermal cycles.

7.7/ Moisture Effects

Introduction of water into the specimen box was responsible for the observed peaks in some of the strain-cycle curves. This effect was most apparent for the sample of cement mortar (Figure 25). The peaks of some 180 microstrain amplitude corresponded identically with the introduction of water into the specimen box during cycles 5, 17, 24, 29 and 36.

Similar moisture expansion peaks were evident in the graphs for Nelson dolostone (Figure 26), Grenville dolomitic marble (Figure 27), and dolomitic sandstone (Figure 29). The peaks were much more pronounced for the unsealed "moist" specimens than for the sealed "dry" ones. The Nelson dolostone had the highest porosity of the rock types tested (7 to 9%, see Figure A4). The rock type with the next highest porosity, the Haldimand dolostone, however, showed less pronounced moisture peaks than the Grenville dolomitic marble which had a porosity of only 0.3 to 0.5% (Figure 27). Porosity was evidently not the sole criterion of whether or not moisture expansion would occur, which is likely to be governed also by such properties as pore size, permeability and clay content.

For most rock types, the effects of moisture on thermal expansion appeared to be transient rather than irreversible. After passing through a strain peak as a result of the introduction of moisture, the specimens resumed their original trend of strain-cycle behaviour. Usually, there were only slight differences, both positive and negative, between the magnitudes of ultimate permanent strain experienced by "dry" and "moist" specimens of the same rock type.

An exception to the transient nature of moisture expansion occurred with both calcite marbles (Figures 28, 29). These rock types showed a permanent expansion after each introduction of moisture into the specimen box, at least during the initial cycles of the test.

In conclusion, there seems to have been little if any permanent disruption caused by ice growth during this test series. This is probably because of the low levels of saturation (15 to 20%), and because of the limited time for ice growth to occur (6 to 7 hours). Adsorbed moisture acquired in environments near 100% relative humidity at 30°C is not considered capable of freezing (Hudec and Sitar, 1975). This is because moisture contained within micropores at low levels of saturation is in equilibrium with high vapour pressures (Litvan, 1972). Any water that does freeze is able to expand into available pore space provided that the degree of saturation remains below a "critical level" of about 90%. The dual role of adsorbed and free water in the frost susceptibility of rock is discussed by Cady (1969).

7.8/ Concrete Deterioration Hypotheses

This research points to three possible mechanisms whereby concrete might deteriorate as a result of thermal cycling. These are identified as follows:

Thermal Incompatibility of Mortar and Aggregate

Cement mortars have typical thermal expansion coefficients of 12 to 16 microstrain per °C, whereas rock aggregates have values that are much lower, typically 4 to 9 microstrain per °C (Appendix B). In the sub-freezing range some rock types, such as calcitic marbles, have near-zero or even negative thermal coefficients. Non-linear expansion characteristics could also increase the degree of thermal incompatibility.

Cooling of concrete is therefore likely to result in the generation of tensile stresses in the mortar which contracts more than the enclosed aggregate particles. Repeated thermal cycling could lead to thermal fatigue characterized by cracking in the cement paste.

Anisotropic Thermal Expansion of Aggregates

Certain rock types expand more in the direction perpendicular to the bedding or foliation. The severity of such effects is likely to be much greater than is suggested by results of the current research program, from which grossly anisotropic rock types were excluded. Such differential thermal expansion could result in tensile stresses in the mortar matrix of a concrete and might well lead to cracking.

Shrinkage of Mortar and Growth of Aggregates

The research has also demonstrated that mortars shrink and some aggregates grow as a result of thermal cycling (Section 7.6). The combination of shrinkage and permanent expansion would generate additional stresses at the aggregate-mortar interface. Microcracking might result if these stresses were to reach sufficient magnitude.

The three mechanisms, which are strictly thermal and do not require the presence of moisture, are likely to act in combination and to supplement each other to a greater or lesser extent, depending on the nature of the aggregates and mortar. Microcracks generated by one or all three mechanisms will weaken the concrete and contribute to the access of moisture. The combined effects of reduced strength and increased permeability will accelerate freeze-thaw deterioration of the concrete.

8/ Conclusions

The test technique proved satisfactory and gave reliable results. A complete record of temperature-strain cycling and moisture movements was obtained.

Measured values of the coefficients of thermal expansion for standard materials agreed closely with those reported in literature, confirming the reliability of the test method.

Rock types had lower coefficients of thermal expansion than those of typical cement mortars, and negative ones in some cases. The lowest values were recorded for calcite marbles. These coefficients decreased with decreasing temperature in most cases, resulting in non-linear temperature-strain graphs.

Anisotropic thermal expansion occurred in rock types containing bedding or foliation. Thermal expansion was up to ten times greater perpendicular to the rock fabric.

The strain-temperature curve followed a hysteresis loop, both for standard materials and for the rock specimens.

Irreversible growth often occurred when the rock specimens were temperature-cycled. The amount of permanent expansion was greatest during the initial 10 to 20 thermal cycles. Growth was greatest for calcite marbles, with permanent strains of up to 500 microstrains. Shrinkage occurred in the mortar and "moist" diabase specimens, probably as the result of moisture losses during thermal cycling.

Moisture effects were recorded in the form of temporary expansions coinciding with increases of humidity within the specimen box. However, the various thermal effects of non-linearity, hysteresis, anisotropy and growth were not influenced by changes in moisture content in the range of saturations tested (3 to 20%).

These thermal effects are likely to generate stress concentrations at contacts between aggregate particles and the mortar matrix. In combination, they may cause microcracking, particularly for those aggregate types with thermal characteristics contrasting most with those of cement mortar. Such cracking will increase the permeability of the concrete and reduce its strength and resistance to more aggressive types of freeze-thaw mechanism.

References

Adie, A.J. (1836), "On the expansion of different kinds of stone from an increase of temperature with a description of the pyrometer used in making the experiments", Royal Society of Edinburgh *Transcripts*, Vol. 13, pp. 354-372.

Baldwin-Wiseman, W.R. and Griffith, O.W. (1909), "Physical properties of building materials," Institute of Civil Engineers, *Proceedings*, Vol. 3, p. 179.

Barlett, W.H. (1832), "Experiments on the expansion and contraction of building stone," *American Journal of Science and Arts*, Vol. 22, pp. 136-140.

Bayer, G. (1971), "Thermal expansion anisotropy of dolomite-type borates $Me^{2+}Me^{4+}B_2O_6$," *Zeitschrift fur Kristallographie*, Vol. 133, pp. 85-90.

Brandes, E.A. (Ed.) (1983), "The physical properties of alloys and steels," in *Smithells Metals Reference Book*, 6th Edition, London: Butterworth and Co., pp. 14.4-14.39.

Cady, P.D. (1969), "Mechanisms of frost action in concrete aggregates," *Journal of Materials*, JMLSA, Vol. 4, No. 2, pp. 294-311.

Callan, E.J. (1950), "The relationship of thermal expansion to the durability of concrete," Bulletin No. 34, Waterways Experimental Station, Corps of Engineers, U.S. Army, Vicksburg, Mississippi.

Callan, E.J. (1952), "Thermal expansion of aggregates and concrete durability," *Journal of the American Concrete Institute*, Proceedings, Vol. 48, pp. 485-504.

Cook, H.K. (1966), "Thermal properties" in "Significance of tests and properties of concrete making materials," *ASTM STP No. 169-A*, American Society for Testing and Materials, pp. 476-486.

Davis, R.E. (1930), "A summary of investigations of volume changes in cements, mortars, and concretes produced by causes other than stress," *ASTM Proceedings*, Vol. 30, Part 1, pp. 668-685.

Finke, T.E., and Heberling, T.G. (1978), "Determination of thermal-expansion characteristics of metals using strain gauges," April, *Experimental Mechanics*, pp. 155-159.

Griffith, J.H. (1936), "Thermal expansion of typical American rocks," Iowa Engineering Experiment Station Bulletin 128, 36 pp.

Hahn, T.A. (1970), "Thermal expansion of copper from 20-800 K: Standard reference material 736," *Journal of Applied Physics*, Vol. 41, No. 13, pp. 5096-5102.

Hallock, W. (1891), "Preliminary notes on the coefficients of thermal expansion of certain rocks," U.S. Geological Survey Bulletin, Vol. 78, pp. 109-118.

Harvey, R.D. (1967), "Thermal expansion of certain Illinois limestones and dolomites," Illinois Geological Survey, Circular, No. 415, pp. 1-33.

Harvey, R.D. (1968), "Nonlinear thermal expansion of coarse grain limestones," *Materials Research and Standards*, Vol. 7, No. 7, pp. 502-506.

Hockman, A. and Kessler, D.W. (1950), "Thermal and moisture expansion studies of some domestic granites," *Journal of Research of the National Bureau of Standards*, Research Paper RP 2087, Vol. 44, pp. 395-410.

Hudec, P.P. (1980), "Durability of carbonate rocks as a function of their thermal expansion, water sorption and mineralogy," 1980, in *Durability of Building Materials and Components*, ASTM STP 691, P.J. Sereda and G.G. Litvan, Eds., American Society for Testing and Materials, pp. 497-508.

Hudec, P.P. and Sitar, N. (1975), "Effect of water sorption on carbonate rock expansivity," *Canadian Geotechnical Journal*, Vol. 12, pp. 179-186.

Johnson, W.H. and Parsons, W.H. (1944), "Thermal expansion of concrete aggregate materials," *National Bureau of Standards Journal of Research*, Vol. 32, pp. 101-126.

Koenitzer, L.H. (1936), "Elastic and thermal expansion properties of concrete as affected by similar properties of the aggregate," *ASTM Proceedings*, Vol. 36, Part 2, pp. 393-406.

Kohlbeck, F., and Scheidegger, A.E. (1984), "Applications of strain gauges on rock and concrete," in *Field Measurements in Geomechanics, Proceedings International Symposium*, Zurich, September, 1983, Vol. 1, K. Kovari (Ed.), A.A. Balkema, Rotterdam, pp. 197-207.

Litvan, G.G. (1972), "Phase transitions of adsorbates, III: Heat effects and dimensional changes in non-equilibrium temperature cycles," *Journal of Colloid and Interface Science*, Vol. 38, No. 1, pp. 75-83.

Litvan, G.G. (1973), "Frost action in cement paste," *Materials and Structures, Research and Testing*, Vol. 6, No. 34, pp. 293-298.

Loubser, P.J., and Bryden, J.G. (1972), "An apparatus for determining the coefficient of thermal expansion of rocks, mortars, and concretes," *Magazine of Concrete Research*, Vol. 24, No. 79, pp. 97-100.

Mather, B., Callan, E.J., Mather, K., and Dodge, N.B. (1953) "Laboratory investigations of certain limestone aggregates for concrete," 1953, *Technical Memorandum No. 6-371*, Waterways Experimental Station, Corps of Engineers, Vicksburg, Mississippi.

Meyers, S.L. (1940), "Thermal coefficient of expansion of Portland cement," *Industrial and Engineering Chemistry*, Vol. 32, pp. 1107-1112.

Pearson, J.C. (1941), "A concrete failure attributed to aggregate of low thermal coefficient," *Journal of the American Concrete Institute, Proceedings*, Vol. 38, No. 1, pp. 29-34.

Pearson, J.C. (1943), "Supplementary data on the effect of concrete aggregate having low thermal coefficient of expansion," *Journal of the American Concrete Institute*, Vol. 15, No. 33.

Poore, M.W. and Kesterson, K.F. (1978), "Measuring the thermal expansion of solids with strain gauges," *Journal of Testing and Evaluation*, Vol.6, No. 2, pp. 98-102.

Roy, R.F., Beck, A.E., and Touloukian, Y.S. (1981), "Thermophysical properties of rocks," in *Physical Properties of Rocks and Minerals*, McGraw-Hill/-CINDAS Data Series on Material Properties Vol. II-2, Y.S. Touloukian and C.Y. Ho (Editors), McGraw-Hill Book Company, New York, pp. 409-502.

Richter, D. and Simmons, G. (1974), "Thermal expansion behaviour of igneous rocks," *International Journal of Rock Mechanics and Mining Science, and Geomechanical Abstracts*, Vol. II, pp. 403-411.

Shah, G.N. (1974), "Rigid pavement investigations — growth characteristics and blowups," Maryland State Highway Administration, Bureau of Research, Final Report, AW 74-96-46.

Skinner, B.J. (1966), "Thermal Expansion" in *Handbook of Physical Constants —Revised Edition*, Geological Society of America Memoir 97, S.P. Clarke Jr., Ed., pp. 76-96.

Smith, G.M. (1956), "Physical incompatibility of matrix and aggregate in concrete," *Journal of the American Concrete Institute, Proceedings*,Vol. 52, pp. 791-798.

Souder, W.H., and Hidnert, P. (1919), "Thermal expansion of insulating materials," U.S. National Bureau of Standards, Scientific Paper SP352, Vol. 15, pp. 387-417.

Thomlinson, J. (1940), "Temperature variations and consequent stresses produced by daily and seasonal temperature cycles," *Concrete and Construction Engineering*, Vol. 35, pp. 298-307, 352-360.

Valentich, J. (1981), "Tube type dilatometers," Instrumentation Society of America, North Carolina.

Walker, S., Bloem, D.L., and Mullen, W.G. (1952), "Effects of temperature changes on concrete as influenced by aggregates," *Journal of the American Concrete Institute, Proceedings*, Vol. 48, pp. 661-678.

Wheeler, N.E. (1910), "On the thermal expansion of rocks at high temperatures," Royal Society of Canada Transactions, Series 3, Vol. 4, pp. 19-44.

Willis, T.F. and DeReus, M.E. (1939), "Thermal volume change and elasticity of aggregates and their effect on concrete," *ASTM Proceedings*, Vol. 39, pp. 919-929.

Zoldners, N.G. (1971), "Thermal properties of concrete under sustained elevated temperatures," American Concrete Institute, Special Publication SP25, pp. 1-31.

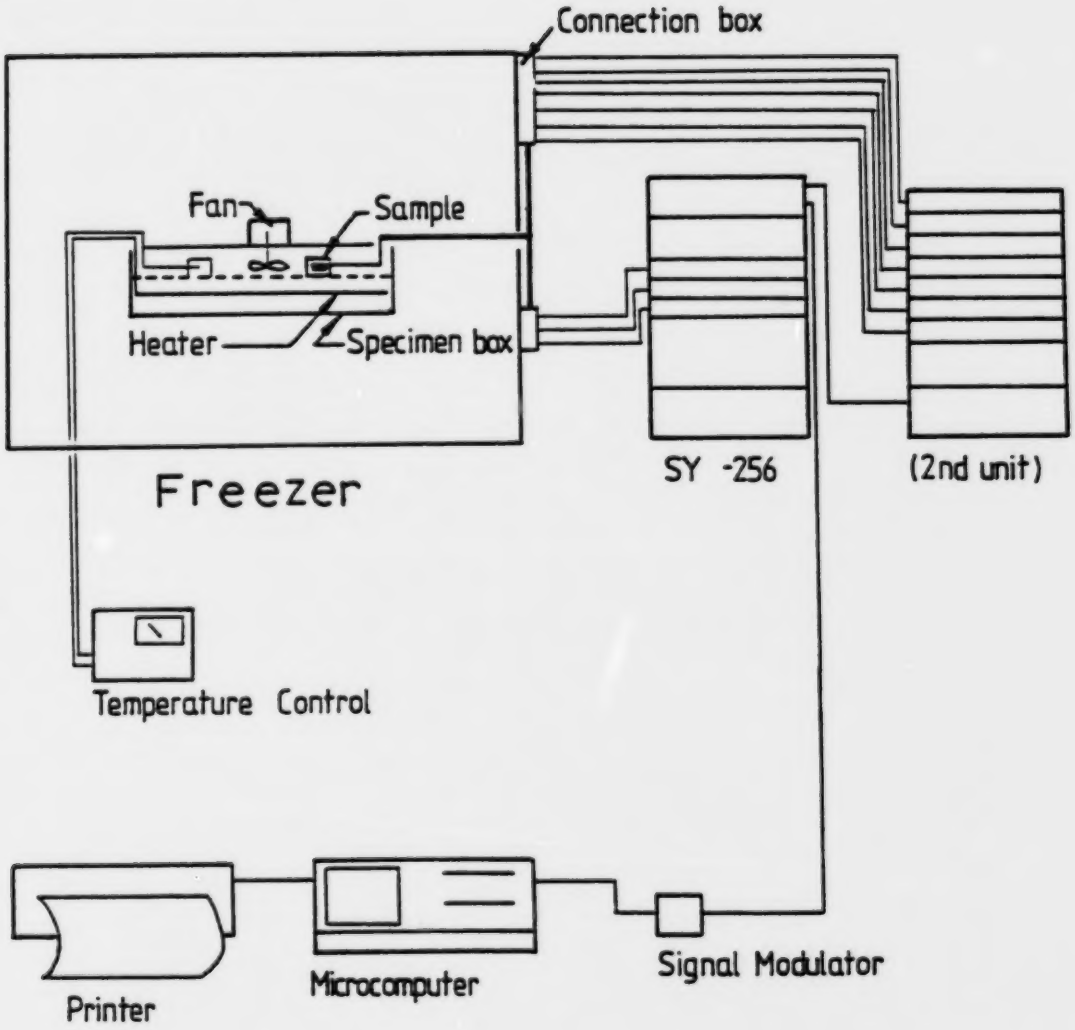

Figure 1/ Wiring Connections of System Apparatus

Figure 2a/ Specimen Box Showing Fan and Water Tubes

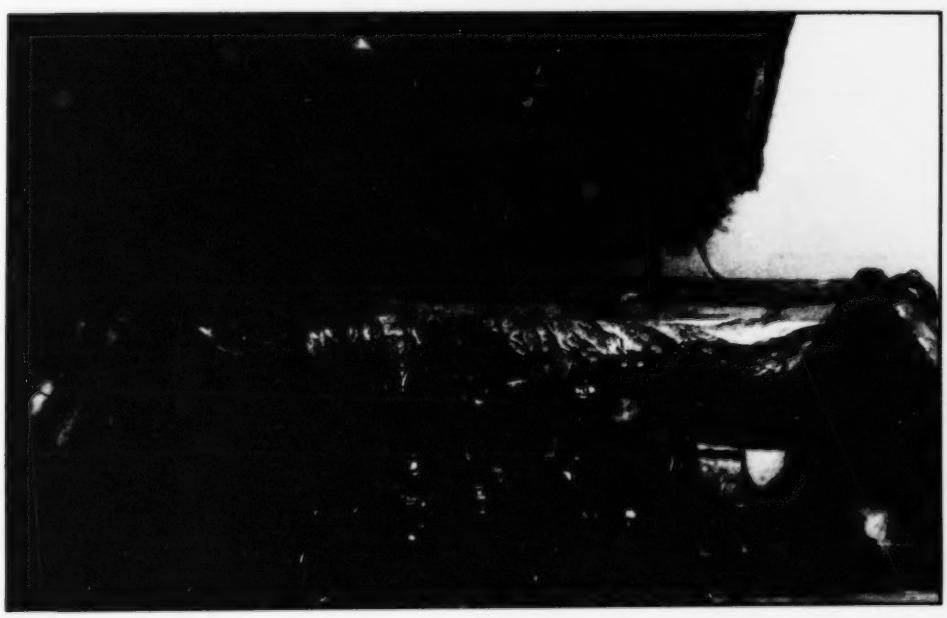

Figure 2b/ Specimen Box Open, Showing Assembled Specimens

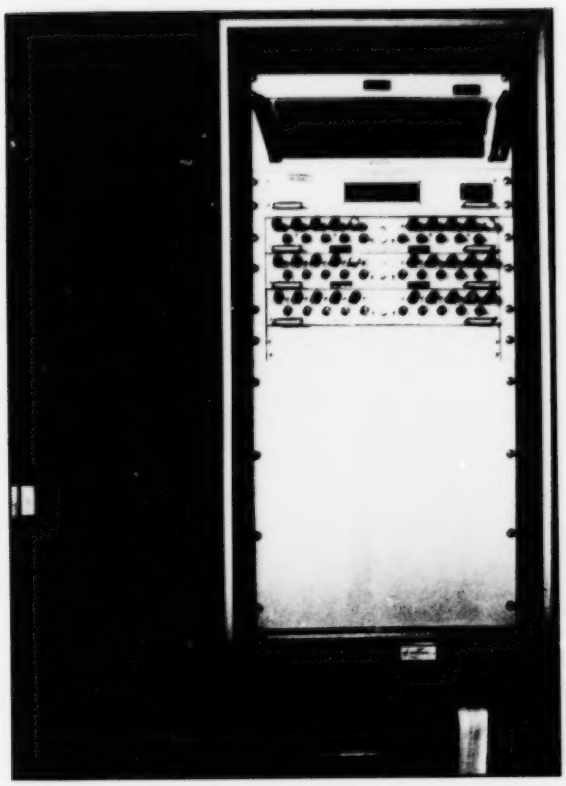

Figure 3/ Data Logger
(B & F Instruments SY256-17)

Figure 4/ Large Freezer with Connection Boxes for Strain Gauge Leads

Figure 5a/ Attaching Strain Gauge Leads to a Specimen

Figure 5b/ Strain-gauged Rock Specimens

Figure 6/ Humidity Control Box

Figure 7/ Epoxy Coating of "Dry" Specimens

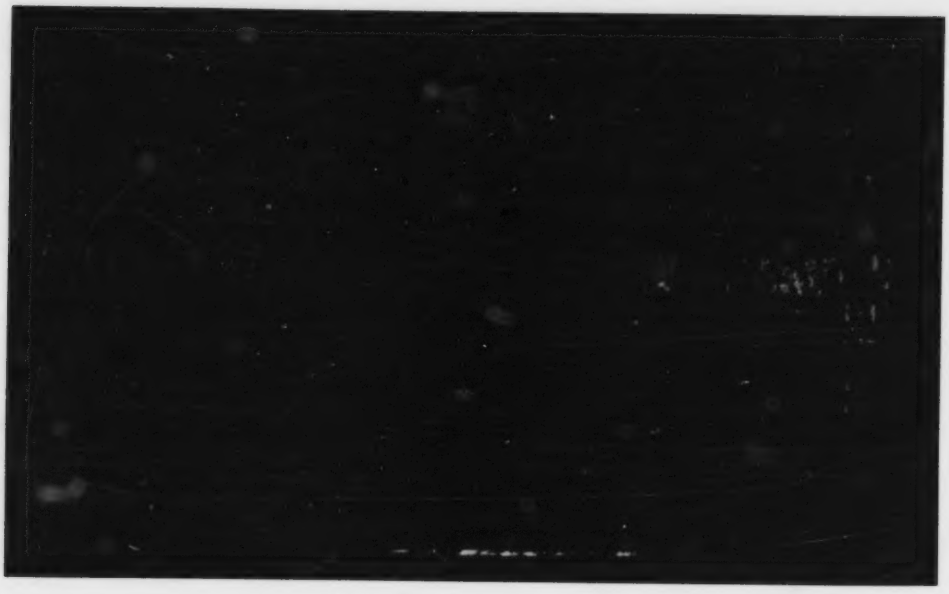

Figure 8a/ Calibration Specimens in Thermal Control Box
Thermofoil Heaters can be seen beneath the wire mesh.

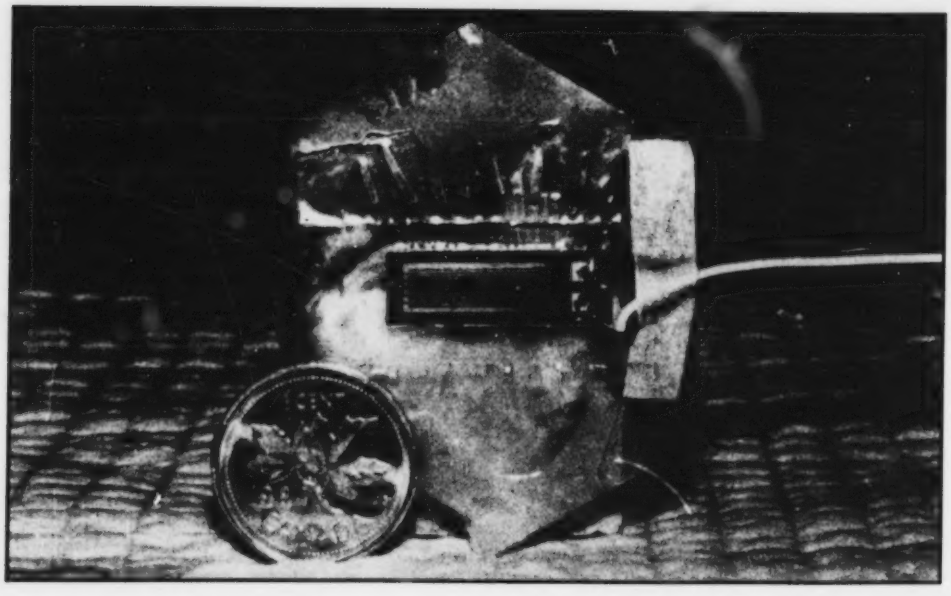

Figure 8b/ Quartz Crystal Calibration Specimen

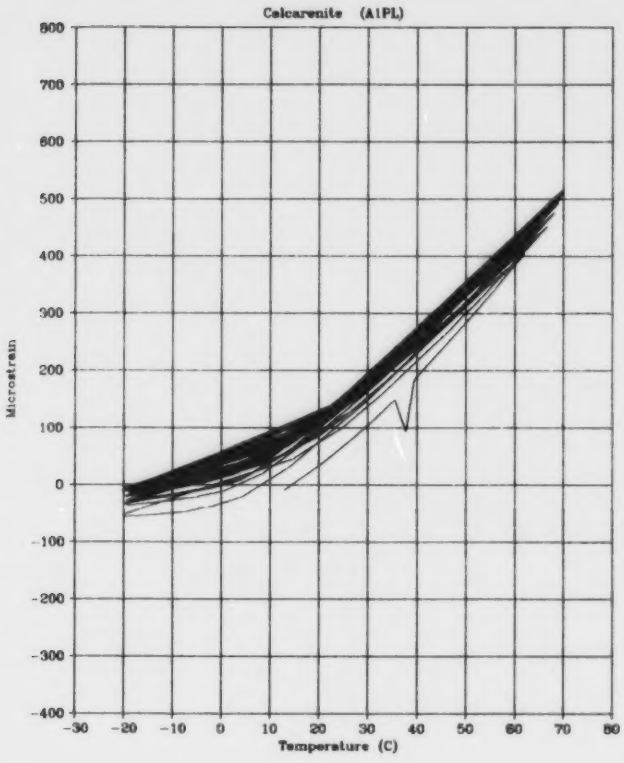

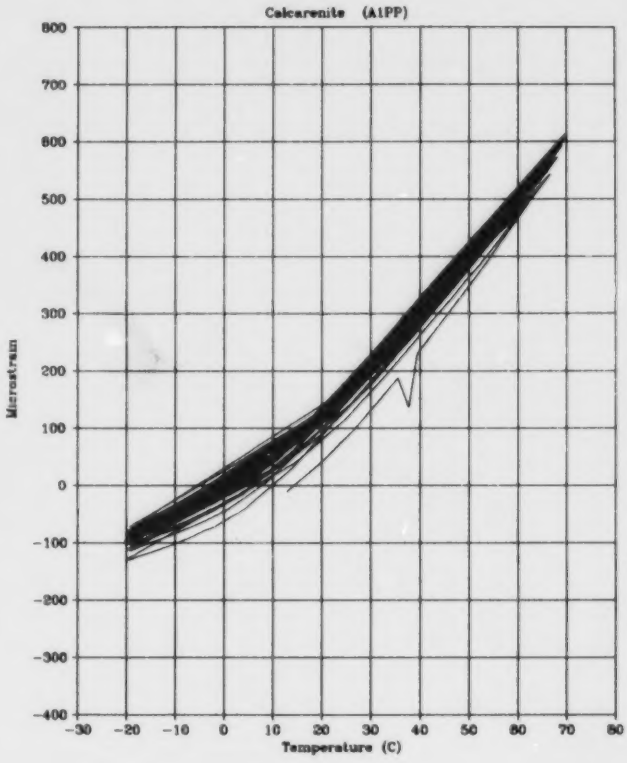

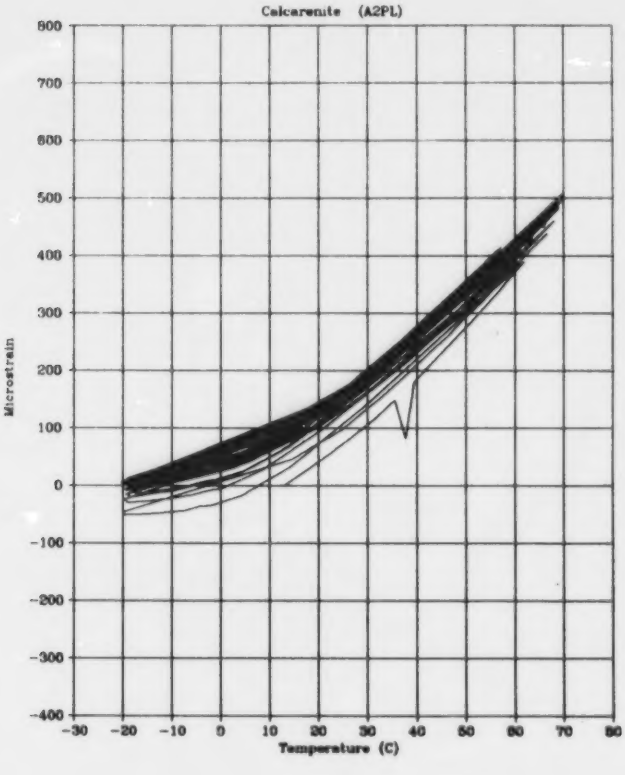

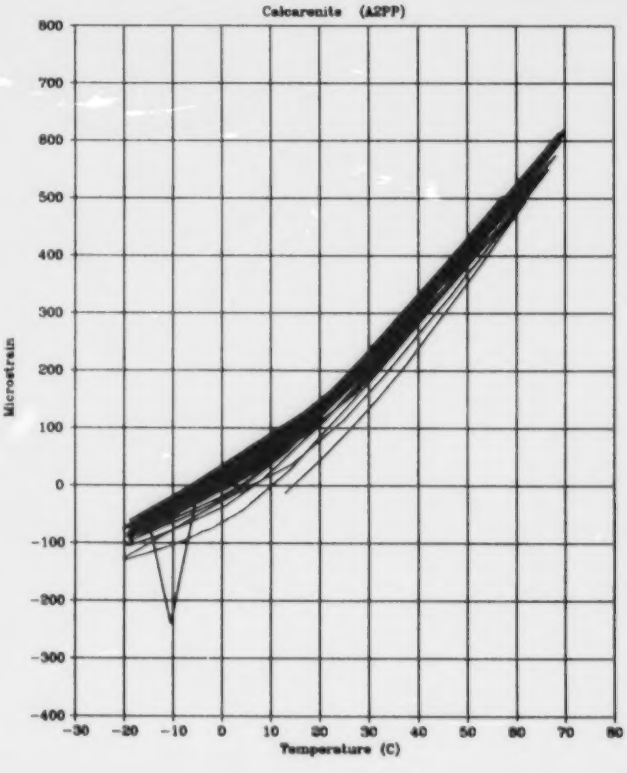

Figure 9a/ Strain versus Temperature, Sample A, Calcarenite Moist Specimens A1, A2

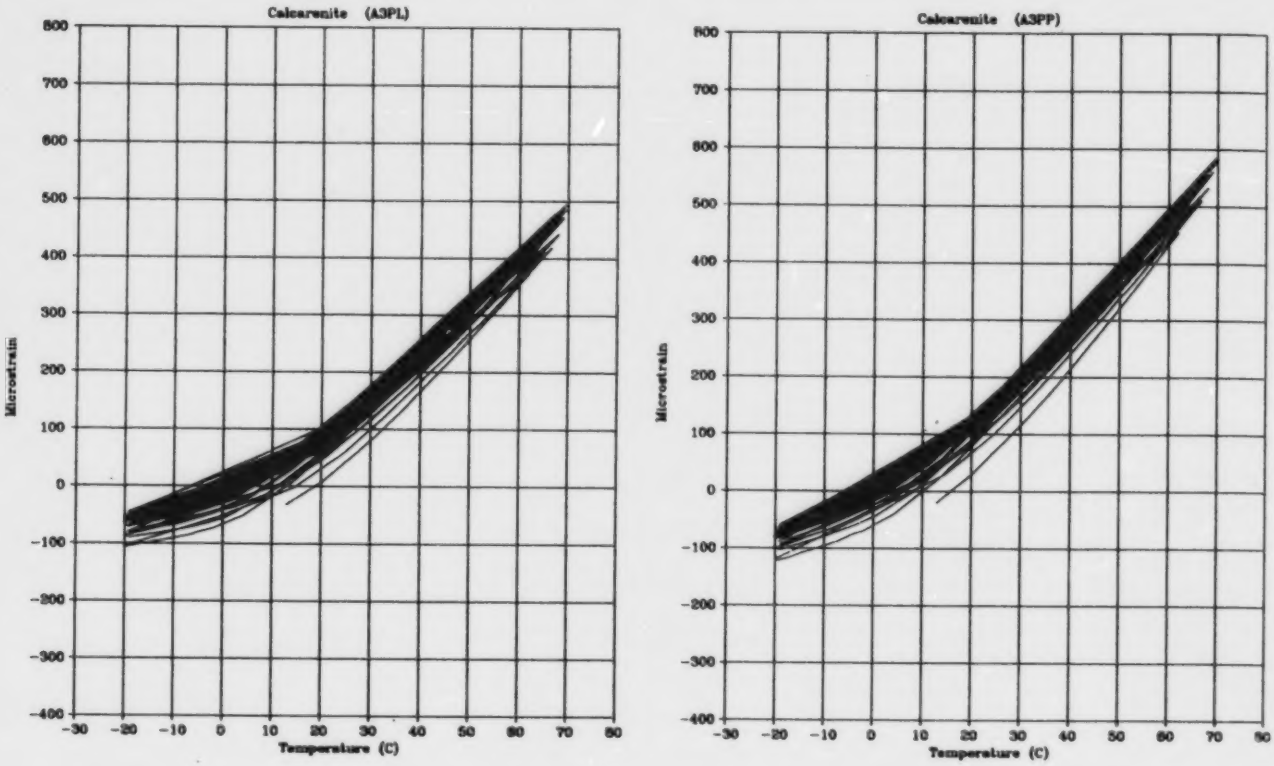

Figure 9b/ Strain versus Temperature, Sample A, Calcarenite, Air-dried Specimen A3

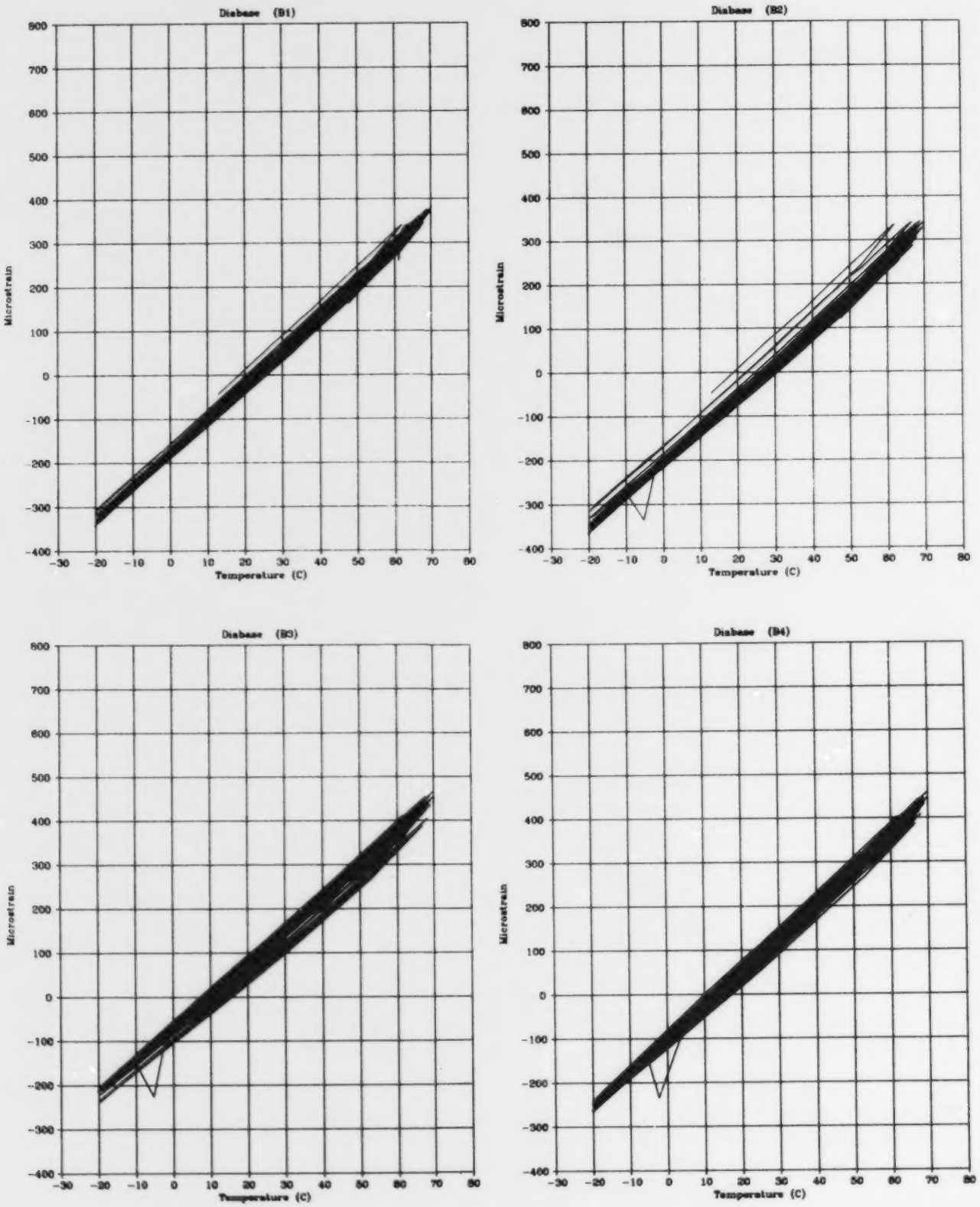

Figure 10/ Strain versus Temperature, Sample B, Logan Diabase,
Moist Specimens B1, B2
Air-dried Specimens B3, B4

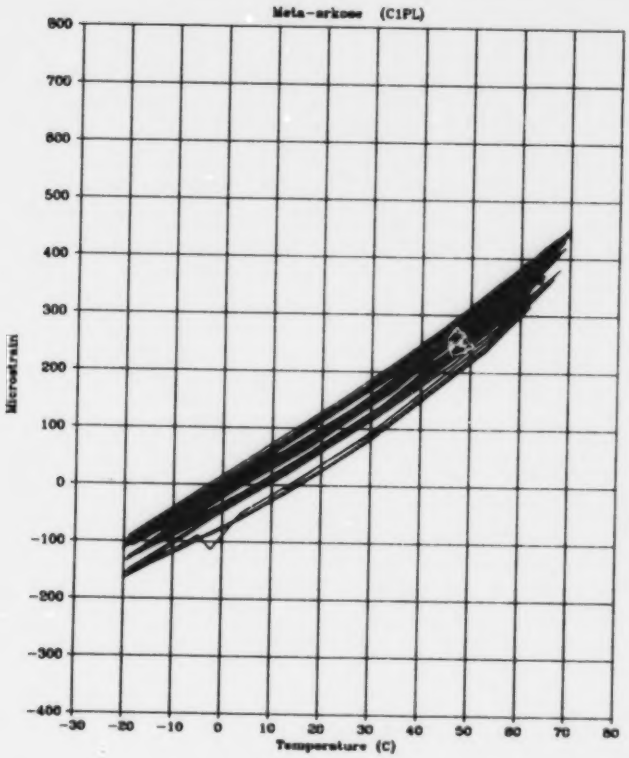

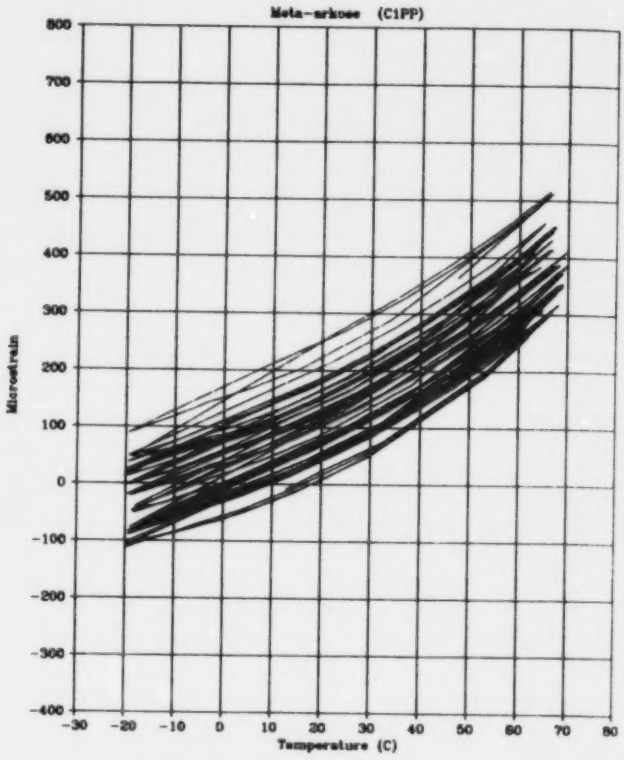

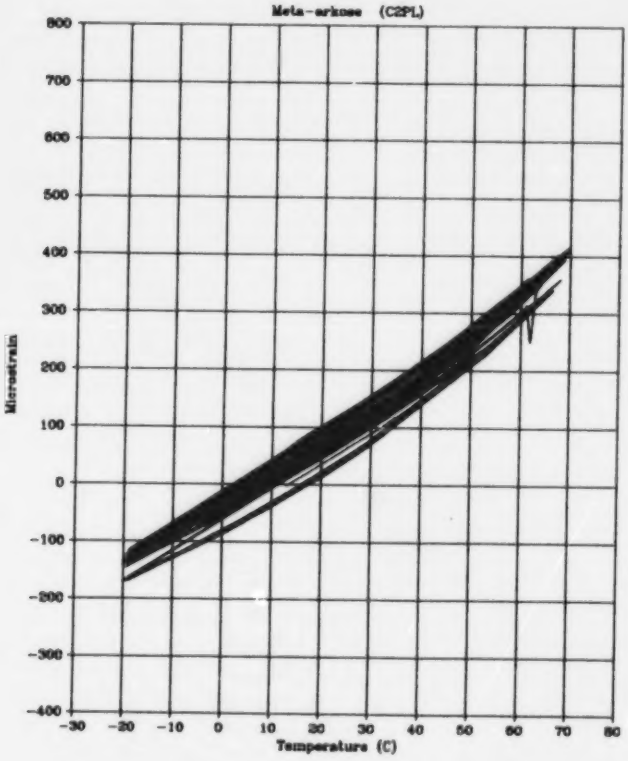

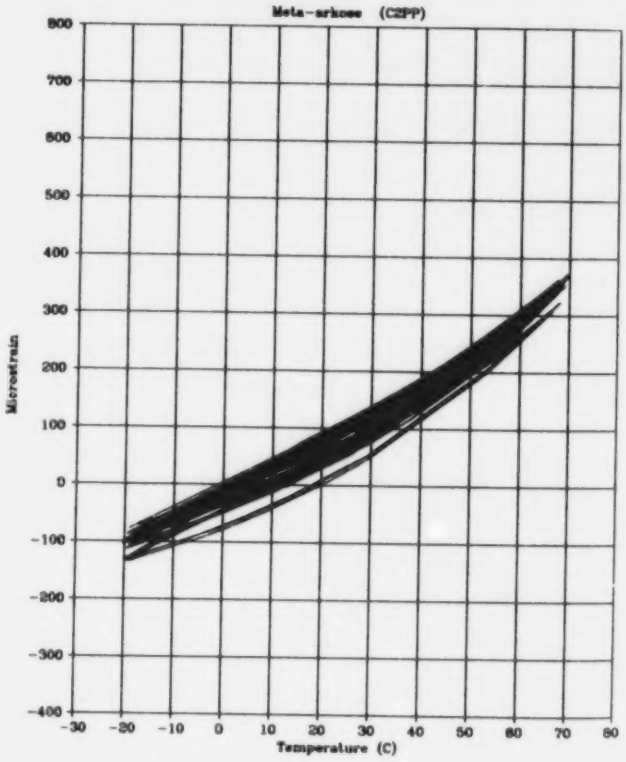

Figure 11a/ Strain versus Temperature, Sample C, Meta-arkose, Moist Specimens C1, C2

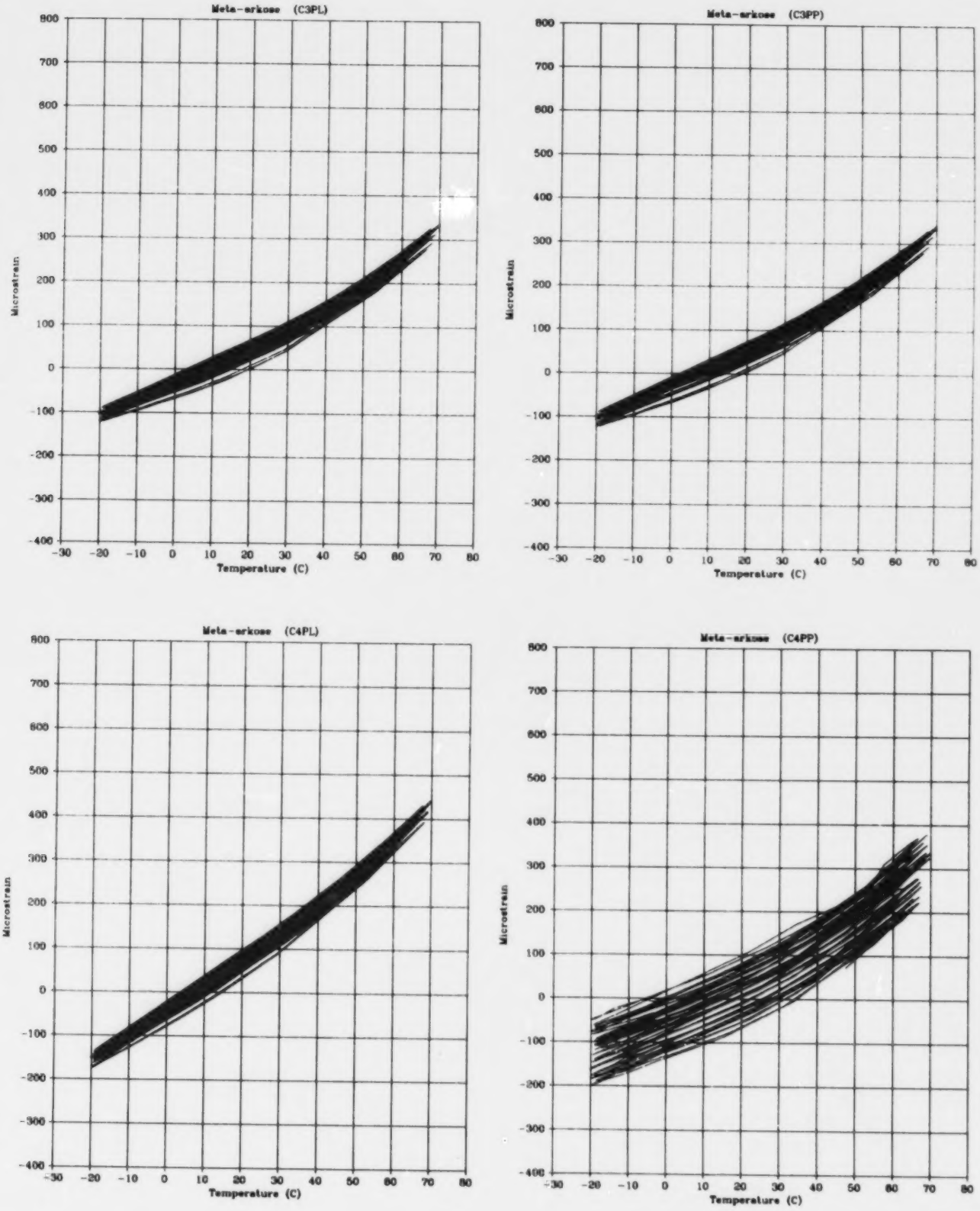

Figure 11b/ Strain versus Temperature, Sample C, Meta-arkose, Air-dried Specimens C3, C4

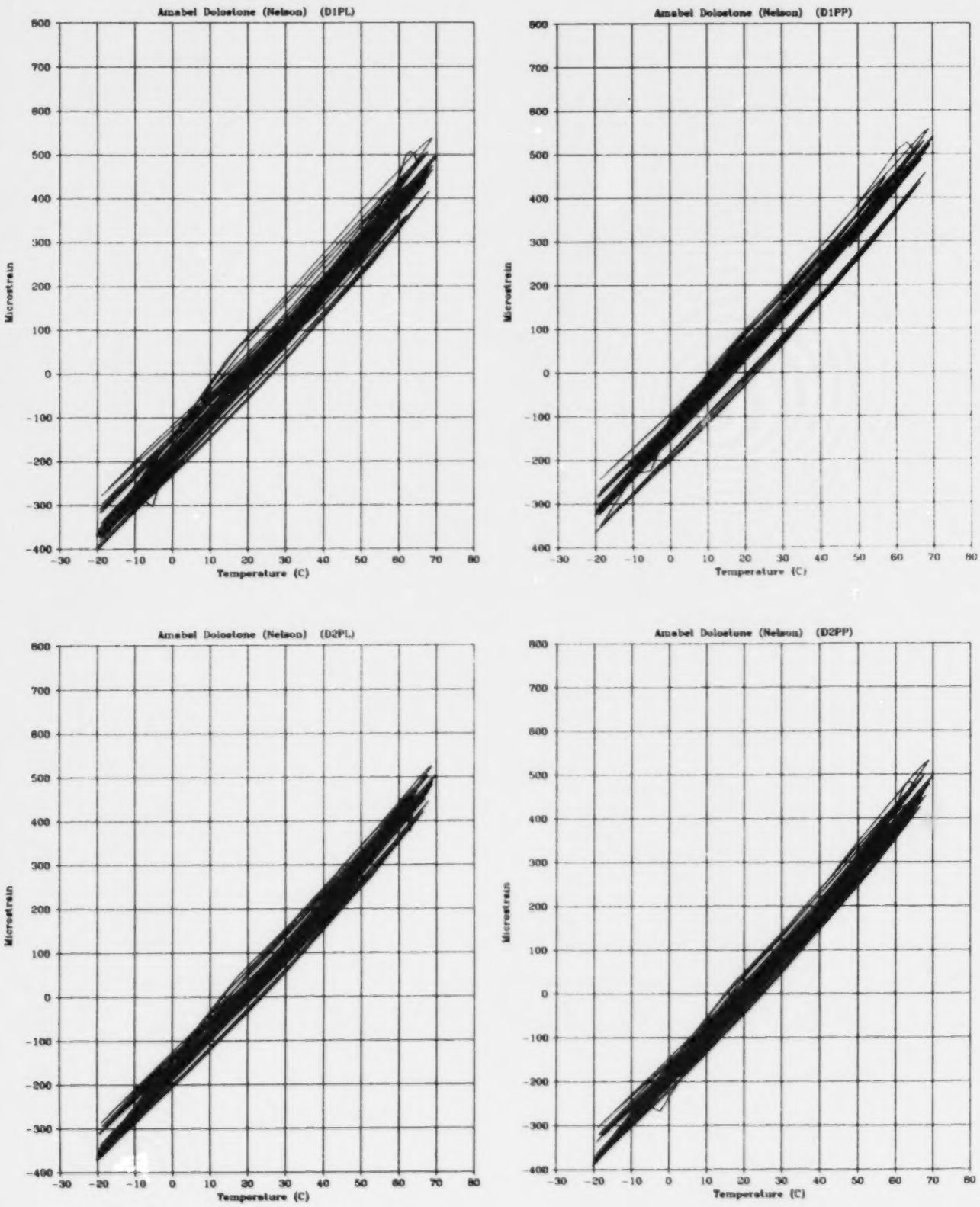

Figure 12a/ Strain versus Temperature, Sample D, Nelson Dolostone, Moist Specimens D1, D2

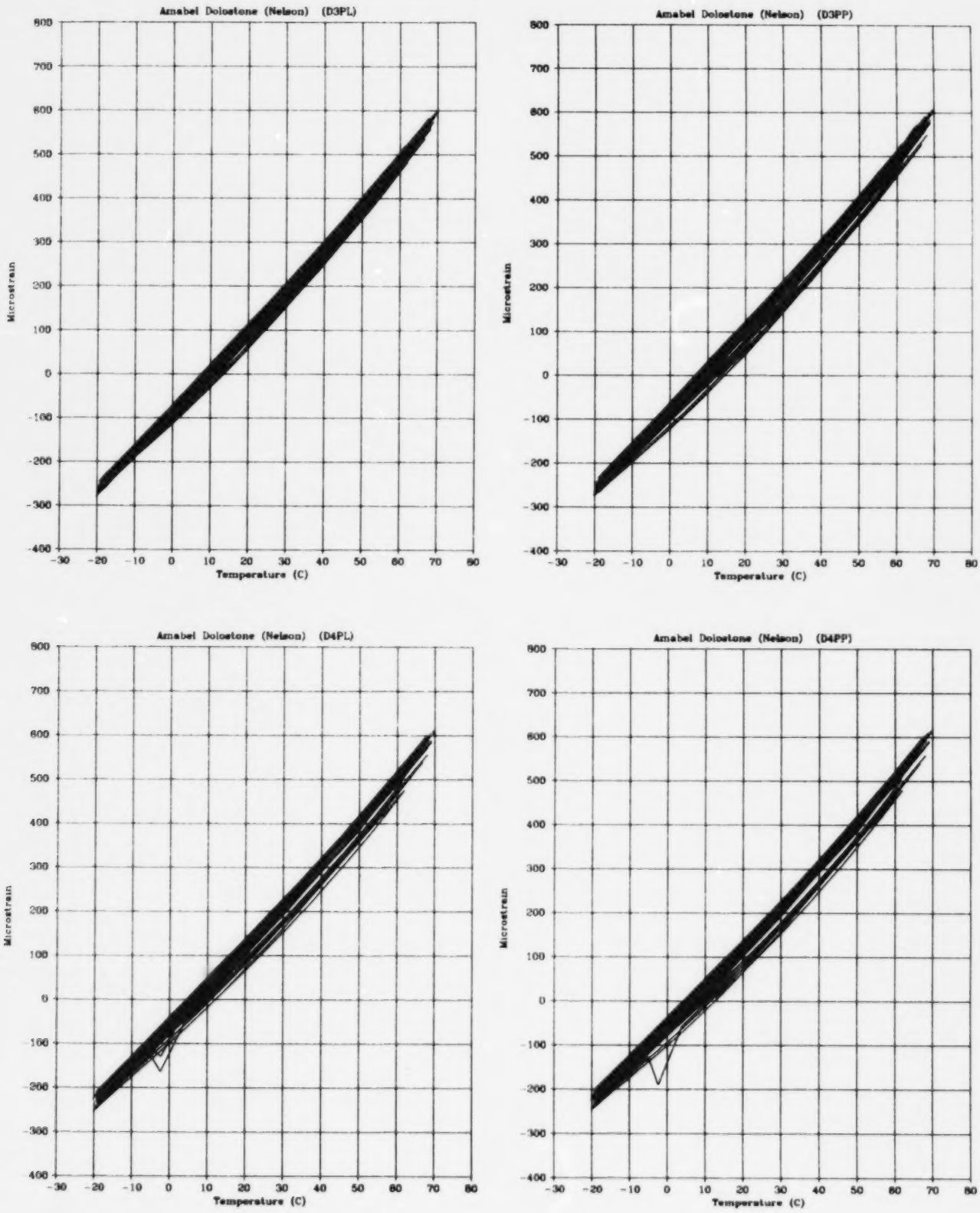

Figure 12b/ Strain versus Temperature, Sample D, Nelson Dolostone, Air-dried Specimens D3, D4

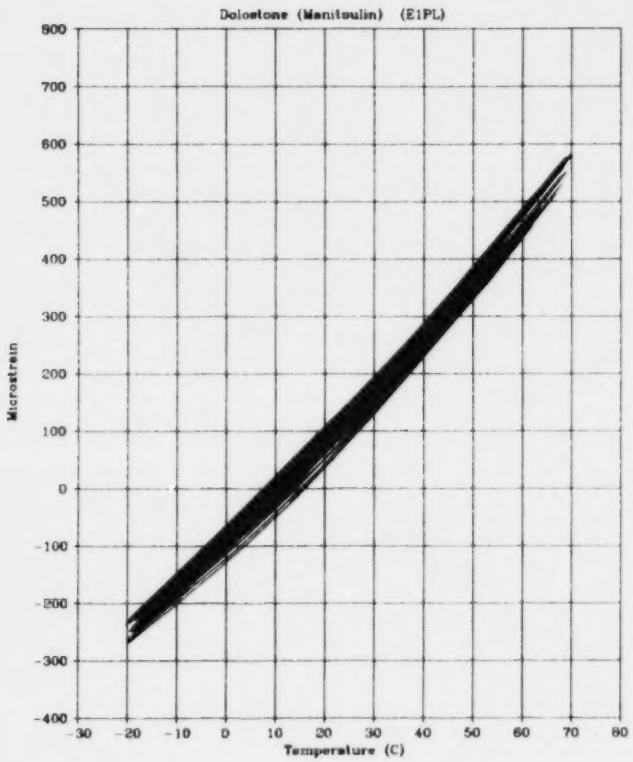

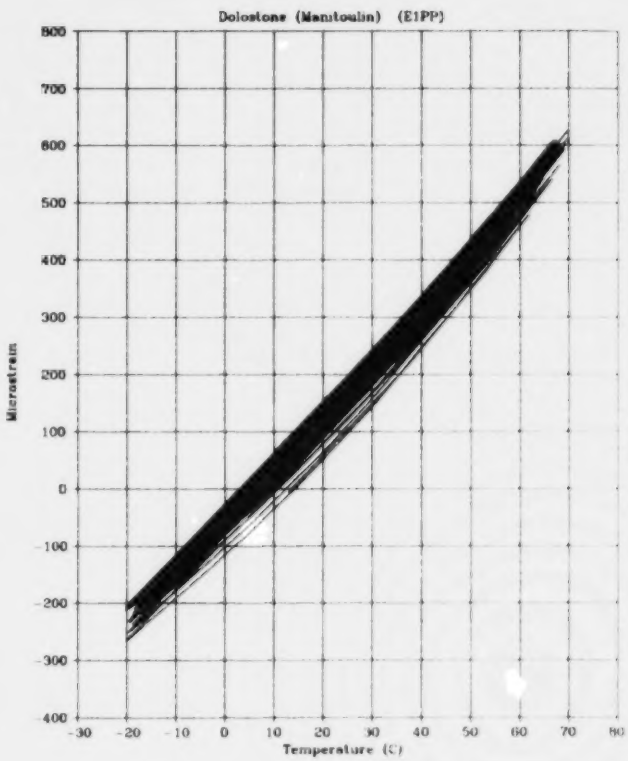

Figure 13a/ Strain versus Temperature, Sample E, Manitoulin Dolostone, Moist Specimen E1

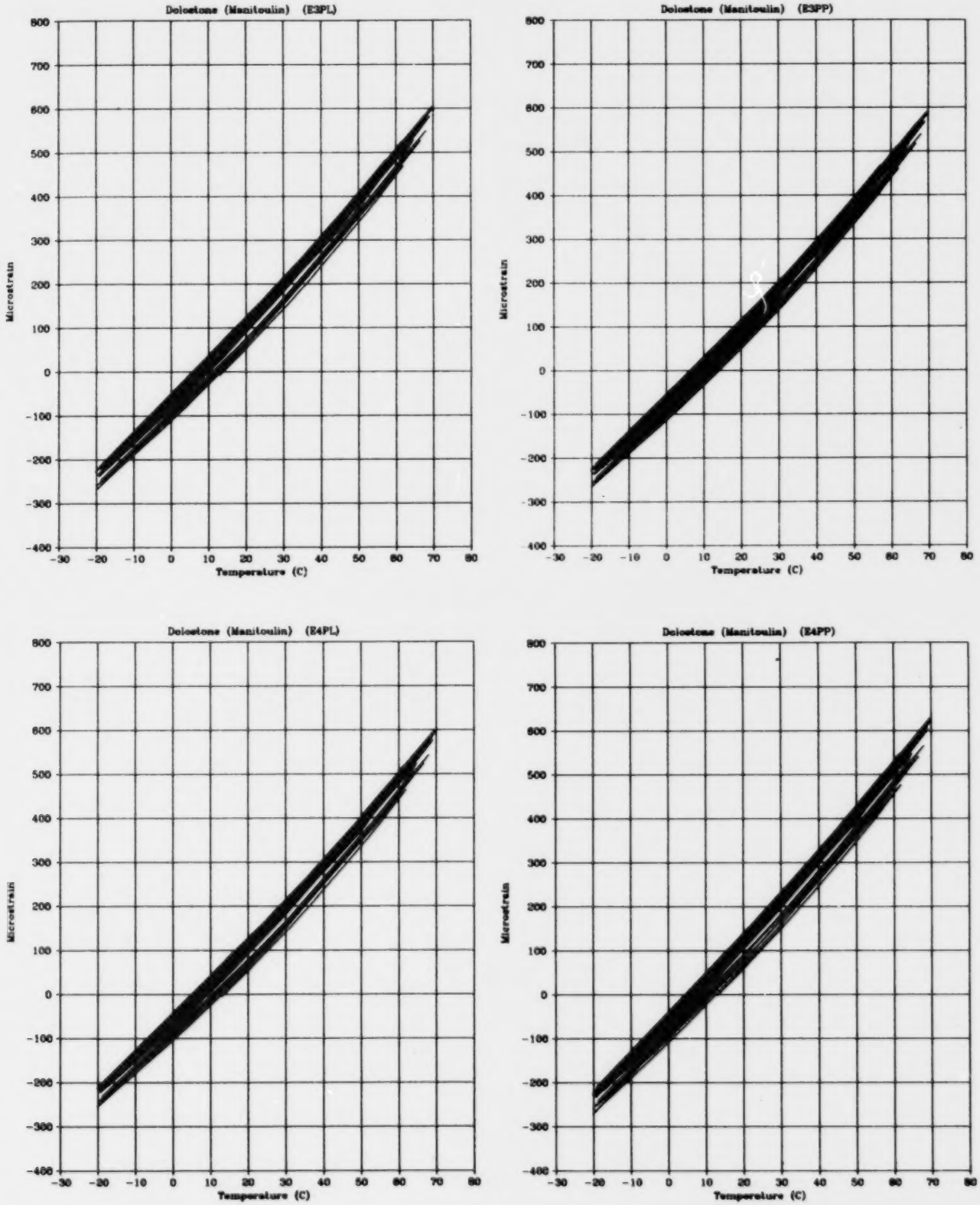

Figure 13b/ Strain versus Temperature, Sample E, Manitoulin Dolostone, Air-dried Specimens E3, E4

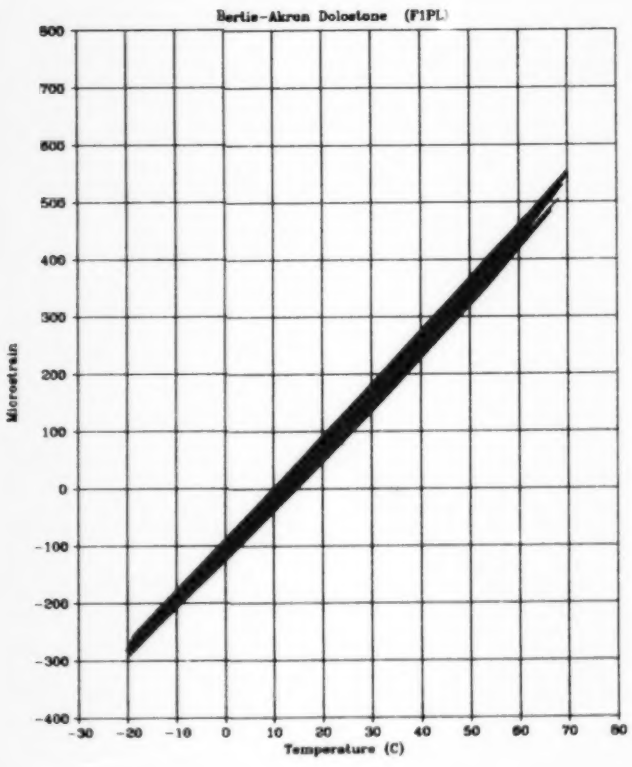

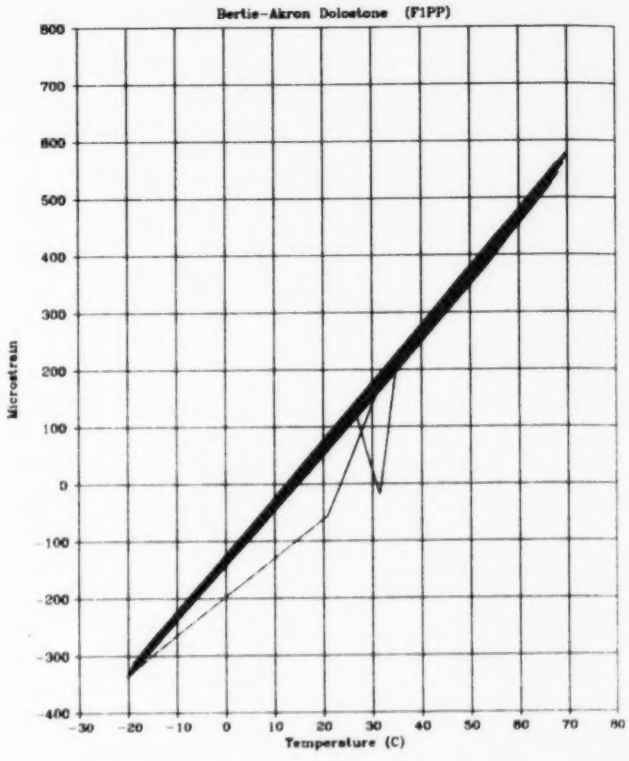

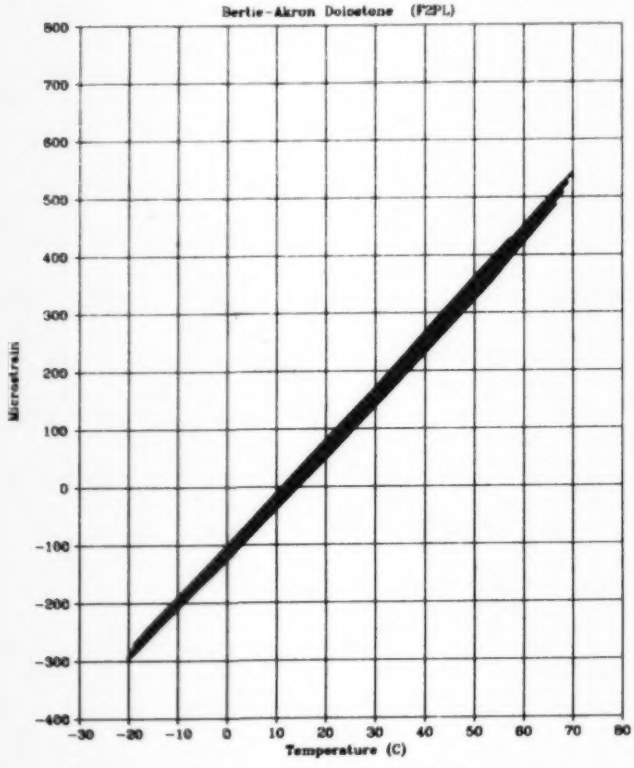

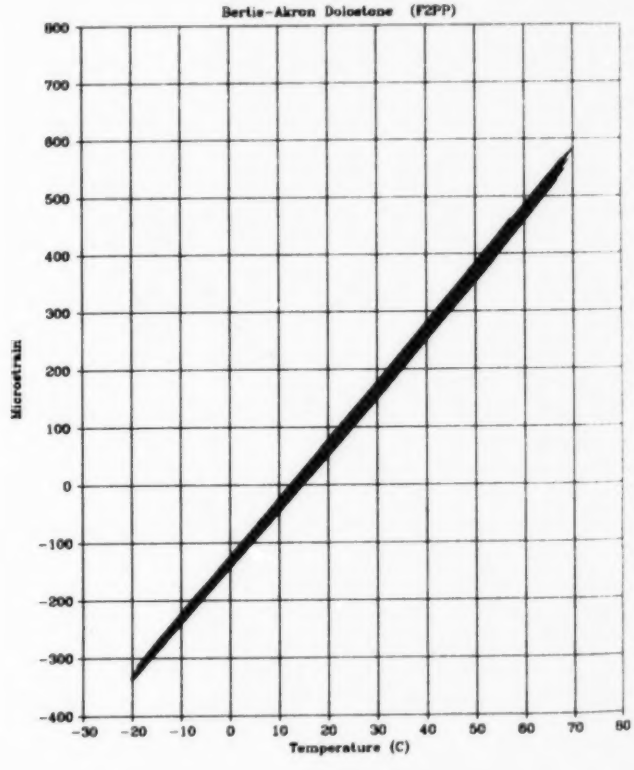

Figure 14a/ Strain versus Temperature, Sample F, Bertie-Akron Dolostone, Moist Specimens F1, F2

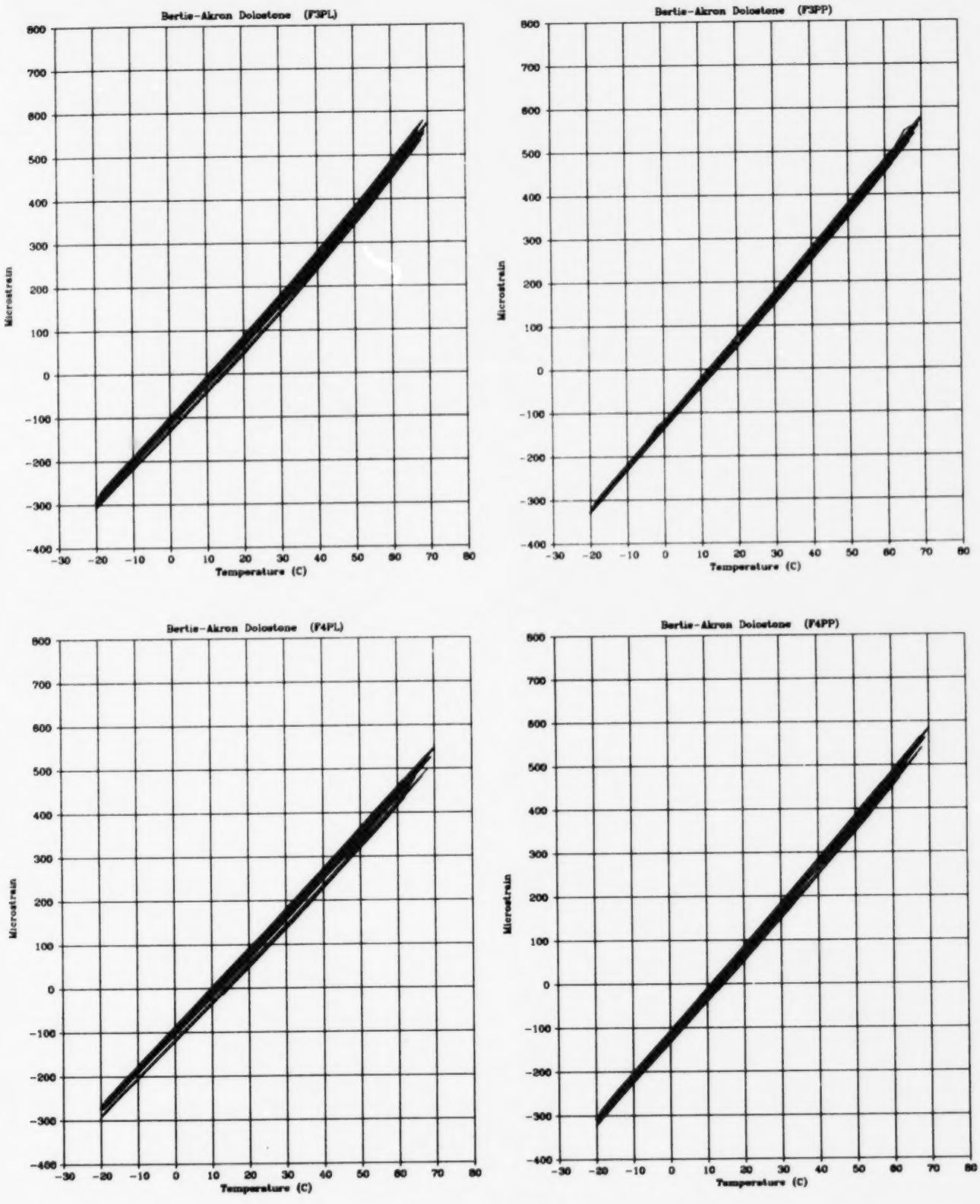

Figure 14b/ Strain versus Temperature, Sample F, Bertie-Akron Dolostone, Air-dried Specimens F3, F4

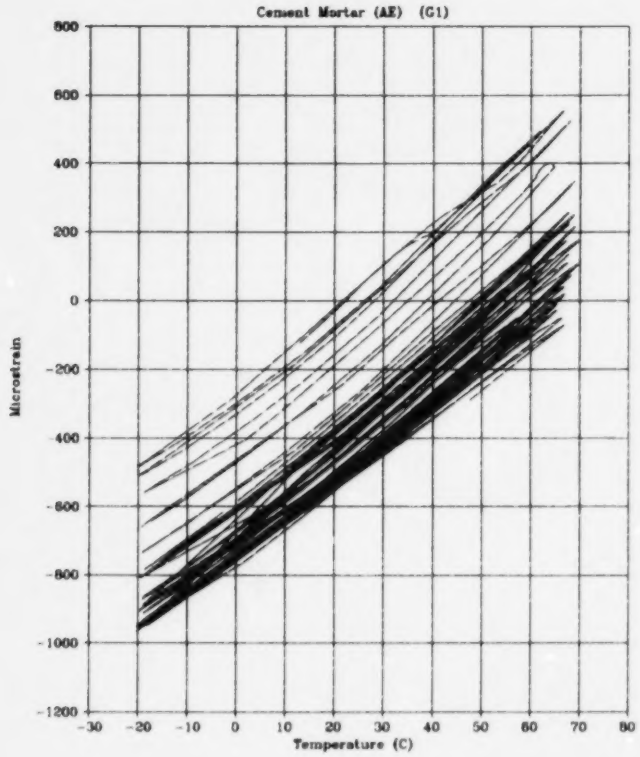

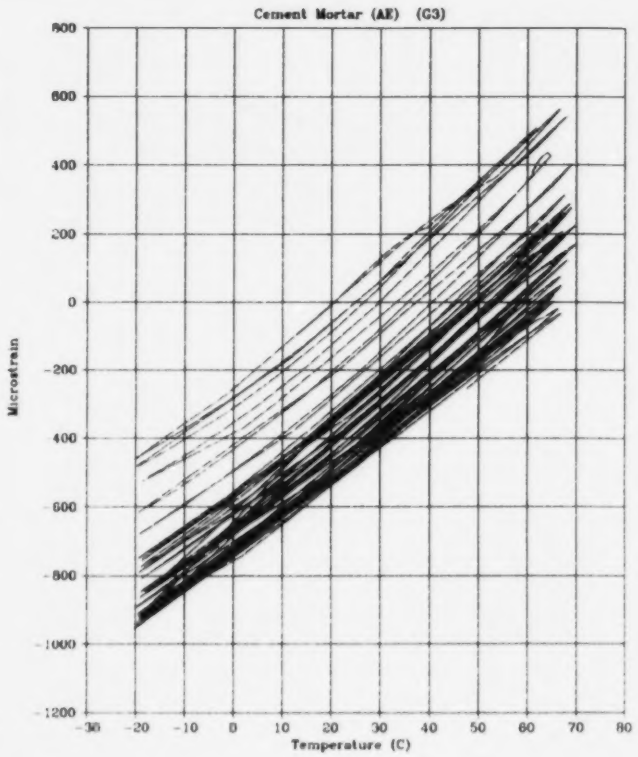

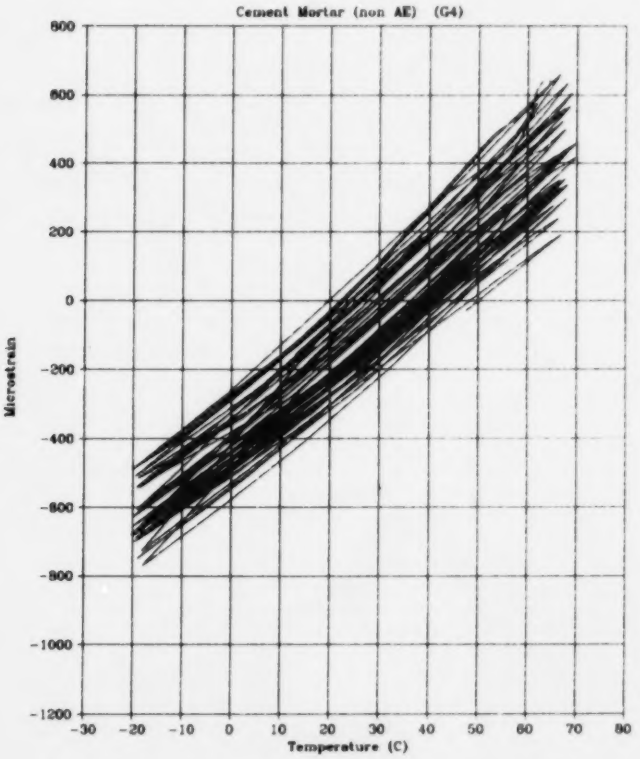

Figure 15/ Strain versus Temperature, Sample G, Cement Mortar,
Air-entrained Specimens G1, G3
Non Air-entrained Specimen G4

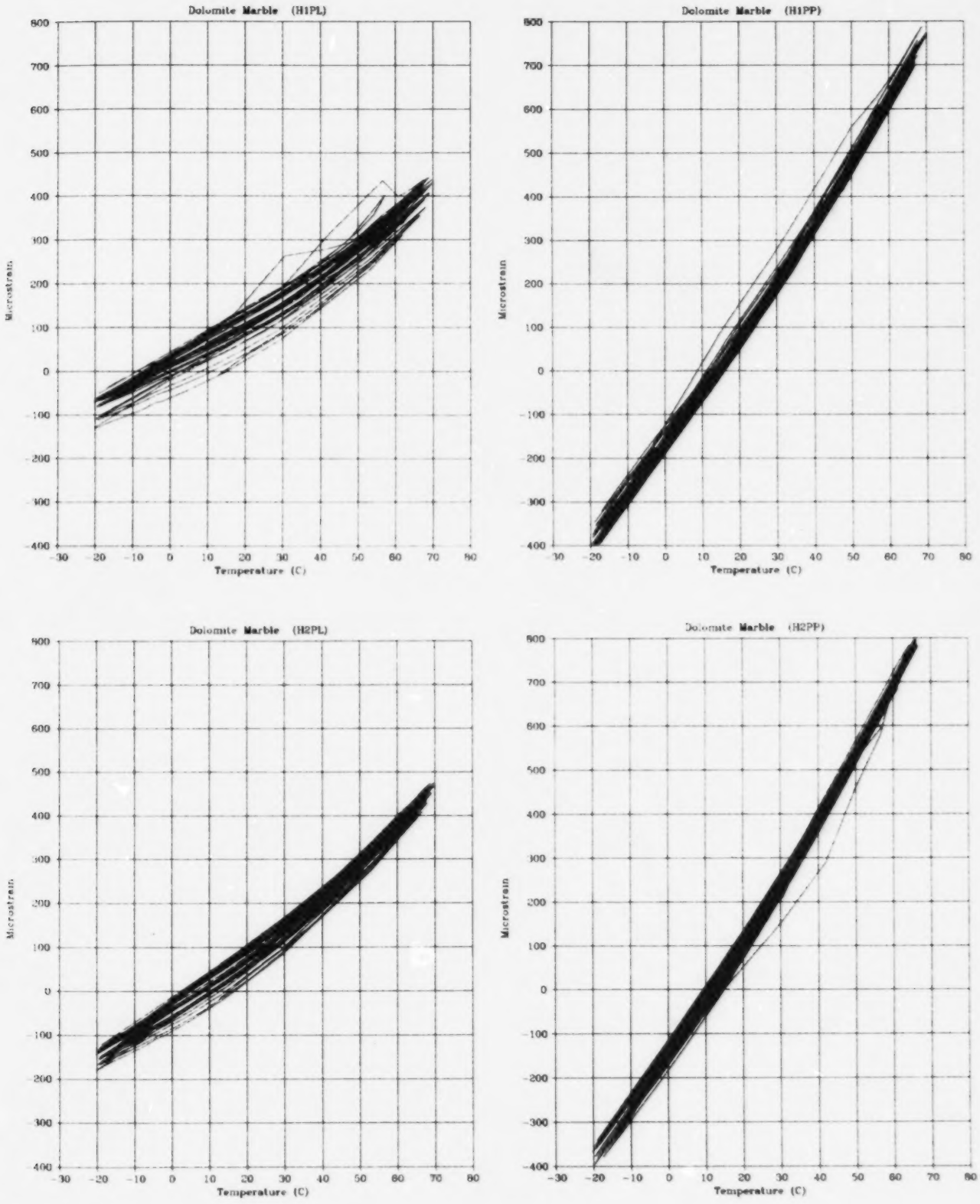

Figure 16a/ Strain versus Temperature, Sample H, Dolomite Marble, Moist Specimens H1, H2

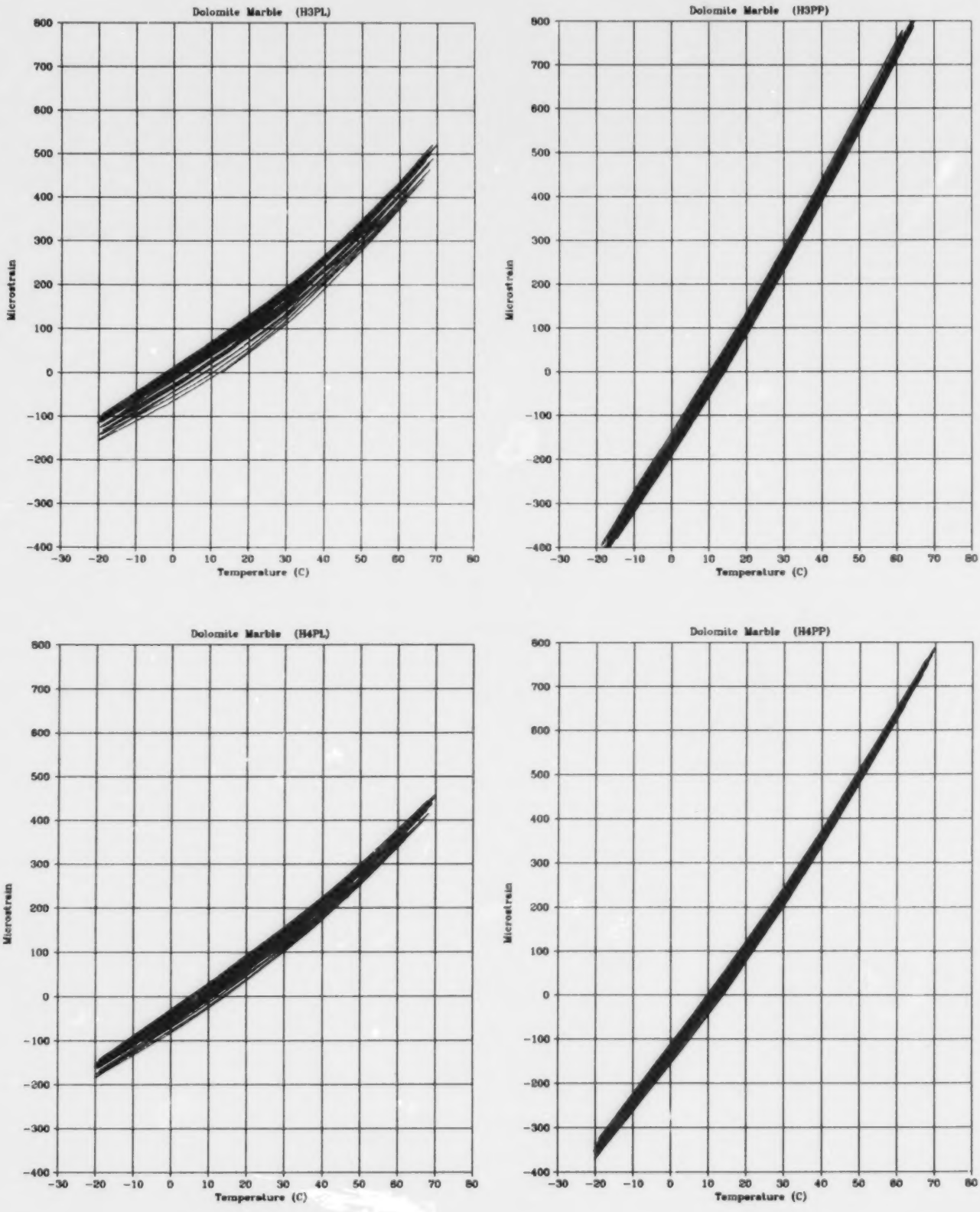

Figure 16b/ Strain versus Temperature, Sample H, Dolomite Marble, Air-dried Specimens H3, H4

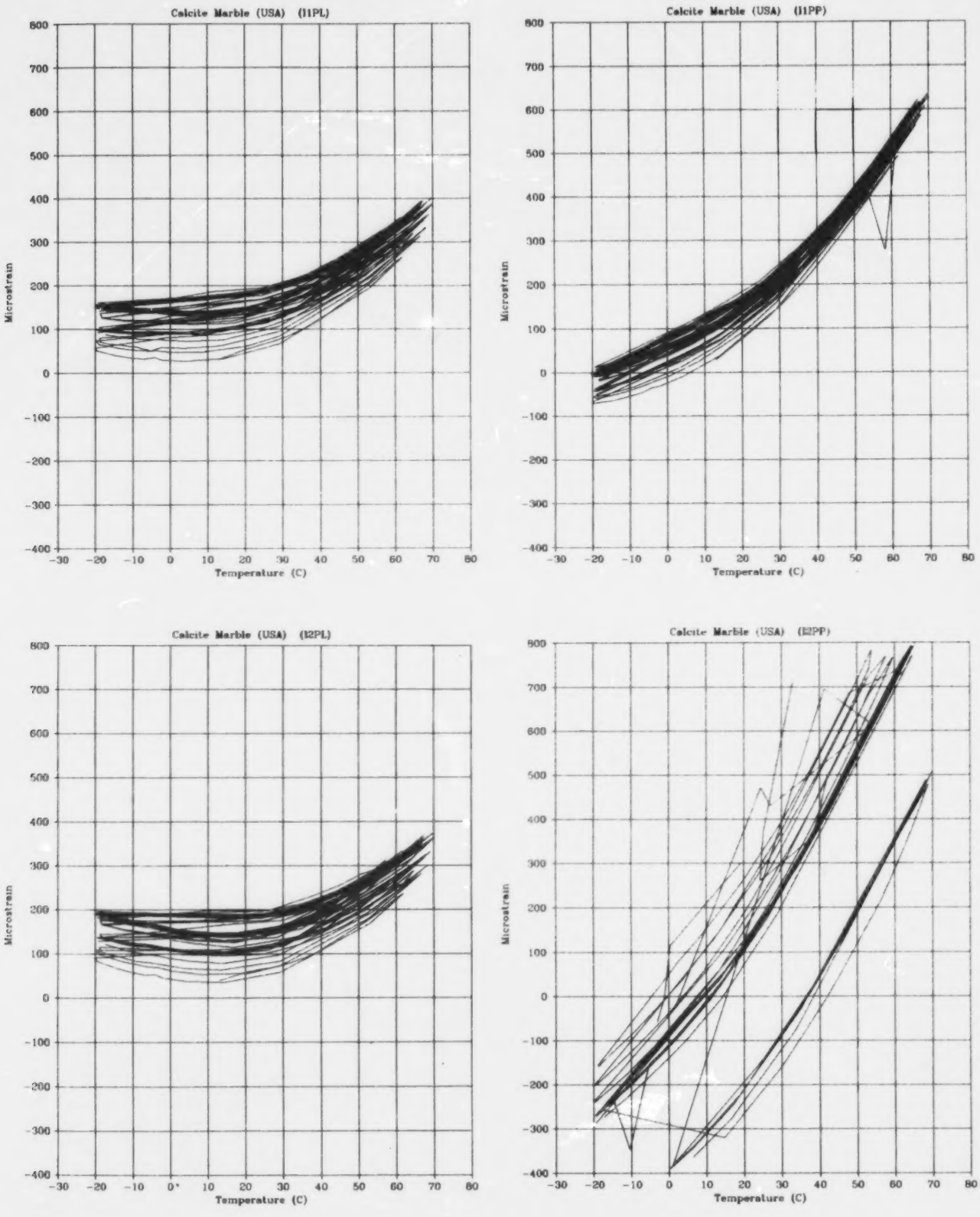

Figure 17a/ Strain versus Temperature, Sample I, Calcite Marble, Moist Specimens I1, I2

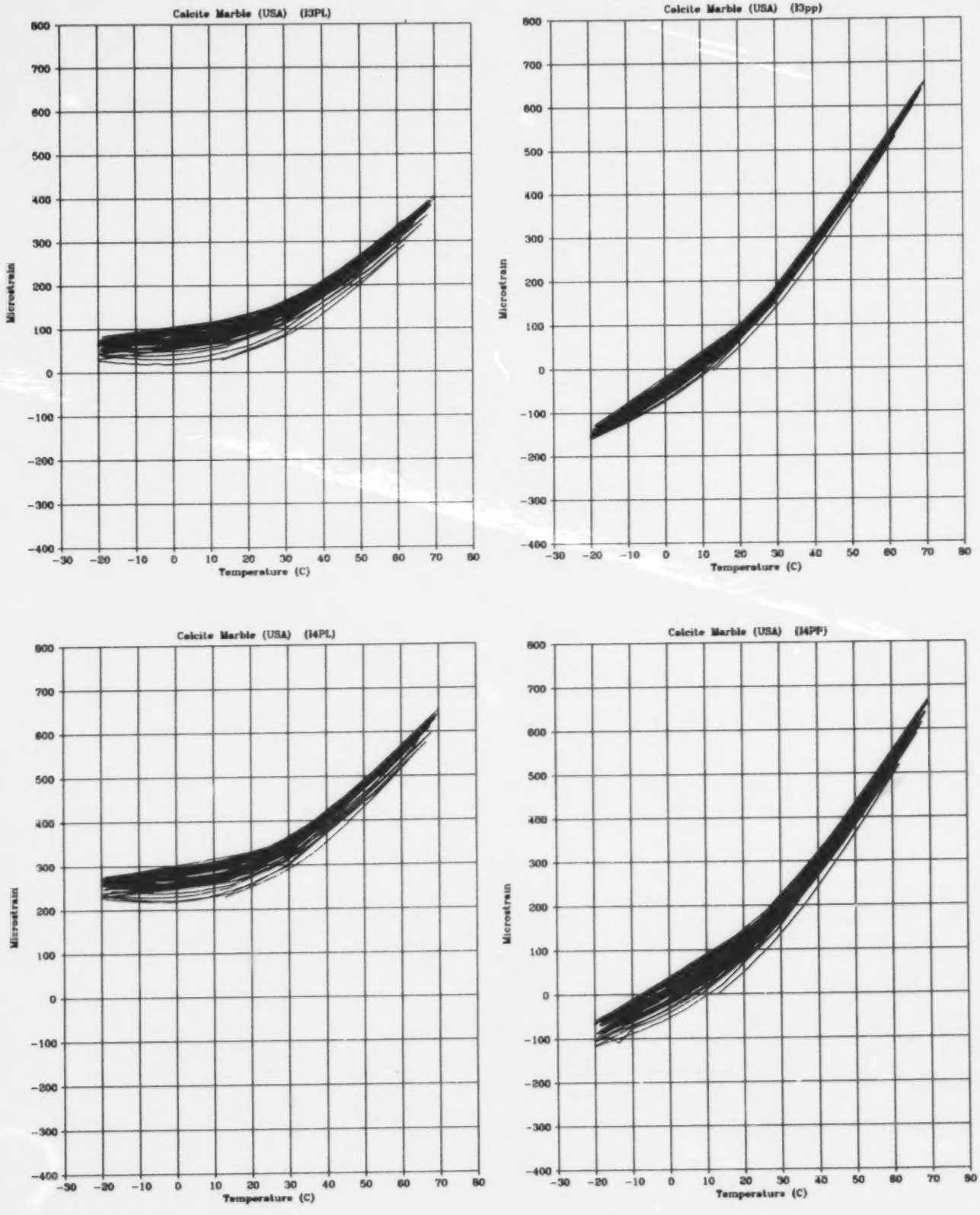

Figure 17b/ Strain versus Temperature, Sample I, Calcite Marble (USA), Air-dried Specimens I3, I4

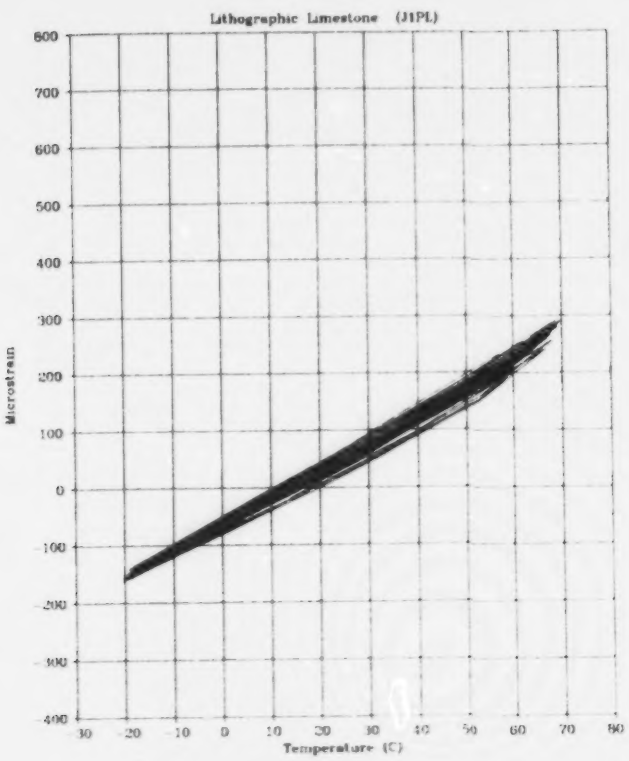

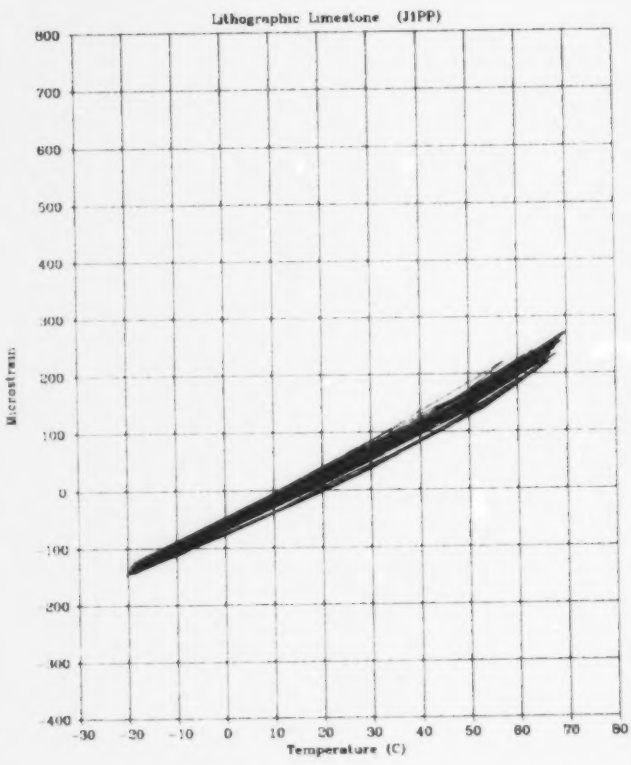

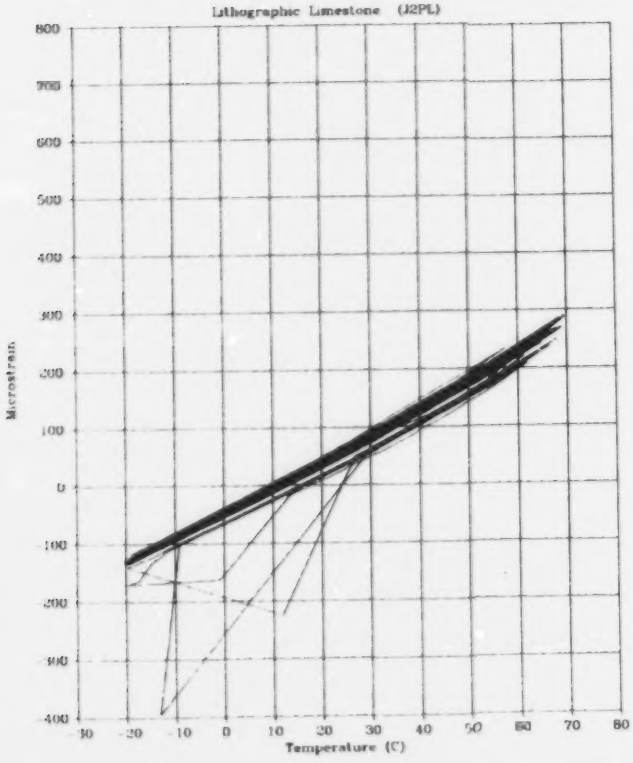

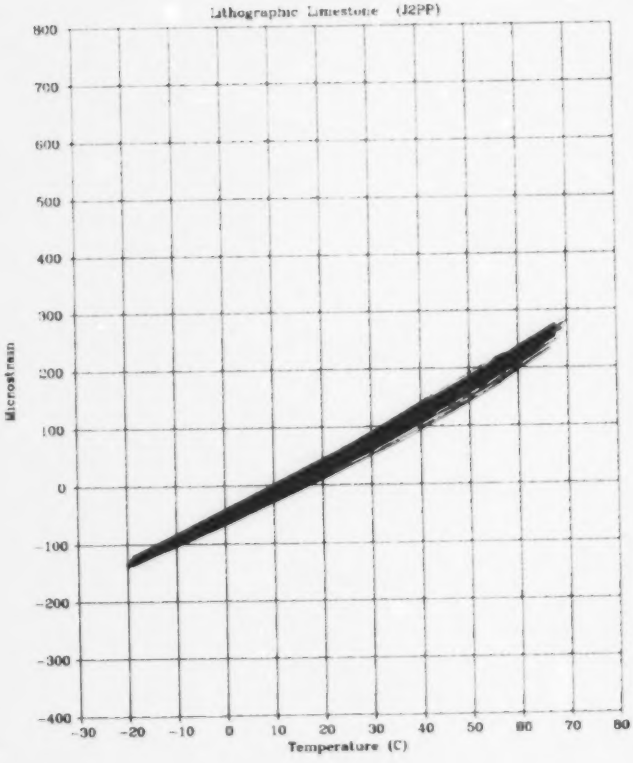

Figure 18a/ Strain versus Temperature, Sample J, Lithographic Limestone, Moist Specimens J1, J2

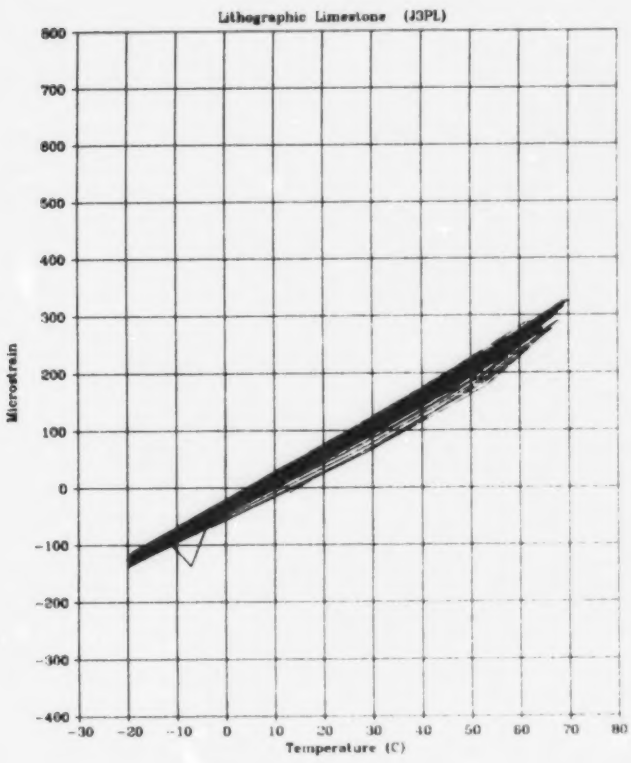

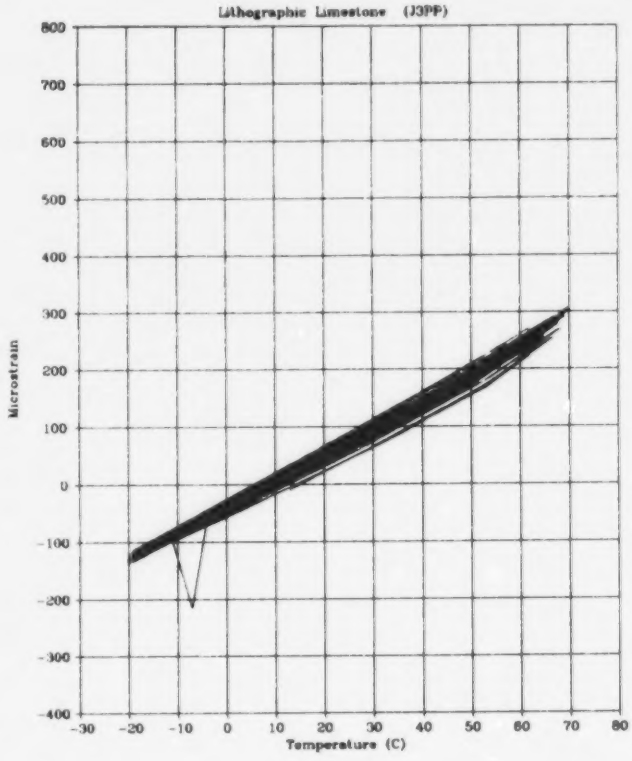

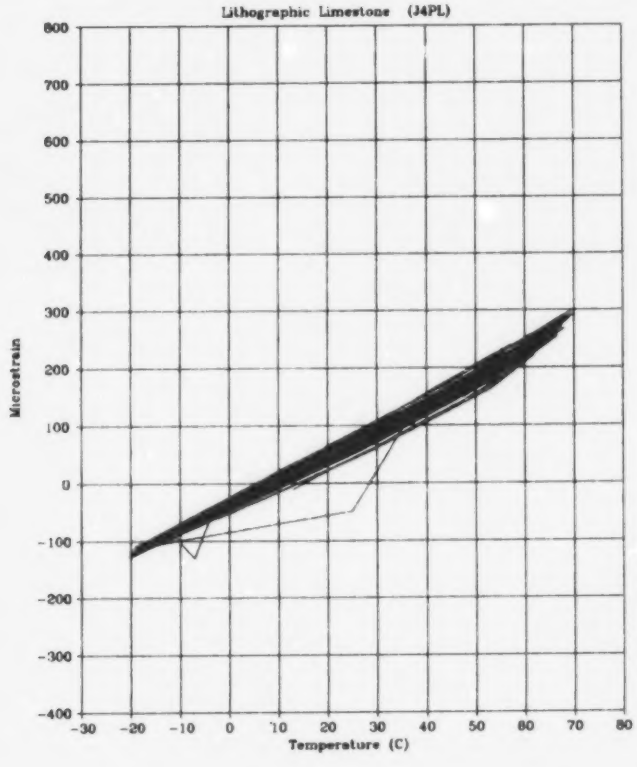

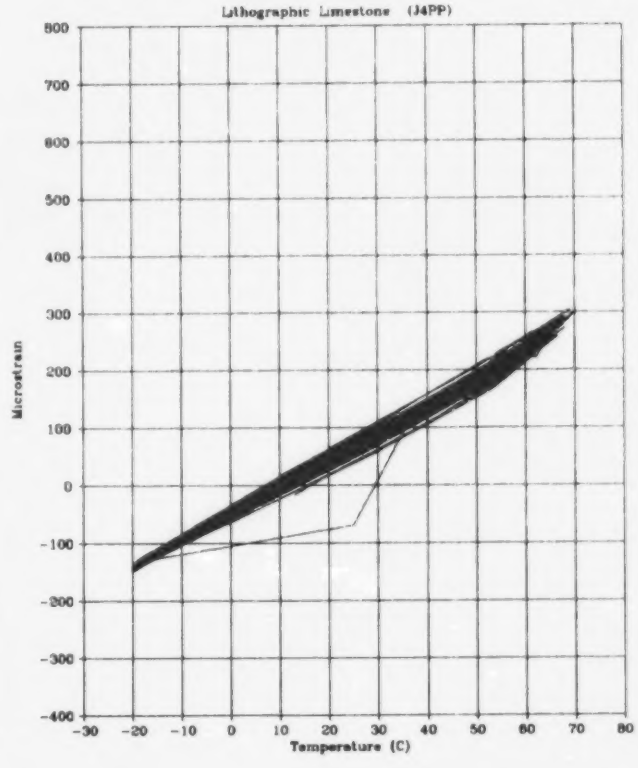

Figure 18b Strain versus Temperature, Sample J, Lithographic Limestone, Air-dried Specimens J3, J4

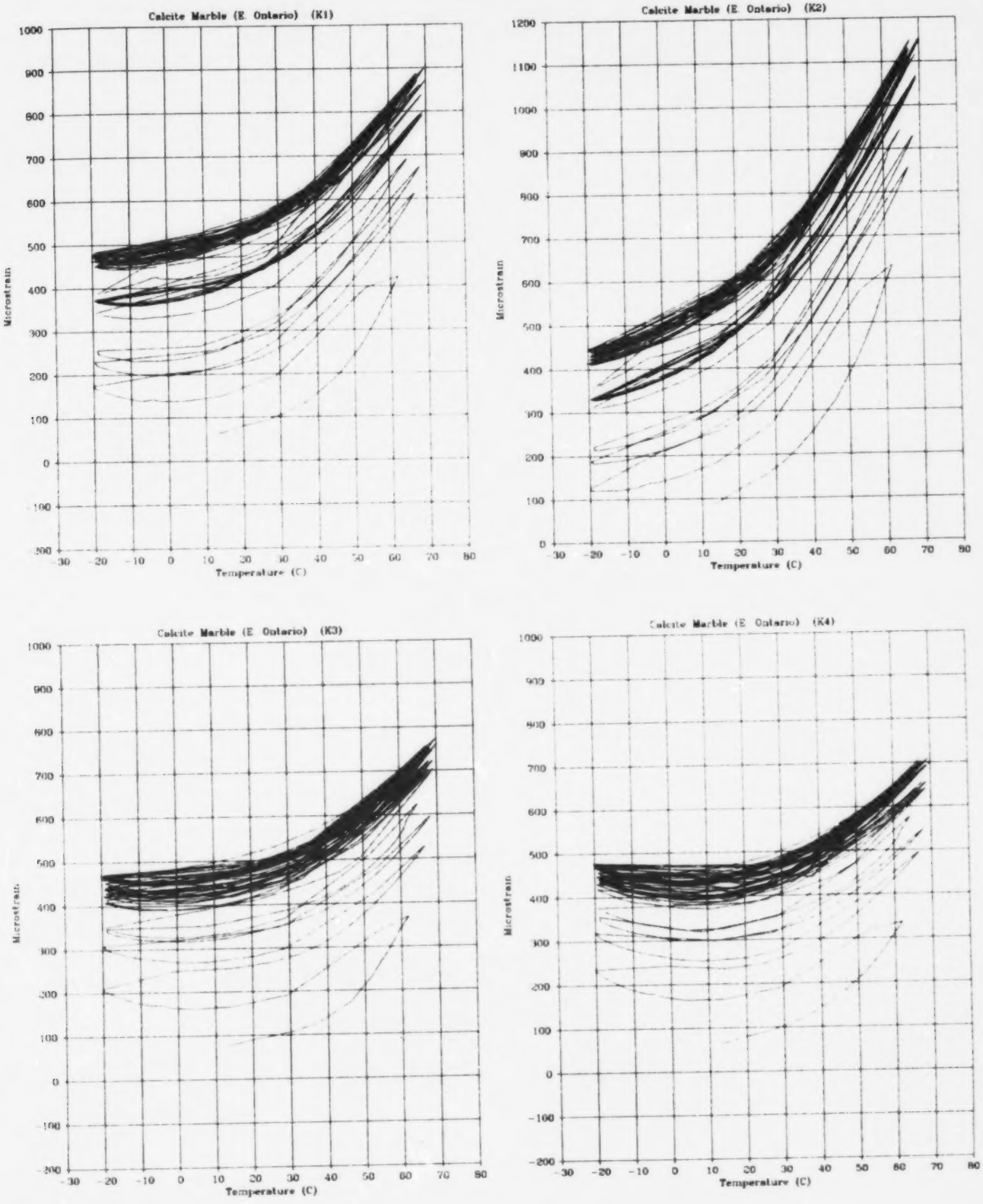

Figure 19/ Strain versus Temperature, Sample K, Calcite Marble (E. Ont.), Moist Specimens K1, K2; Air-dried Specimens K3, K4

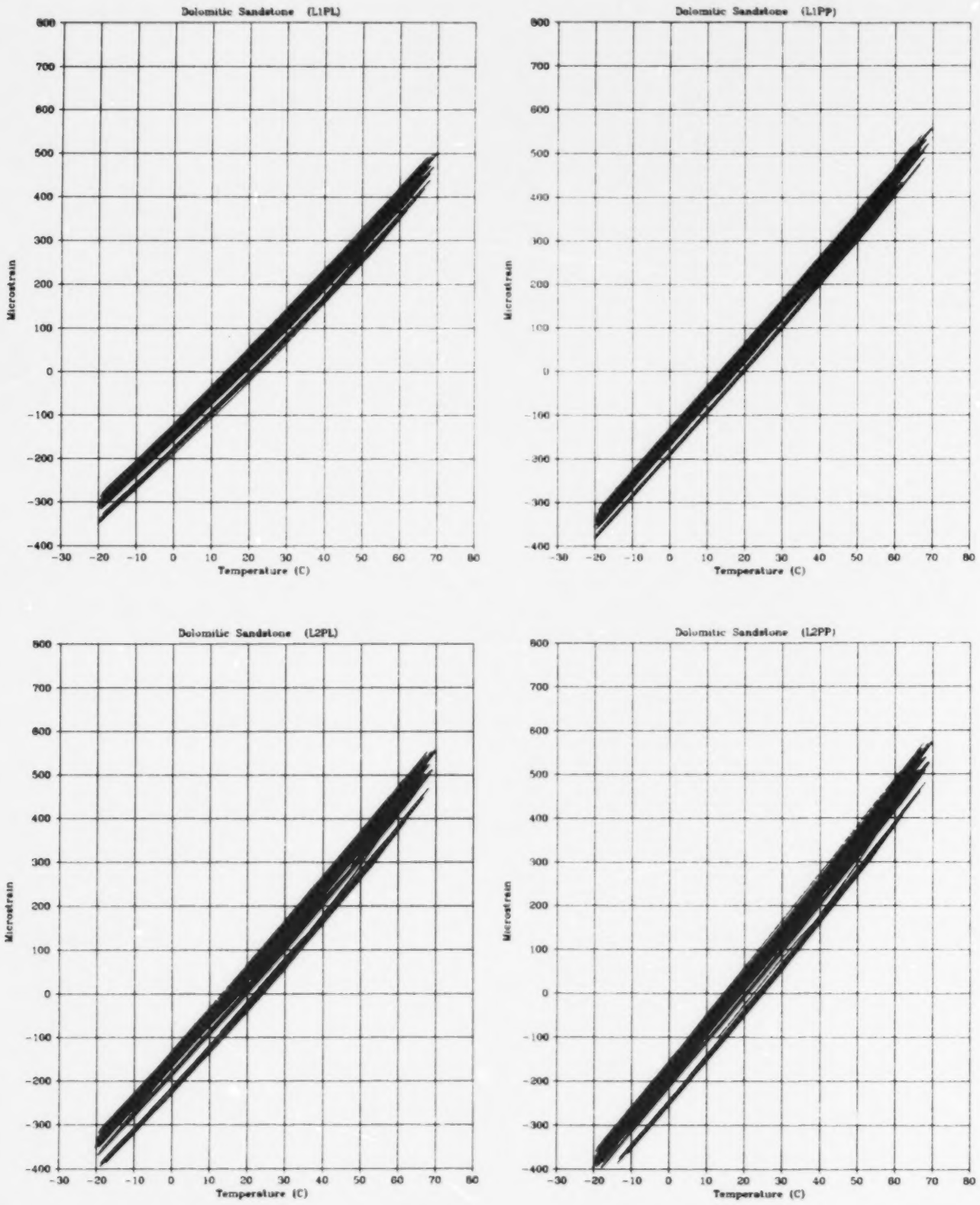

Figure 20a/ Strain versus Temperature, Sample L, Dolomitic Sandstone, Moist Specimens L1, L2

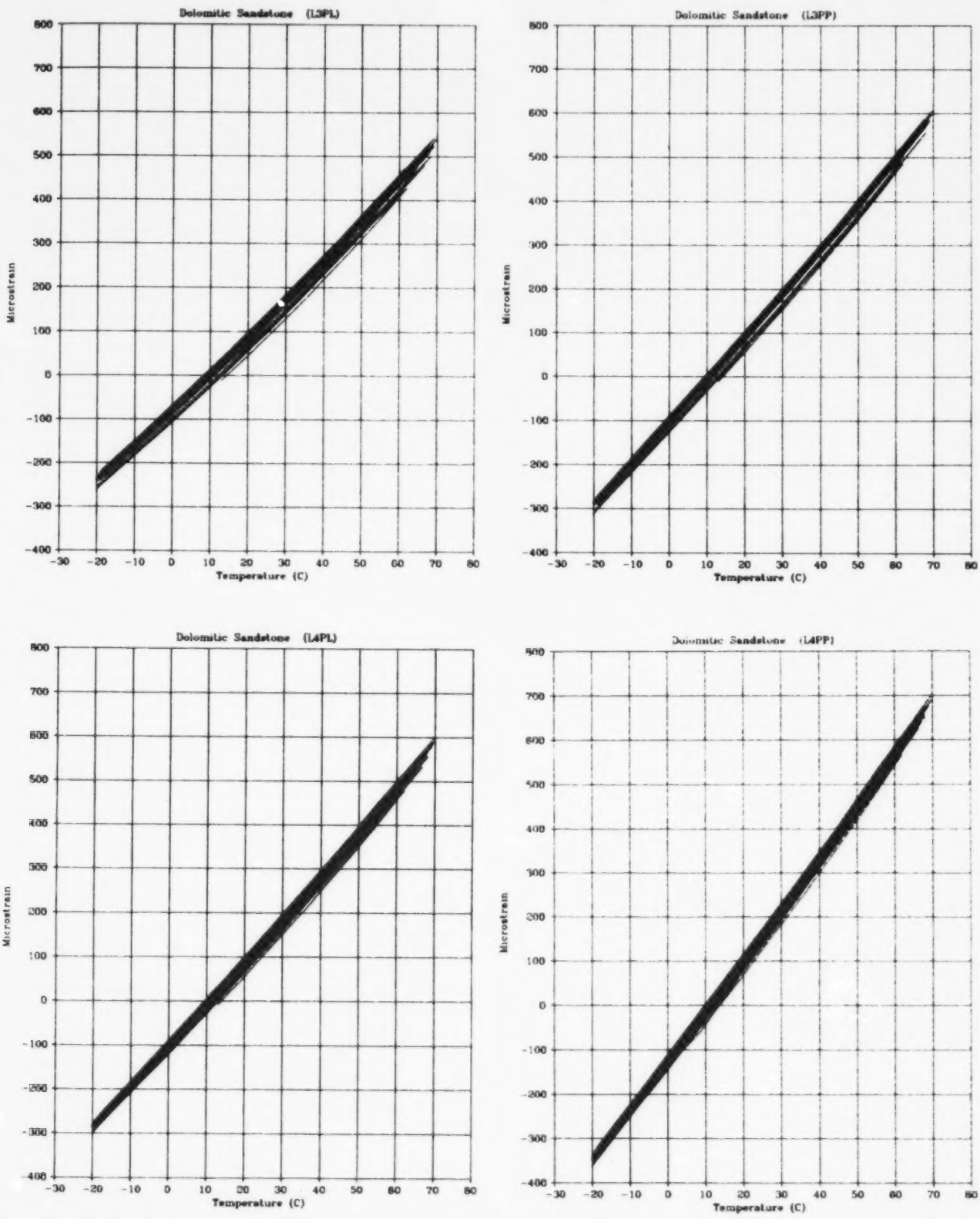

Figure 20b/ Strain versus Temperature, Sample L, Dolomitic Sandstone, Air-dried Specimens L3, L4

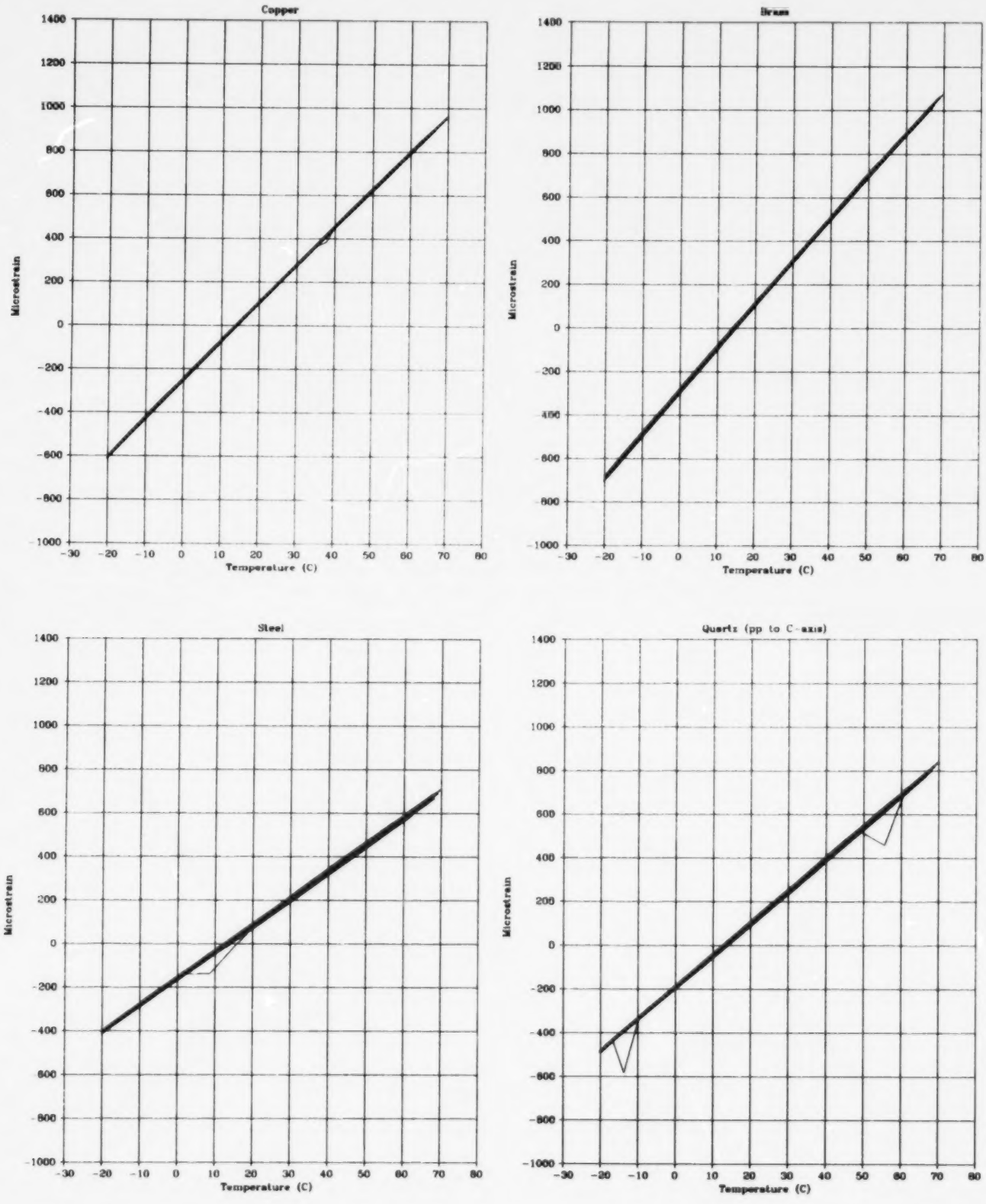

Figure 21/ Strain versus Temperature, Standard Materials, Copper, Brass, Steel, Quartz

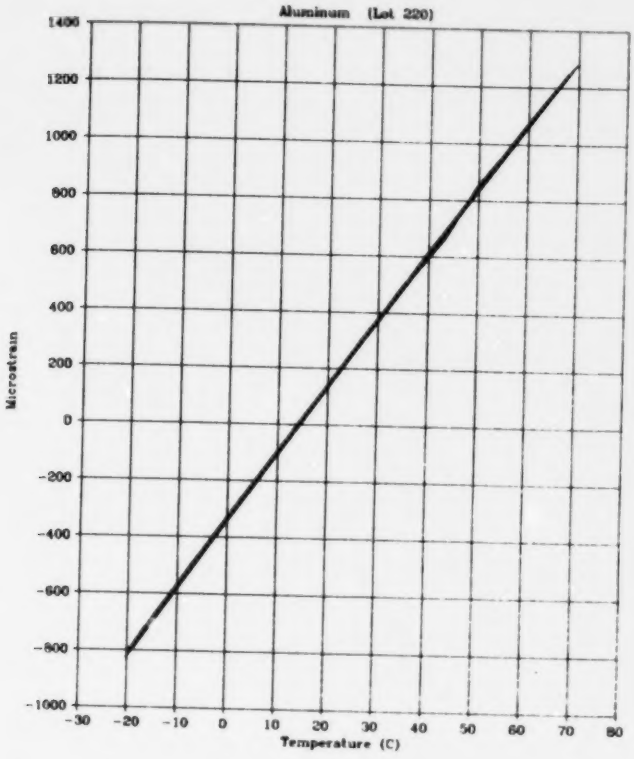

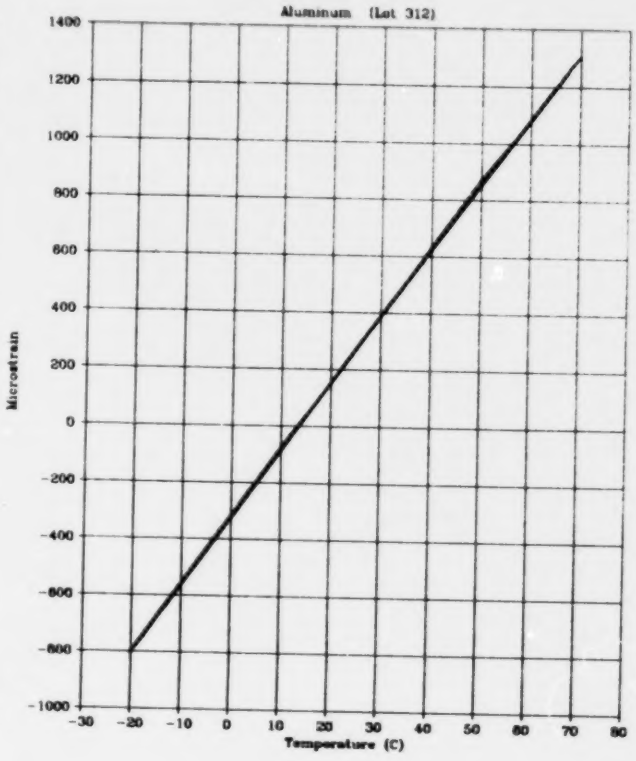

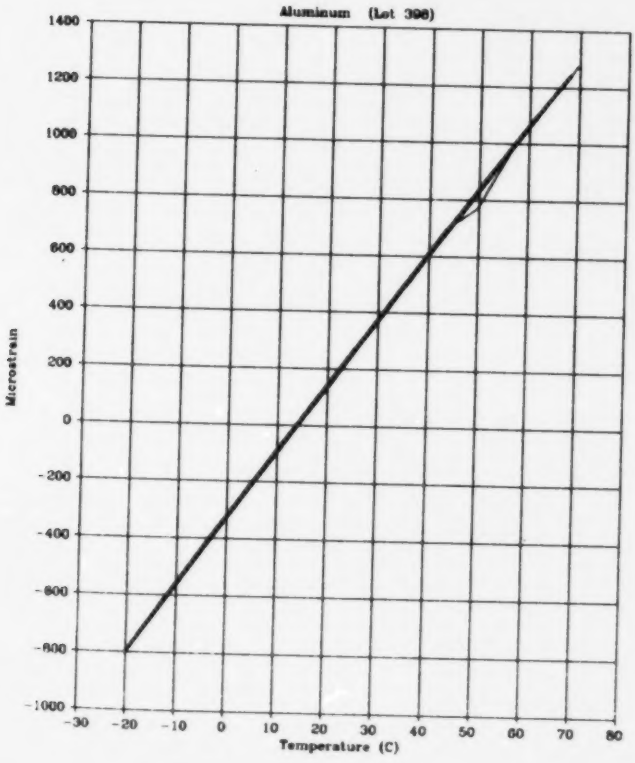

Figure 21/ Strain versus Temperature, Standard Material, Aluminum

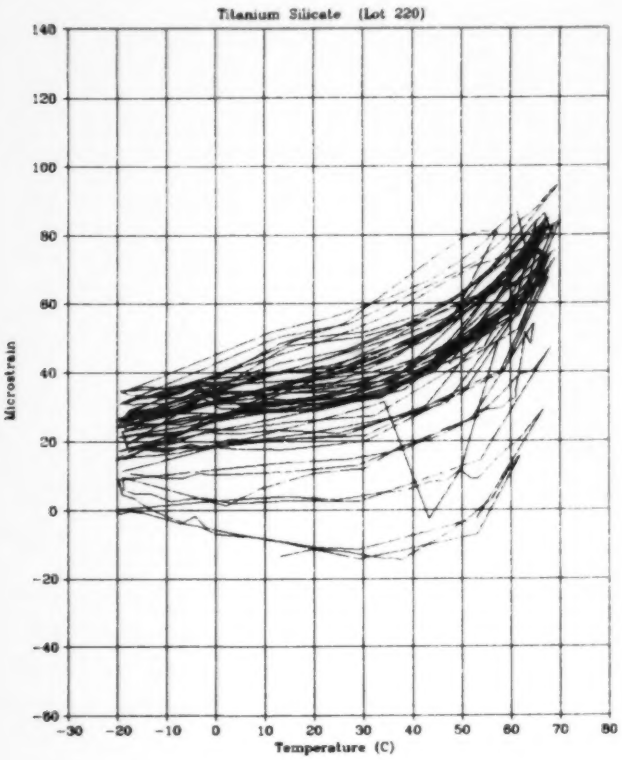

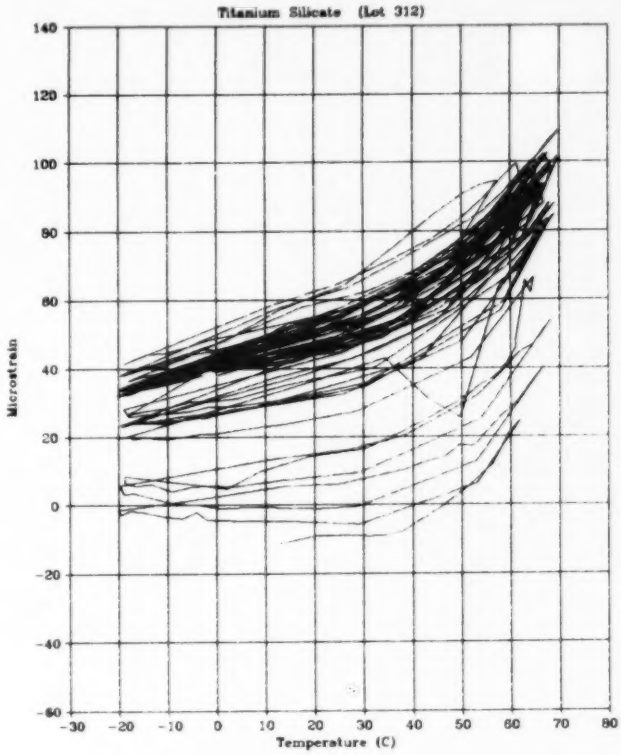

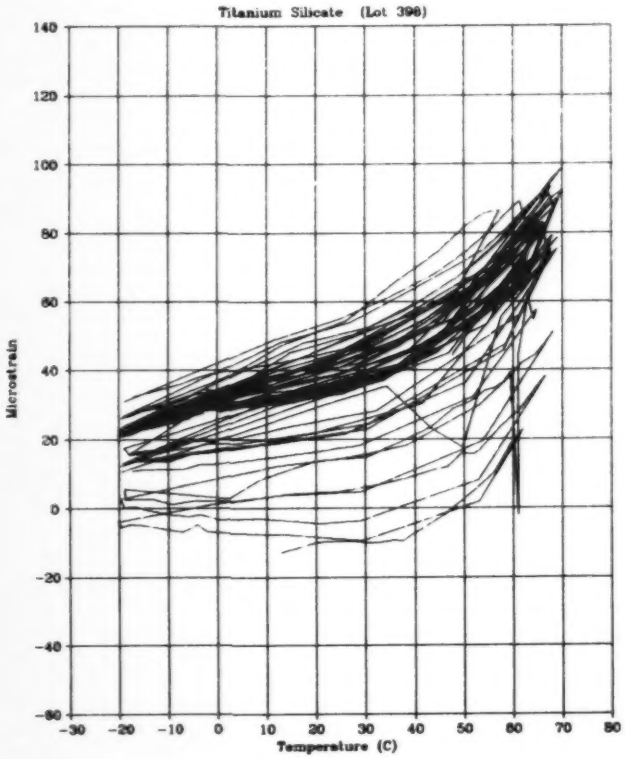

Figure 23/ Strain versus Temperature, Titanium Silicate

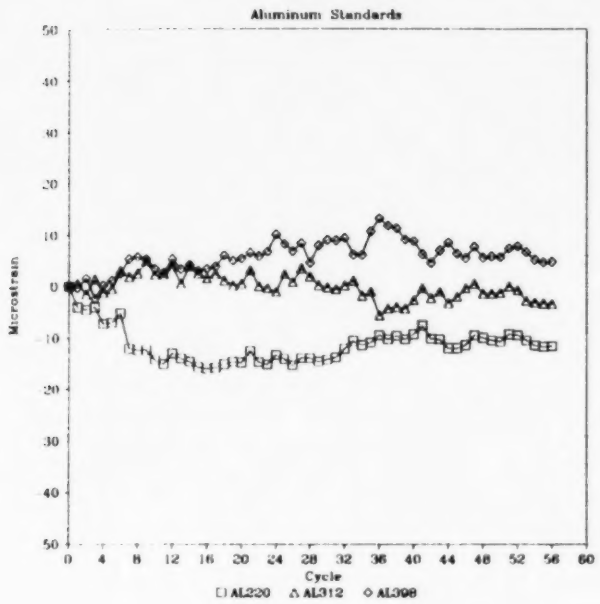

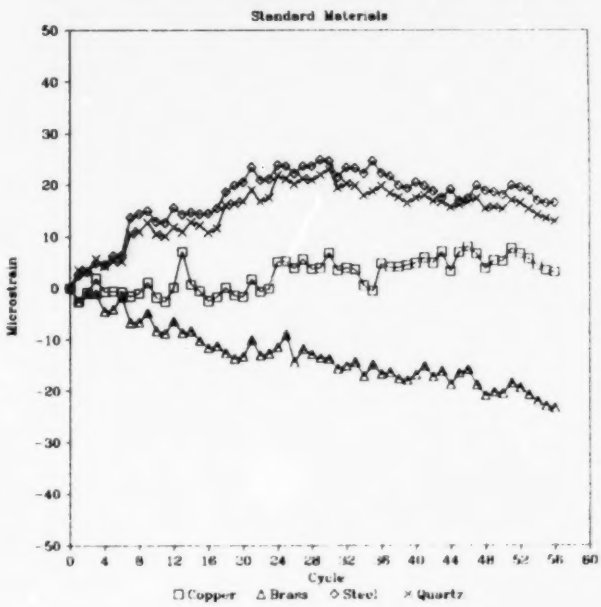

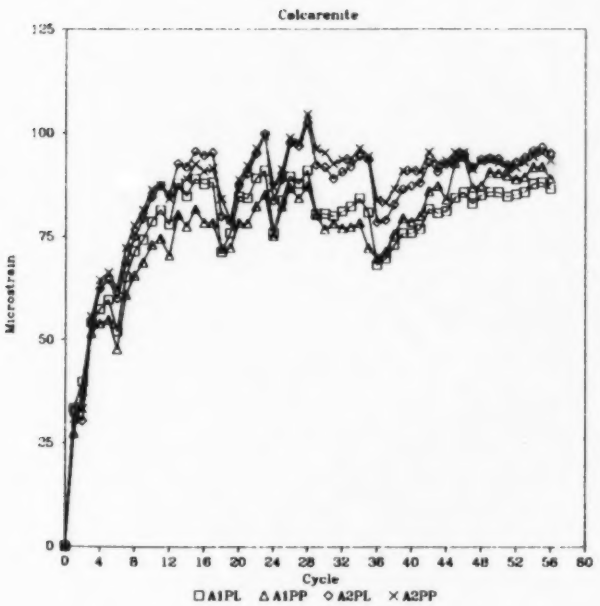

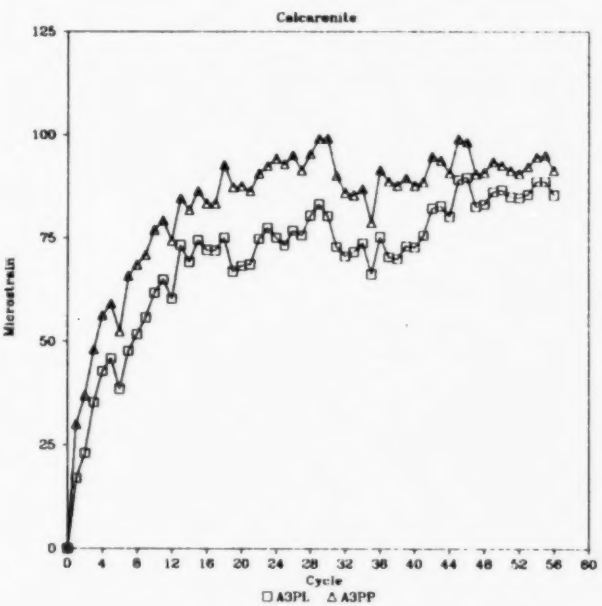

Figure 24/ Residual Strain at 20°C versus Cycle
Standard Materials and Calcarenite (A)

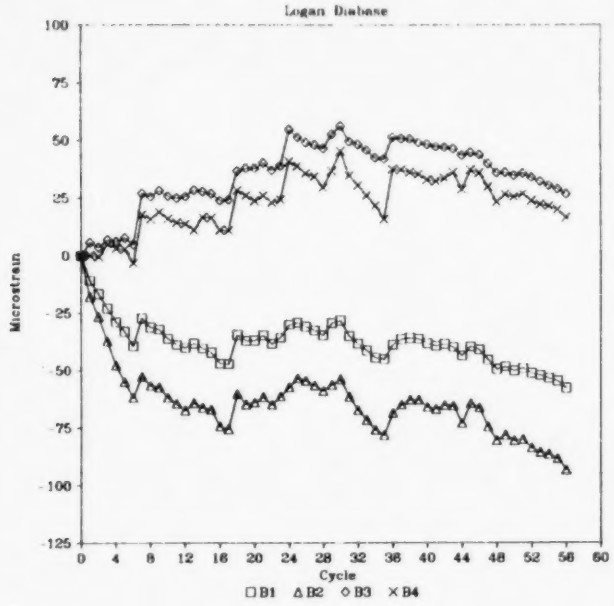

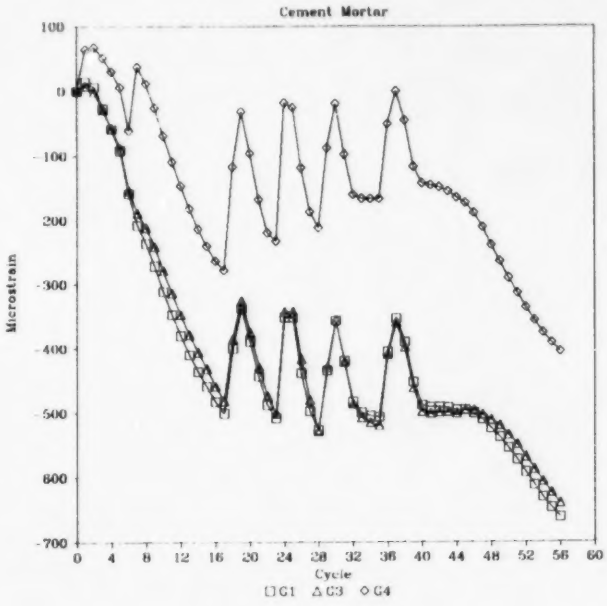

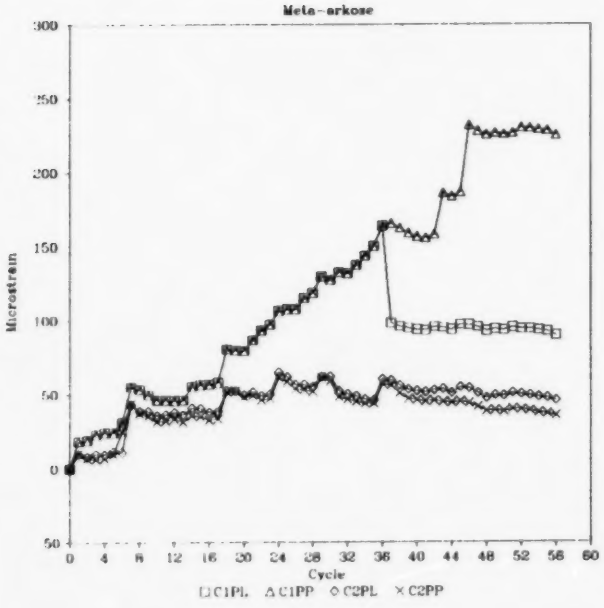

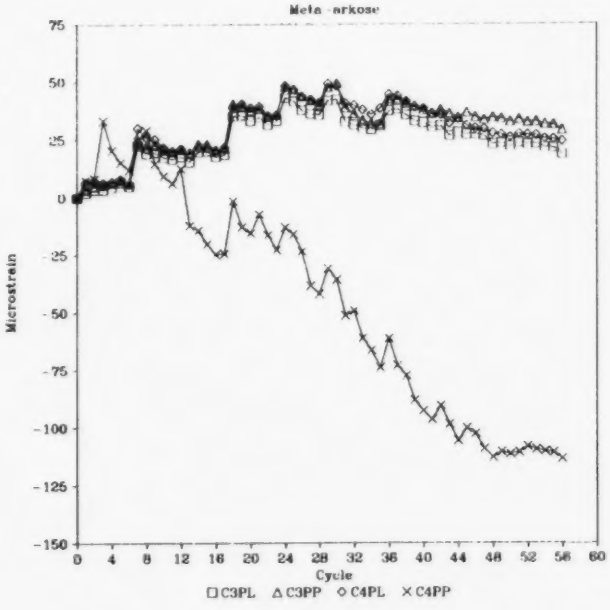

Figure 25/ Residual Strain at 20°C versus Cycle
Diabase (B), Cement Mortar (G) and Meta-arkose (C)

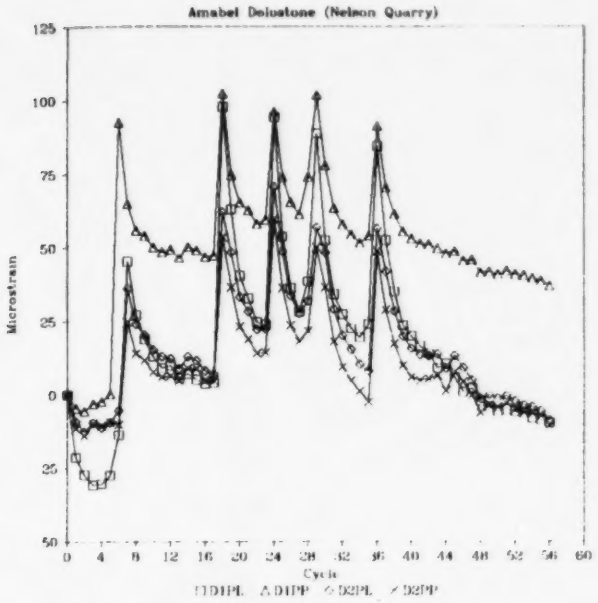

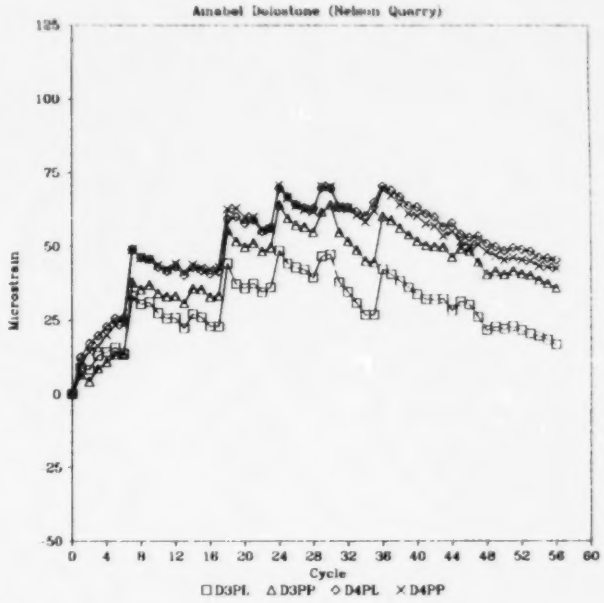

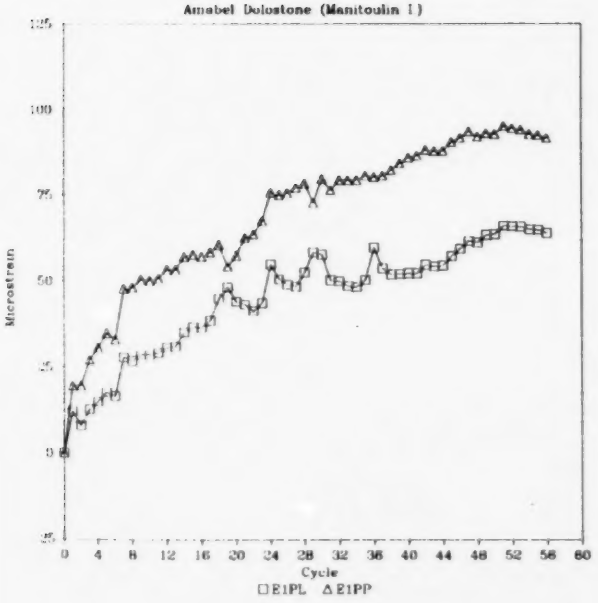

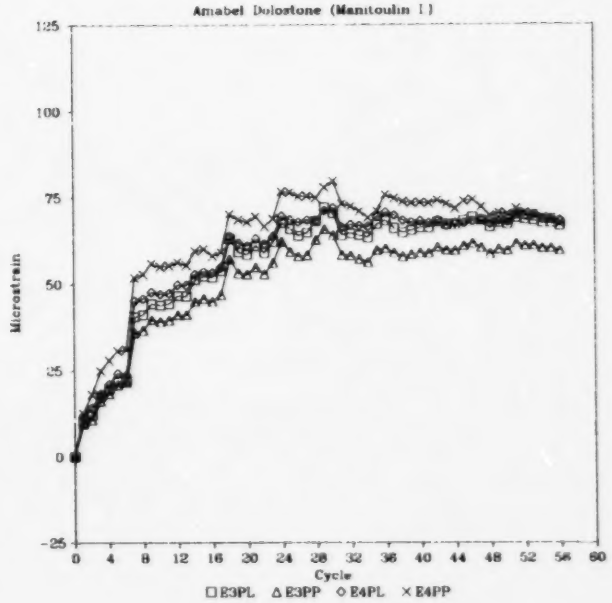

Figure 26/ Residual Strain at 20°C versus Cycle
Nelson Dolostone (D) and Manitoulin Dolostone (E)

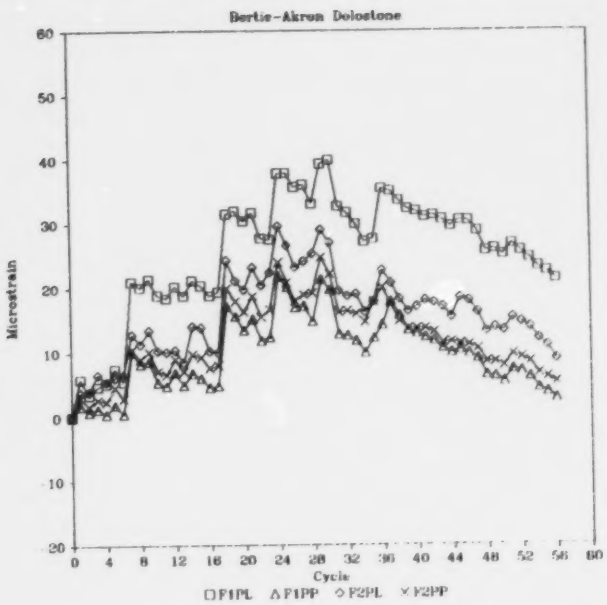

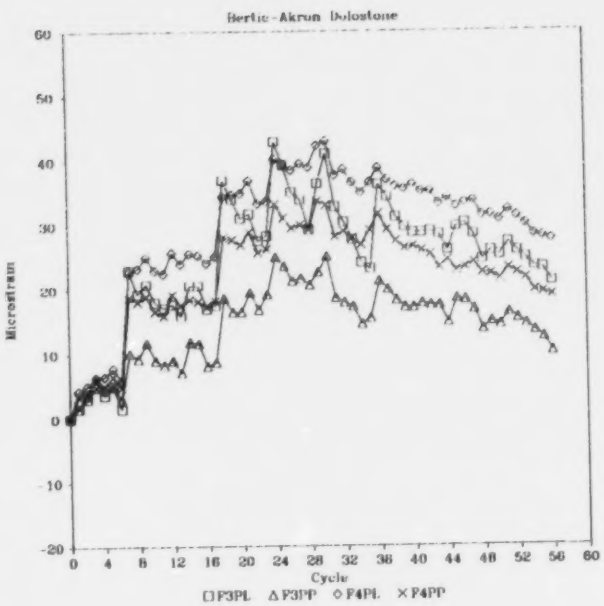

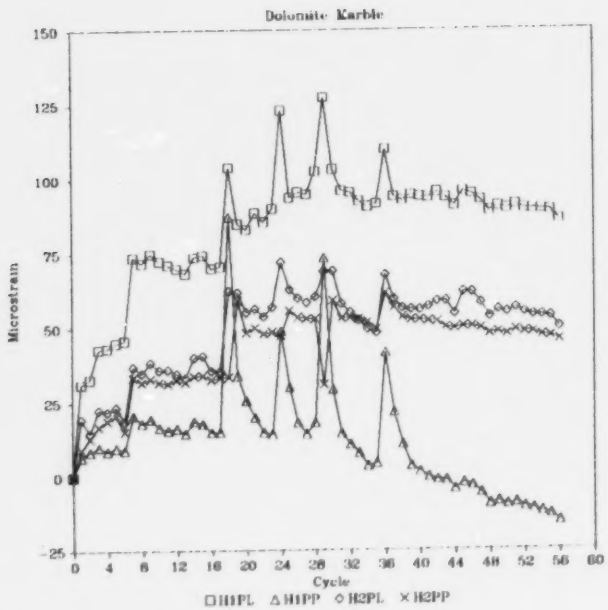

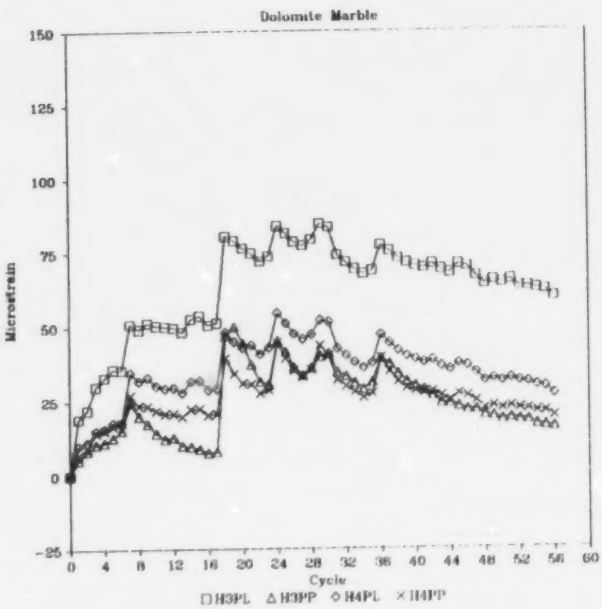

Figure 27/ Residual Strain at 20°C versus Cycle
Bertie-Akron Dolostone (F) and Dolomite Marble (H)

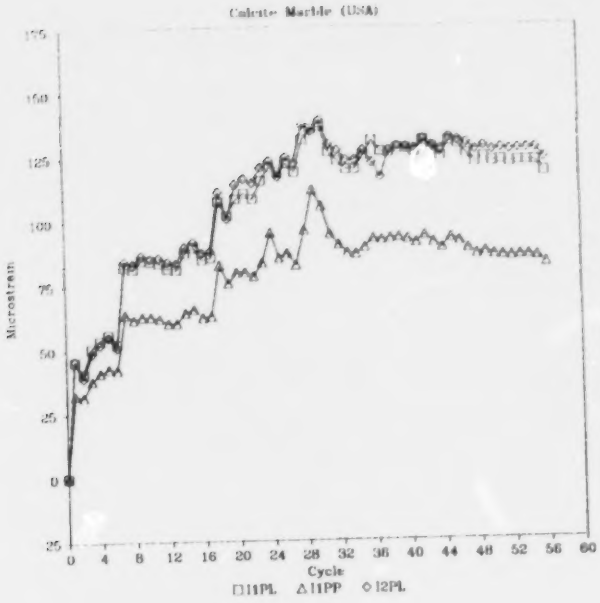

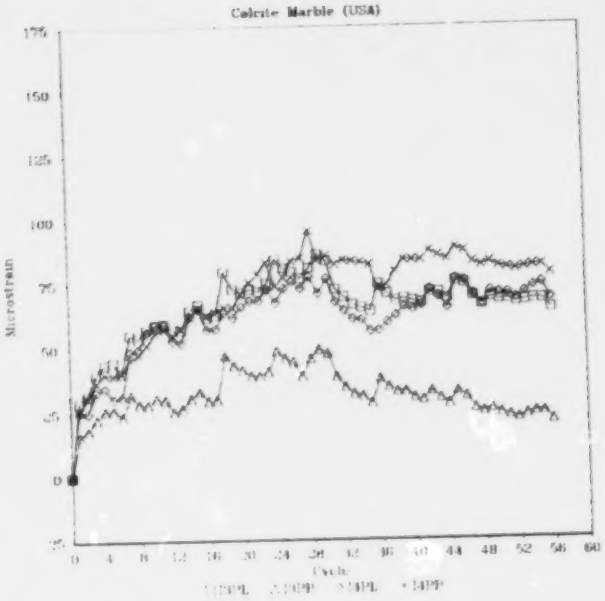

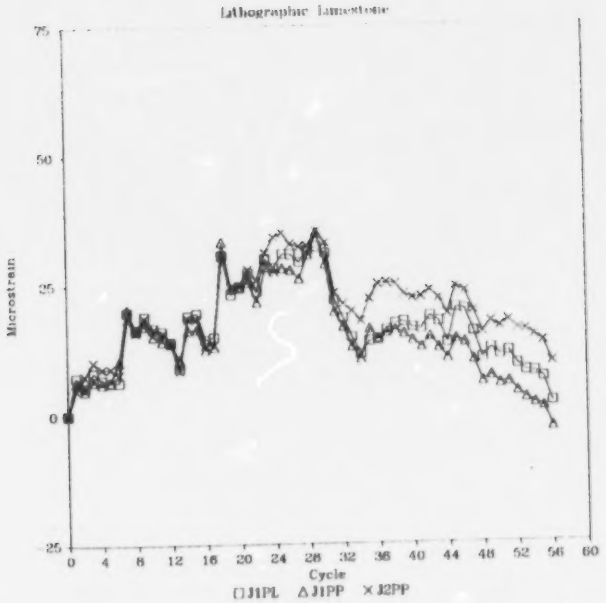

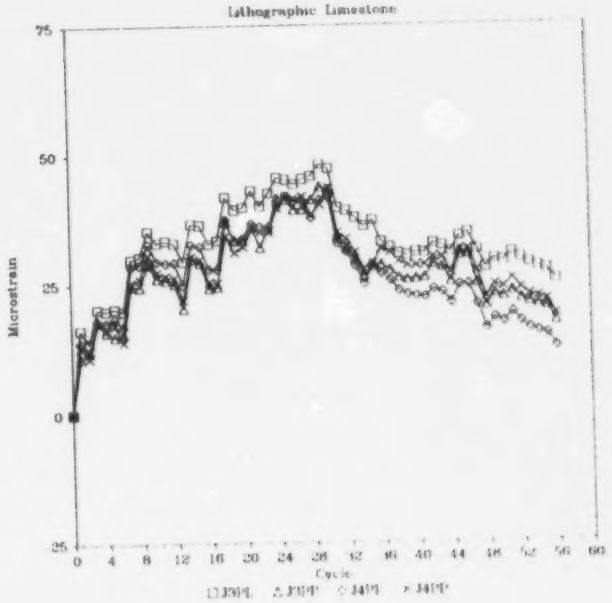

Figure 28/ Residual Strain at 20°C versus Cycle
Calcite Marble (I) and Lithographic Limestone (J)

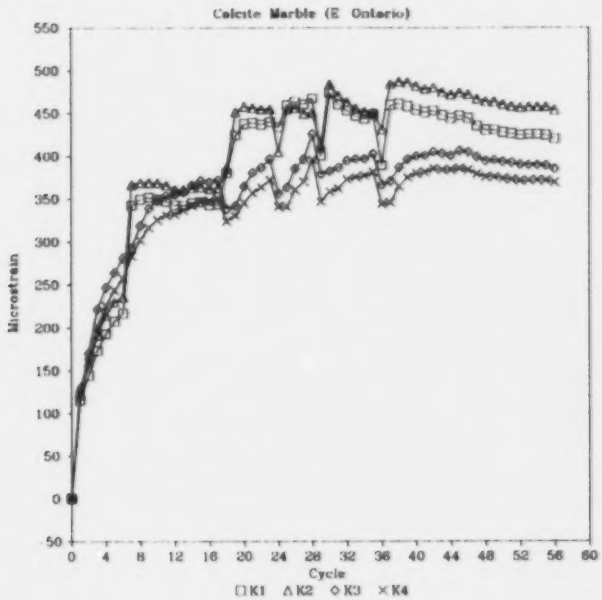

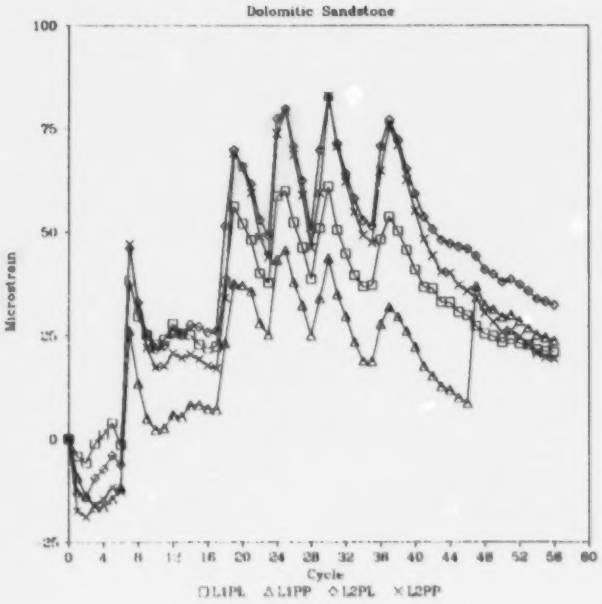

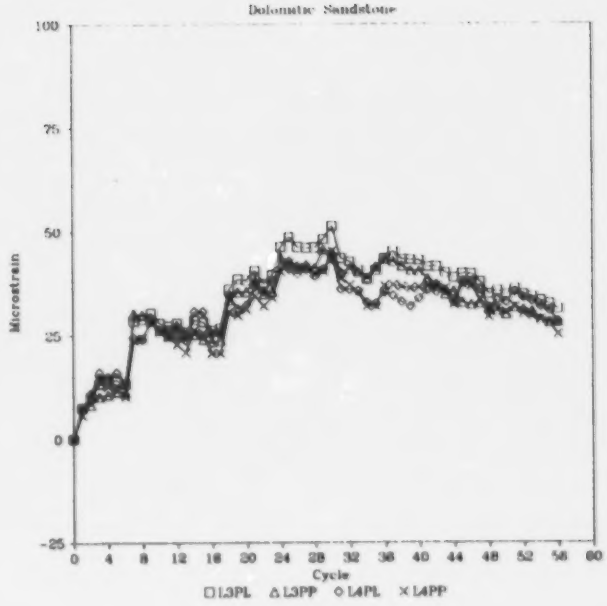

Figure 29/ Residual Strain at 20°C versus Cycle
Calcite Marble (K) and Dolomitic Sandstone (L)

Appendix A/ Sample Designations, Locations and Thin Section Descriptions

Sample: **A (Plate 1)**

Rock Type: Coquinoid Calcarenite (Bobcaygeon Fm.)
Location: Francon Quarry, Ottawa, Ontario
Topo Map: Ottawa, Grid Reference: 560323
Repository: A522 University of Waterloo

The thin section exhibited bedding as alignment of the brachiopod fragments, grain size variations in the crystalline portion, and occasional stylolites. Argillaceous content and organic material also varied, being richer within the finer grained beds. The stylolites were marked by organic material accumulations. The rock is predominantly crystalline calcite and calcite replaced bioclastic fragments. It is composed of large irregular anhedral calcite crystals (up to 1 mm diameter) in a very fine grained, very poorly sorted matrix of fine granular calcite (<0.1 mm). The calcite did not exhibit prominent twinning lammellae but had a high birefringence and uniaxial negative character. The cement is mainly crystalline spar. The larger calcite crystals contained in interior zone rich in inclusions surrounded by clear exterior boundaries modified by crystalline sparry cement. Grain boundaries are highly irregular, ranging from crystal face contacts between the large spar to diffuse granular boundaries between the allochemical grains. The fossil component is mostly broken and incomplete, elongated articulated brachiopod fragments (to 5 mm in length) which exhibit a fibrous texture parallel to bedding. Minor algaloncolites and numerous fine (0.2 mm) collophane fragments are also noted.The noncarbonate fraction contains subangular quartz, muscovite and minor feldspars and comprises less than 5% of the total volume.

Sample: **B (Plate 2)**

Rock Type: Diabase (Logan Fm.)
Location: Zysko Quarry, Thunder Bay, Ontario
Topo Map: Thunder Bay Grid Reference: 400730
Repository: A523 University of Waterloo

The diabase consists predominantly of subhedral plagioclase laths (0.5 mm) and anhedral pyroxene aggregate crystals in the interstices giving the mineral assemblage typical diabasic to sub-diabasic textures. Large (2.0 mm) pyroxene crystals exhibiting high birefringence often enclose the smaller plagioclase laths so that ophitic textures are also displayed in the thin section. The plagioclase is highly sericitised with alteration of the laths almost 70-80% complete. The alteration masks most of the crystal twins. No fluidal textures were observed with the plagioclase orientation being completely randomized.

Sample: **C (Plate 3)**

Rock Type: Meta-arkose (Grenville)
Location: Fleming Quarry, Orillia, Ontario
Topo Map: Orillia Grid Reference: 317532
Repository: A524 University of Waterloo

The mineralogy of this rock is dominantly microcline feldspar (40%) and anhedral quartz (35%). Agglomerations of hematite/magnetite comprise 7 to 10%. The foliation is poorly identified in the thin section, being marked by mineral banding. The quartz crystals are equidimensional, generally 1.0 to 1.5 mm in diameter with individual grains up to 2.0 mm. The extinction of the quartz is often strongly strained. The feldspar exhibits typical microcline cross-hatched twinning with occasional polysynthetic twins of plagioclase. The feldspar twins often show irregular and distorted extinction patterns indicating strain at the grain boundaries. The quartz grain boundaries are highly sutured. Disseminated hematite inclusions surround the feldspar crystals and along their cleavage traces. The feldspars show only minor alteration to sericite. Numerous accessory minerals are also present. Rutile forms needle-like (0.2 mm length) capillary crystal insertions in association with the quartz and minute euhedral crystals of sphene occur as quartz inclusions. Large orange-pink subhedral garnets (0.5 - 1.0 mm) occur in bands as the dominant ferro-magnesian mineral present, and calcite is found interstitially between crystals throughout the slide.

Sample: **D (Plate 4)**

Rock Type: Dolostone (Amabel Fm.)
Location: Nelson Quarry, Burlington, Ontario
Topo Map: Burlington Grid Reference: 909055
Repository: A525 University of Waterloo

The thin (10 mm) beds are marked by incipient stylolitic formations and changes in argillaceous and organic content. Large open pores (0.1 - 3 mm) comprise approximately 15% of the area of the slide. They are slightly elongated and aligned in the bedding direction. Allochemical composition cannot be determined because of complete recrystallization of the constituents. The argillaceous content varies throughout the rock and minor quartz; feldspar and gypsum have been identified from acid residues. The thin section mineralogy is dominated by subhedral

rhombic dolomite crystals (80 - 85%) up to 2.0 mm diameter with an average of 0.2 mm. Inclusions are sparse, with opaque minerals (pyrite) occurring interstitially within the dolomite matrix. Disseminated pyrite also occurs as crystalline aggregates in roughly spheroidal shaped masses within the finer grained beds. The cement is dolomite spar which is indistinguishable from the recrystallized matrix except for the occasional larger forms of the mineral dolomite.

Sample: **E (Plate 5)**

Rock Type: Dolostone (Amabel Fm.)
Location: Manitoulin Dolostone Quarry, Manitoulin Island, Ontario
Topo Map: Meldrum Bay
Grid Reference: 277862
Repository: A526 University of Waterloo

The main mineralogic component is subhedral to anhedral crystalline dolomite. Grain size variations and crystal orientation distinguish the 10 mm thick beds. The overall structure is free of any noticeable voids and the argillaceous component and organic content of the rock is minimal. Beds containing the larger grain sizes (0.4 - 0.5 mm) show polygonal grain boundaries between crystals that exhibit a high birefringent character while beds containing the smaller sized grains contain better defined crystal shapes, although no prominent rhombic crystals are present. Coarse polygonal dolomite, noticeably lacking in inclusions, is observed to infill minor fractures within the rock structure which typically cross-cut the bedding direction.

Sample: **F (Plate 6)**

Rock Type: Dolostone (Bertie-Akron Fm.)
Location: Haldimand Quarry, Simcoe Country, Ontario
Topo Map: Simcoe Grid Reference: 785573
Repository: A527 University of Waterloo

The thin section exposes very fine laminations (0.1 - 1.0 mm thick) differentiated on grain size and argillaceous content. The argillaceous rich beds contain extremely fine grained crystalline dolomite (<0.01 mm) with occasional subhedral crystals up to 0.03 mm. The cement is comprised of micrite with no sparry cement observed. The coarser grained beds contain grain sizes of typically 0.1 to 1.0 mm with angular quartz grains in addition to dolomite crystals. These beds contain a few irregular voids. Pyrite aggregations are rare, with the majority of the sulphides disseminated throughout the slide.

Sample: **G (Plate 7)**

Type: Cement Mortar

Air entrained mortar: Canada Cement LaFarge (Woodstock) Type 10
Guelph Sand and Gravel, concrete sand
Cement: aggregate ratio (by weight) = 1:1.66
W/C ratio = 0.31
Air content = 10.9%
28 day strength = 42.1 and 40.2 MPa

Non air-entrained mortar:
Cement and aggregate as above

Cement: aggregate ratio (by weight) = 1:1.26
W/C ratio = 0.37
Air content = 4.8%
28 day strength = 55.1 and 54.6 MPa

Sample: **H (Plate 8)**

Rock Type: Dolomite Marble (Grenville)
Location: Hwy 41 roadcut, Lennox and Addington County, Ontario
Topo Map: Denbigh Grid Reference: 253102
Repository: A586 University of Waterloo

The rock contains 95% of subhedral, dolomite with polysynthetic twinning. Grain boundaries are transitional, with granulations and evidence of recrystallization. Alteration fringes are common at the crystal contacts. The dolomite often contains disseminated, banded inclusions of opaque grains. Equidimensional interstitial muscovite and minor phlogopite occur as subhedral to anhedral crystals, commonly with broken boundaries. Quartz grains are small (0.2 mm) and irregular, showing corroded grain contacts and containing inclusions of muscovite. Disseminated magnetite and hematite are present in small amounts. A few crystals of altered tremolite are present with incomplete crystalline form and iron-stained boundaries. No alteration minerals are identifiable.

Sample: **I (Plate 9)**

Rock Type: Calcite Marble (Cockeysville Fm.)
Location: Arundel Corp., Greenspring, Maryland, USA
Topo Map: N/A
Repository: A774 University of Waterloo

Anhedral to subhedral calcite dominates the minerology of this rock type. Calcite crystals (1.0 - 2.0 mm) make up 75 to 80% of the rock and occur as polygonal grains surrounding minor amounts of prismatic phlogopite and muscovite. There is 10 to 12% of equigranular (0.5 mm) quartz and feldspar. Boundaries between the calcite crystals are commonly sutured, showing irregular forms and interpenetration. The micas are situated interstitially between the calcite and are occasionally enclosed by them. Phlogopite is the dominant phyllosilicate (8 - 10% of the rock), distinguished by its slightly pleochroic light brown colour and small 2V angle. These grains are

commonly <1.0 mm in length. The rounded quartz grains occur with the anhedral equigranular plagioclase interstitially between the calcite grains. They sometimes occur in linear agglomerations with the phyllosilicates and may indicate remnant bedding.

Sample: **J (Plate 10)**

Rock Type: Lithographic Limestone (Gull River Fm.)
Location: Medonte Quarry, Coldwater, Ontario
Topo Map: Elmvale Grid Reference: 095507
Repository: A775 University of Waterloo

This microcrystalline limestone consists of 80 to 85% micrite matrix surrounding infilled cavities of coarse sparry crystalline calcite. There is no evidence of bedding other than faint, discontinuous stylolites. These are large in amplitude (10 mm) and formed mainly from phosphatic material with minor calcite spar. Thin microfractures also contain spar. There are occasional large calcite crystals with corroded boundaries; negligible clay minerals; and minor organic material. Acid residues contain minor amounts of quartz, pyrite, and possibly gypsum. The few fossil fragments of brachiopod and ostracod shells have been replaced by spar.

Sample: **K (Plate 11)**

Rock Type: Calcite Marble (Grenville)
Location: Tatlock Quarry, Eastern Ontario
Topo Map: Carleton Place
Grid Reference: 825018
Repository: A776 University of Waterloo

This rock consists almost entirely (>95%) of polygonal 3 to 4 mm equigranular crystalline calcite. Smaller rounded quartz and feldspar minerals (0.3 - 0.4 mm) are present in the calcite matrix. Quartz grains are common as inclusions in the calcite crystals. Minor amounts of muscovite are also observed. The overall texture is mosaic with grain boundaries formed between the crystal edges of the individual grains. The calcite crystals exhibit a high degree of individuality. Some of these twins give evidence of straining at the grain boundaries where they are altered and distorted. This is associated with wavy birefringence patterns. The feldspars are mixed, showing both carlsbad and minor albite twins.

Sample: **L (Plate 12)**

Rock Type: Dolomitic Sandstone (March Fm.)
Location: Permanent Quarry, Brockville, Ontario
Topo Map: Brockville Grid Reference: 475398
Repository: A777 University of Waterloo

This rock is composed of 55 to 60% medium to fine sand-sized quartz grains cemented by subhedral dolomite spar. Organic-rich medium grained beds alternate with beds of small subangular quartz and feldspar. The grains are bimodally sorted with large (0.5 mm) rounded, fractured, spherical quartz and smaller (0.1 mm) subangular, equidimensional quartz and feldspar. Quartz dominates the sand fraction by a ratio of 9:1. The cement is comprised of subhedral dolomite crystals 0.1 mm in diameter which account for 40% of the thin section by area. The sand grains are floating in the dolomite matrix without grain-to-grain contact as a result of recrystallized detrital carbonate matrix. Pyrite agglomerations are found in the matrix and finely disseminated pyrite as inclusions within the dolomite. The organic component and the sulphides account for less than 3% of the detrital matrix.

Plate 1: Calcarenite A

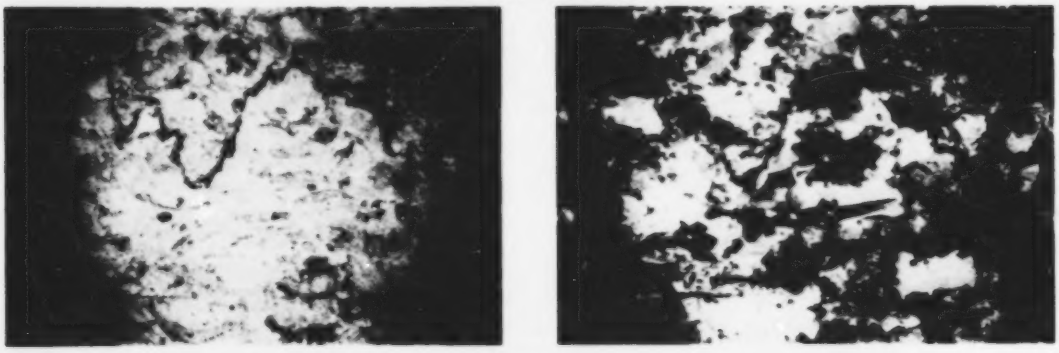

Plate 2: Logan Diabase B

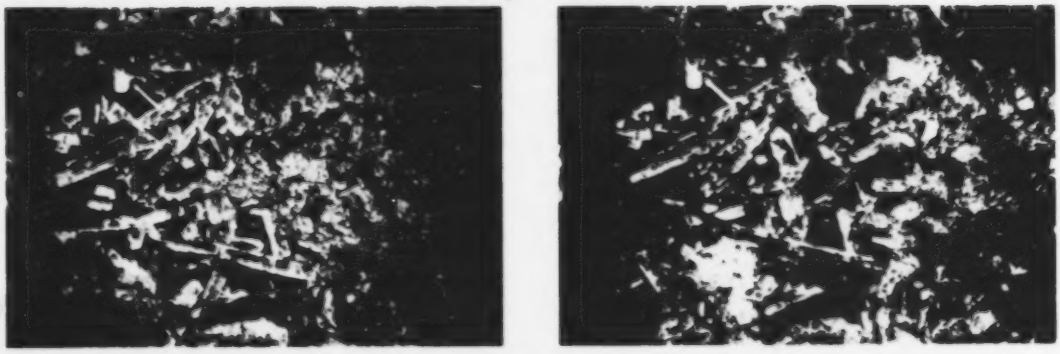

Plate 3: Meta-arkose C

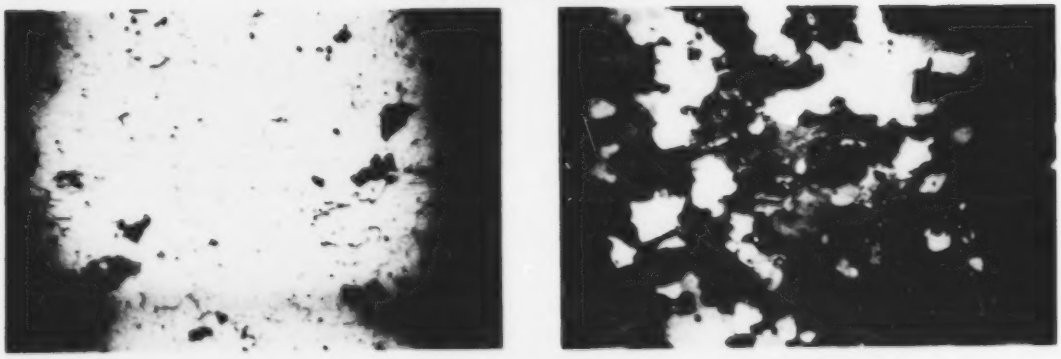

Plate 4: Amabel Dolostone (Nelson) D

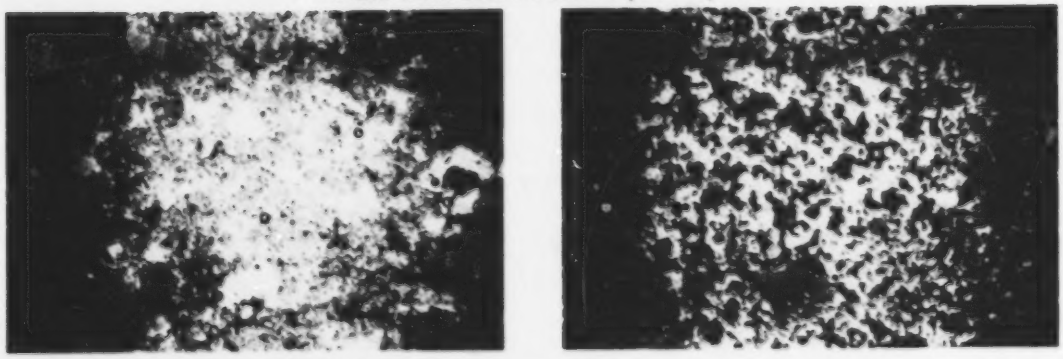

Figure A1/ Photomicrographs of Rock Samples
Fabric horizontal; Photo width 5.5 mm; Polarized light to right

Plate 5: Amabel Dolostone (manitoulin) E

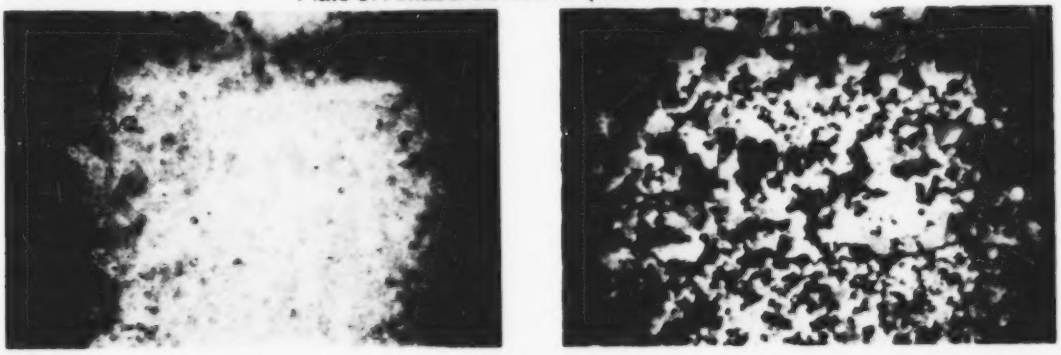

Plate 6: Bertie Akron Dolostone F

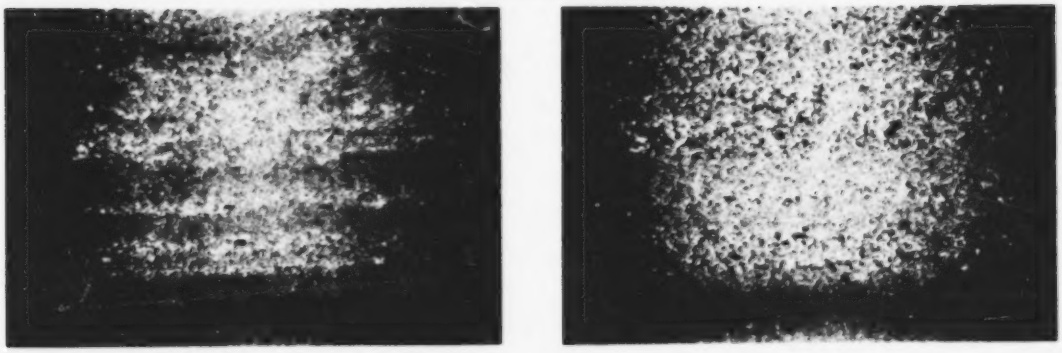

Plate 7: Cement Mortar G

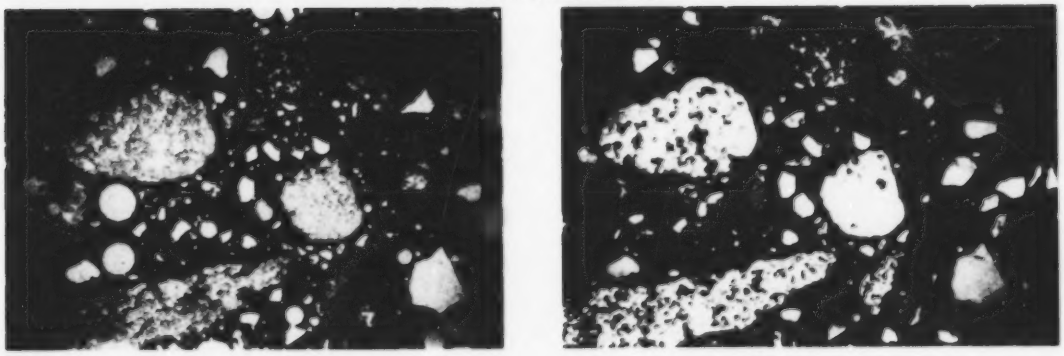

Plate 8: Dolomite Marble H

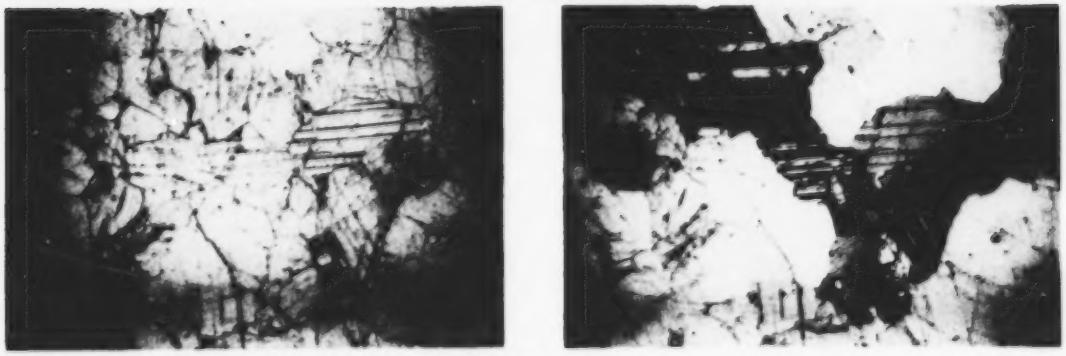

Figure A2/ Photomicrographs of Rock Samples
Fabric horizontal; Photo width 5.5 mm; Polarized light to right

Plate 9: Calcite Marble (USA) I

Plate 10: Lithographic Limestone J

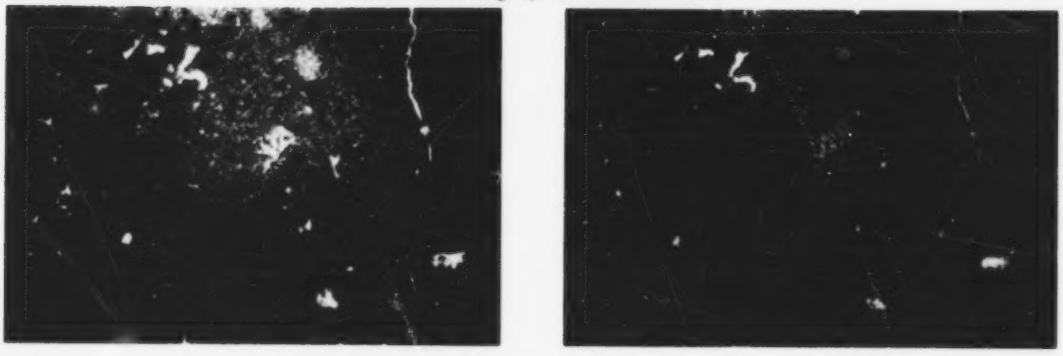

Plate 11: Calcite Marble (E. Ontario) K

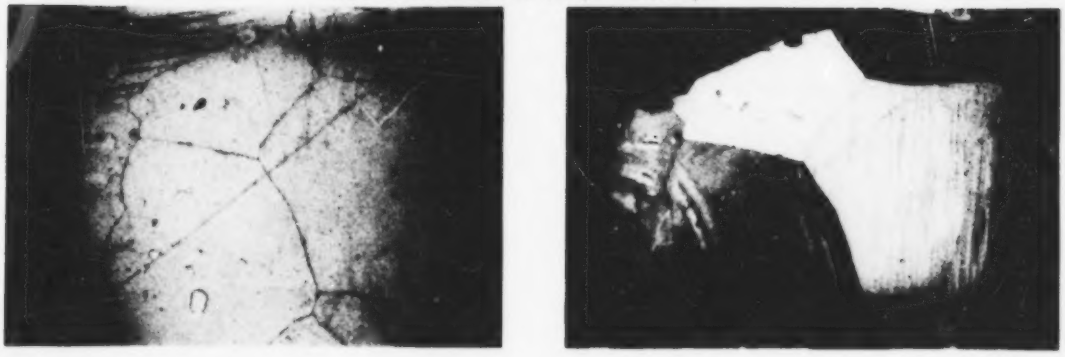

Plate 12: Dolomitic Sandstone L

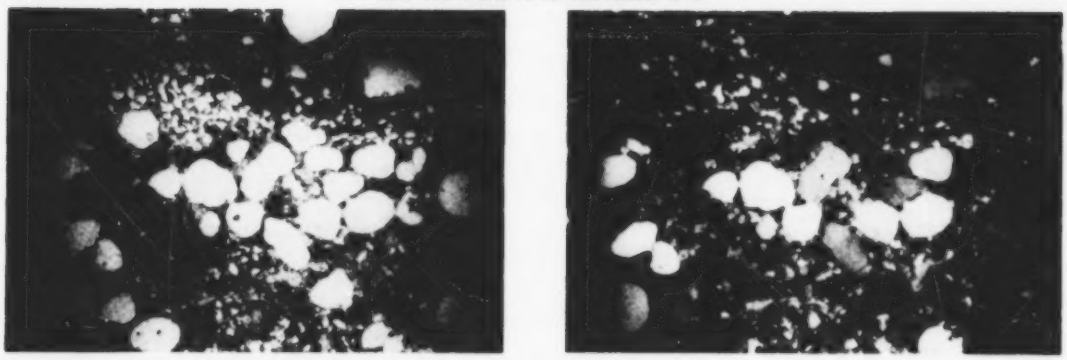

Figure A3/ Photomicrographs of Rock Samples
Fabric horizontal; Photo width 5.5 mm; Polarized light to right

Sample	Mineralogy	Grain Size (mm) Range	Median
A/ Calcarenite (Francon Quarry, Ottawa)	calcite (>85%) quartz, muscovite, feldspar (<5%) organic material (3-5%)	0.01-1.00 (prismatic)	0.50 0.15 0.20
B/ Diabase (Zysko Quarry, Thunder Bay)	plagioclase (55%) pyroxene (40%) sericite (alteration from plagioclase)	0.30-0.75 (prismatic) 0.50-0.75 0.03-0.05	0.50 0.60
C/ Meta-arkose (Fleming Quarry, Orillia)	microcline (40%) quartz (35%) garnet (5%) opaques (7-10%) calcite (1-2%) sphene (<1%)	0.05-1.50 0.05-1.50 0.50-1.00 (insertal)	0.75 0.75 0.65 0.50 0.10 0.07
D/ Dolostone (Nelson Quarry, Burlington)	dolomite (>90%) quartz, feldspar, gypsum (<5%) opaques	0.01-0.50	0.25 0.10 <0.01
E/ Dolostone (Manitoulin Quarry)	dolomite (>90%)	0.05-0.50	0.35
F/ Dolostone (Haldimand Quarry, Simcoe)	dolomite (85%) quartz (5-8%) opaques (5-7%)	0.01-0.10 disseminate	0.03 0.05 <0.01
H/ Dolomite Marble (Hwy 41, Denbigh)	dolomite (95%) muscovite phlogopite quartz	0.30-2.00	1.00 0.30 0.30 0.20
I/ Calcite Marble (Maryland, USA)	calcite (80%) quartz, feldspar (10-12%) phlogopite (8%)	0.40-2.00 0.15-1.00 0.20-1.00	1.50 0.30 0.40
J/ Limestone (Medonte Quarry, Coldwater)	calcite (80-85%) calcite (15%)	(micrite) 0.03-0.20	<0.005 0.10
K/ Calcite Marble (Tatlock Quarry, Carleton Pl.)	calcite (>95%) quartz, feldspar muscovite (<1%)	1.20-4.00 0.10-0.20	3.00 0.15 0.10
L/ Dolomitic Sandstone (Permanent Quarry, Brockville)	quartz (50%) dolomite (45%) pyrite (1-2%) organic material	0.05-1.00 0.03-0.50	0.10; 0.70 0.10 0.05 <0.01

Figure A4/ Rock Minerology and Grain Size

Specimen Designation	Moisture Content "dry" [Saturation %]	"wet" [Saturation %]	Porosity %	S.G. g/cc
A/ Calcarenite (limestone)	0.022%	0.175%		
A1	[4.21]	[33.48]	0.52%	2.76
A3	[2.38]	[18.99]	0.92%	2.34
B/ Diabase	0.063%	0.123%		
B1	[20.26]	[39.55]	0.31%	3.02
B2	[16.34]	[31.90]	0.39%	3.01
C/ Meta-arkose	0.019%	0.091%		
C1	[3.35]	[16.05]	0.57%	2.65
C2	[3.39]	[16.25]	0.56%	2.73
D/ Dolostone (Nelson)	0.008%	0.232%		
D1	[0.09]	[2.63]	8.81%	2.53
D2	[0.12]	[3.36]	6.91%	2.61
E/ Dolostone (Manitoulin)	0.023%	0.050%		
E1	[9.00]	[19.57]	0.26%	2.81
E2	[8.43]	[18.32]	0.27%	2.83
E3	[13.25]	[28.80]	0.17%	2.82
E4	[9.28]	[20.17]	0.25%	2.83
E5	[8.34]	[18.14]	0.28%	2.83
F/ Dolostone (Bertie-Akron)	0.017%	0.486%		
F1	[0.31]	[8.82]	5.51%	2.62
F2	[0.28]	[8.13]	5.98%	2.61
F3	[0.32]	[9.11]	5.34%	2.65
G/ Cement Mortar	—	7.562%		
H/ Marble (dolomite)	0.008%	0.054%		
H1	[1.76]	[11.86]	0.46%	2.85
H2	[1.68]	[11.36]	0.48%	2.85
H3	[2.48]	[16.75]	0.32%	2.87
I/ Marble (calcite, USA)	0.010%	0.025%		
I1	[2.91]	[7.27]	0.34%	2.69
I2	[5.70]	[14.26]	0.18%	2.70
I3	[4.11]	[10.29]	0.24%	2.70
I4	[3.27]	[8.18]	0.31%	2.70
J/ Limestone (lithographic)	0.016%	0.097%		
J1	[2.72]	[16.47]	0.59%	2.69
J2	[3.65]	[22.14]	0.44%	2.69
J3	[3.47]	[21.03]	0.46%	2.42
K/ Marble (calcite, E. Ontario)		0.012%	0.039%	
K1	[2.82]	[9.16]	0.43%	2.68
K2	[1.54]	[5.01]	0.78%	2.61
L/ Sandstone (dolomitic)	0.007%	0.194%		
L1	[0.90]	[24.95]	0.78%	2.78
L2	[0.45]	[12.61]	1.54%	2.65

Figure A5/ Index Test Data for Moisture Contents, Saturation, Porosities, and Dry Unit Weights (S.G.)

Appendix B/ Thermal Coefficients of Expansion

Notes:

1. Temperature is reported in degrees Celsius, and the Coefficients in microstrain per degree Celsius (x 10^{-6}/°C).
2. The reported Coefficients are "chord" values measured between increments of temperature during the "slow" first cycle.
3. The reported temperature is the temperature at midpoint between successive determinations (unless otherwise stated).
4. Specimens designated 1, 2 were tested "wet", and 3, 4 "dry".
5. Specimens designated PL were tested with gauge parallel, and PP perpendicular to the rock fabric (bedding or foliation). Omitting this designation implies an isotropic specimen tested in one direction only.

Sample A: Coquinoid Calcarenite (limestone)

Temp	A1PL	A2PL	A3PL	A4PL	A1PP	A2PP	A3PP	A4PP
-11.1	0.14	0.09	1.17	-	2.56	2.08	1.96	-
-2.7	1.95	2.42	3.61	-	4.58	4.12	4.26	-
2.1	3.79	3.08	3.74	-	4.48	4.12	4.95	-
7.1	4.34	3.02	5.17	-	6.24	5.81	6.37	-
12.6	5.52	4.90	6.33	-	7.79	7.29	7.42	-
24.0	7.25	6.13	7.06	-	9.19	8.56	8.63	-
27.5	7.79	7.40	7.70	-	9.75	9.85	9.13	-
32.1	8.15	7.28	8.03	-	10.23	9.97	9.67	-
38.4	8.56	7.82	7.60	-	10.37	10.35	9.44	-
47.3	8.68	8.02	8.21	-	10.74	10.58	9.94	-
Average coefficients for cooling half-cycle (-20°C - +15°C):								
	2.28	2.39	2.68	-	4.38	4.31	3.85	-
Average coefficients for heating half-cycle (+15°C - +50°C):								
	7.40	6.90	7.29	-	9.38	9.44	8.79	-

Sample B: Diabase

Temp	B1	B2	B3	B4
-11.1	7.49	7.43	6.61	-
-2.7	7.67	8.46	6.60	-
2.1	7.77	6.95	7.15	-
7.1	7.36	7.54	6.29	-
12.6	7.62	7.94	6.67	-
24.0	7.75	8.13	7.56	-
27.5	8.19	7.92	7.70	-
32.1	7.59	7.67	7.28	-
38.4	6.94	6.90	7.01	-
47.3	6.83	6.97	6.72	-
Average coefficients for cooling half-cycle (-20°C - +15°C):				
	7.53	7.49	6.76	-
Average coefficients for heating half-cycle (+15°C - +50°C):				
	8.01	8.05	7.18	-

Sample C: Meta-arkose

Temp	C1PL	C2PL	C3PL	C4PL	C1PP	C2PP	C3PP	C4PP
-11.1	4.59	4.20	2.41	4.27	2.59	2.77	2.61	2.46
-2.7	4.58	4.72	2.40	4.26	2.86	3.19	2.88	3.98
2.1	4.72	4.62	3.46	5.97	3.10	3.62	3.38	4.23
7.1	4.58	4.86	2.90	4.64	2.56	3.61	3.17	-
12.6	5.10	5.21	3.31	5.17	3.44	4.02	3.50	3.90
24.0	5.69	5.69	4.38	6.31	4.38	5.06	4.38	4.88
27.5	7.28	6.53	4.81	6.87	5.72	5.83	4.87	5.19
32.1	4.49	5.92	4.59	-	3.82	5.23	-	-
38.4	5.54	5.88	4.62	6.63	4.62	5.29	4.63	4.37
47.3	6.22	6.13	4.68	6.41	5.21	5.55	4.88	4.92
Average Coefficients for cooling half-cycle (-20°C - +15°C):								
	5.36	5.11	3.43	5.43	3.61	3.94	3.52	3.69
Average Coefficients for heating half-cycle (+15°C - +50°C):								
	6.27	6.16	5.03	6.75	5.33	5.61	5.02	5.12

Sample D: Amabel Dolostone (Nelson)

Temp	D1PL	D2PL	D2PL	D4PL	D1PP	D2PP	D3PP	D4PP
-11.1	7.85	7.77	7.35	7.06	7.58	7.82	7.43	6.66
-2.7	7.23	8.19	8.00	6.81	7.77	8.74	7.96	6.39
2.1	9.23	7.97	8.18	8.77	8.51	8.00	8.18	8.72
7.1	7.24	7.83	7.83	7.07	7.56	8.34	7.71	6.90
12.6	7.87	8.52	8.60	7.87	8.38	9.29	8.48	7.73
24.0	8.19	8.25	9.38	9.25	8.38	8.63	9.44	9.25
27.5	8.89	9.02	10.06	9.57	9.06	9.79	10.15	9.60
32.1	8.10	8.31	10.28	9.64	8.31	9.03	10.41	9.67
38.4	6.74	7.06	10.04	9.66	6.72	7.41	9.69	9.90
47.3	7.08	7.63	9.98	9.39	7.75	7.82	9.85	9.66
Average coefficients for cooling half-cycle (-20°C - +15°C):								
	8.36	8.46	8.17	7.88	8.31	8.68	8.06	7.65
Average coefficients for heating half-cycle (+15°C - +50°C):								
	9.87	9.73	9.63	9.32	9.91	10.36	9.66	9.53

Sample E: Amabel Dolostone (Manitoulin)

Temp	E1PL	E2PL	E3PL	E4PL	E1PP	E2PP	E3PP	E4PP
-11.1	6.36	-	7.49	7.06	6.71	-	7.27	7.60
-2.7	7.11	-	7.58	7.11	7.25	-	7.37	7.86
2.1	8.28	-	8.72	8.41	8.41	-	8.41	8.85
12.6	8.02	-	8.44	8.08	7.92	-	8.13	8.69
24.0	9.13	-	9.00	9.00	9.19	-	8.69	9.25
27.5	10.03	-	9.79	9.51	10.13	-	9.58	9.89
32.1	9.38	-	9.49	9.33	9.49	-	9.26	9.62
38.4	9.32	-	9.59	9.43	9.40	-	9.40	9.66
47.3	9.12	-	9.40	9.26	9.39	-	9.28	9.48
Average coefficients for cooling half-cycle (-20°C - +15°C):								
	7.57	-	7.95	7.65	8.06	-	7.80	8.26
Average coefficients for heating half-cycle (+15°C - +50°C):								
	9.75	-	9.40	9.26	9.89	-	9.33	9.53

Sample F: Bertie-Akron Dolostone

Temp	F1PL	F2PL	F3PL	F4PL	F1PP	F2PP	F3PP	F4PP
-11.1	8.22	8.54	8.28	9.14	9.14	9.32	9.32	9.10
-2.7	7.96	8.32	8.63	7.96	9.05	9.12	9.25	8.70
2.1	9.05	9.03	9.49	9.28	10.31	10.38	10.15	10.26
7.1	7.33	8.00	8.24	7.63	8.68	8.83	8.75	8.34
12.6	8.40	8.63	8.92	8.23	9.38	9.37	9.42	9.00
24.0	8.75	8.88	10.25	9.19	9.81	9.81	9.50	9.81
27.5	9.70	9.62	11.02	9.45	10.51	10.62	10.38	10.32
32.1	8.97	9.08	10.69	8.92	9.87	10.05	9.67	9.82
38.4	8.87	9.06	9.18	8.76	9.74	9.82	9.63	9.59
47.3	8.72	8.92	10.02	8.45	9.45	9.55	9.40	9.22
Average coefficients for cooling half-cycle (-20°C - +15°C):								
	8.19	8.37	8.58	8.26	9.31	9.37	9.27	9.07
Average coefficients for heating half-cycle (+15°C - +50°C):								
	8.95	8.96	10.23	8.87	9.83	9.94	9.66	9.70

Sample G: Cement Mortar, Specimens 1 and 3 are Air-entrained

Temp	G1	G2	G3	G4
-11.1	8.76	-	8.58	9.38
-2.7	9.28	-	9.12	9.89
2.1	10.72	-	10.49	12.05
7.1	9.53	-	9.66	10.54
12.6	10.85	-	10.85	11.71
24.0	12.19	-	11.81	13.50
27.5	13.26	-	12.81	14.30
32.1	12.05	-	12.18	14.03
38.4	9.94	-	11.29	10.65
47.3	9.88	-	10.68	11.53
Average coefficients for cooling half-cycle (-20°C - +15°C):				
	11.01	-	10.87	11.56
Average coefficients for heating half-cycle (+15°C - +50°C):				
	15.92	-	15.64	18.12

Sample H: Dolomite Marble

Temp	H1PL	H2PL	H3PL	H4PL	H1PP	H2PP	H3PP	H4PP
-11.1	3.32	4.12	4.21	4.71	10.41	10.41	12.33	9.91
-2.7	3.89	4.95	4.63	5.00	10.67	11.00	12.05	10.12
2.1	4.10	5.23	5.10	6.03	11.95	12.79	14.05	11.56
7.1	3.86	5.17	4.85	5.36	10.68	11.12	12.36	10.17
12.6	4.38	5.96	5.92	6.04	11.79	12.85	14.04	11.75
24.0	5.75	6.63	7.31	6.50	13.25	13.94	14.88	12.88
27.5	6.98	7.96	7.60	7.23	14.36	14.94	15.55	13.68
32.1	6.38	7.76	8.24	6.90	14.08	14.95	14.13	13.56
38.4	6.37	7.54	8.24	7.32	13.84	14.88	15.88	13.84
47.3	6.43	7.68	8.40	7.35	13.96	14.76	15.57	13.61
Average coefficients for cooling half-cycle (-20°C - +15°C):								
	2.75	5.24	5.13	5.49	11.29	11.69	13.03	10.88
Average coefficients for heating half-cycle (+15°C - +50°C):								
	6.44	7.72	7.72	7.11	14.32	15.16	15.51	13.63

Sample I: Calcite Marble (USA)

Temp	I1PL	I2PL	I3PL	I4PL	I1PP	I2PP	I3PP	I4PP
-11.1	-3.46	-5.05	-2.95	-2.42	-0.41	5.05	2.12	0.32
-2.7	-1.21	-2.05	-0.75	0.44	1.68	7.47	3.93	2.47
2.1	-0.28	-1.05	0.79	3.23	3.51	10.10	5.90	4.72
7.1	0.49	0.44	1.58	-	3.80	9.22	5.42	5.14
12.6	1.08	0.44	2.23	2.60	4.96	10.94	6.71	6.12
24.0	1.56	2.00	3.38	3.94	7.25	14.44	8.88	8.75
27.5	4.49	4.04	4.85	5.60	9.42	15.85	9.87	9.72
32.1	4.38	3.74	5.10	5.79	9.51	16.56	9.72	9.31
38.4	5.04	4.38	5.72	6.44	9.88	17.03	10.74	9.97
47.3	5.47	4.95	6.13	7.31	10.37	17.37	11.55	11.13
Average coefficients for cooling half-cycle (-20°C - +15°C):								
	0.41	-0.30	0.79	0.40	3.57	9.06	4.92	4.04
Average coefficients for heating half-cycle (+15°C - +50°C):								
	4.66	3.99	5.11	5.99	9.53	16.15	10.60	10.40

Sample J: Lithographic Limestone

Temp	J1PL	J2PL	J3PL	J4PL	J1PP	J2PP	J3PP	J4PP
-11.1	4.08	3.77	4.09	3.70	3.50	3.77	3.95	4.23
-2.7	4.14	3.47	4.16	3.86	3.60	3.79	4.09	4.25
2.1	4.28	4.41	4.46	4.00	3.97	4.00	4.18	4.44
7.1	3.88	3.47	3.86	3.54	3.41	3.73	3.88	3.92
12.6	4.15	3.75	4.02	3.75	3.63	3.96	4.02	4.08
24.0	4.25	3.94	4.50	4.19	3.69	4.00	4.00	4.38
27.5	4.40	3.96	5.28	4.74	3.72	3.98	4.81	5.04
32.1	4.21	4.10	4.54	4.21	3.74	4.10	4.21	4.05
38.4	4.04	3.79	4.75	4.32	3.53	3.97	4.50	4.22
47.3	4.14	3.79	4.59	4.12	3.68	3.95	4.35	4.28
Average coefficients for cooling half-cycle (-20°C - +15°C):								
	4.11	3.75	4.18	3.78	3.65	3.75	3.95	4.20
Average coefficients for heating half-cycle (+15°C - +50°C):								
	4.48	4.16	4.51	4.05	4.07	4.09	4.15	4.30

Sample K: Calcite Marble (E. Ontario)

Temp	K1	K2	K3	K4
-11.1	-3.98	-2.71	-4.86	-5.49
-2.7	-2.05	0.00	-2.42	-2.65
2.1	-0.97	1.64	-2.28	-2.18
7.1	-0.17	2.75	0.51	-0.03
12.6	0.58	2.90	1.40	0.73
24.0	2.63	4.94	2.63	3.31
27.5	4.11	7.35	3.49	3.92
32.1	4.21	7.33	3.72	3.79
38.4	4.82	8.21	4.24	4.37
47.3	7.72	12.19	5.75	6.29
Average coefficients for cooling half-cycle (-20°C - +15°C):				
	0.17	2.67	-0.17	-1.20
Average coefficients for heating half-cycle (+15°C - +50°C):				
	4.87	8.14	3.55	3.65

Sample L: Dolomitic Sandstone

Temp	L1PL	L2PL	L3PL	L4PL	L1PP	L2PP	L3PP	L4PP
-11.1	7.74	9.81	7.36	8.63	9.37	9.69	8.91	10.41
-2.7	7.65	8.72	7.40	8.70	9.16	9.40	8.63	10.47
2.1	9.18	10.23	8.51	9.56	10.62	10.97	10.05	11.59
7.1	7.59	8.58	7.31	8.49	5.59	9.36	8.39	10.19
12.6	8.27	9.42	7.88	9.31	9.60	10.12	9.08	11.04
24.0	8.50	9.13	8.38	9.63	17.63	9.94	10.00	11.50
27.5	9.42	10.45	8.92	10.17	10.36	11.11	10.32	12.09
32.1	8.67	9.46	8.62	9.85	9.74	10.10	10.03	11.69
38.4	6.74	7.74	8.68	9.99	8.01	7.50	9.96	11.79
47.3	6.86	7.72	8.50	9.75	7.82	7.67	9.56	11.59
Average coefficients for cooling half-cycle (-20°C - +15°C):								
	8.13	9.19	7.50	8.71	9.36	10.04	8.99	10.56
Average coefficients for heating half-cycle (+15°C - +50°C):								
	9.45	10.84	8.44	9.57	10.64	11.56	9.77	11.46

Standard Materials

Temp	Aluminum 1	Aluminum 2	Aluminum 3	Copper	Brass	Steel	Quartz
-11.1	22.96	23.39	23.41	17.53	19.89	11.84	14.14
-2.7	22.84	22.70	22.72	17.21	19.16	11.40	13 82
2.1	24.77	25.21	25.23	18.56	21.36	12 95	15.46
7.1	21.41	21.53	21.59	16.08	18.49	10.95	13.10
12.6	23.12	23.33	23.42	17.48	19.75	11.87	14.23
24.0	23.81	24.00	24.31	17.44	19.94	12.31	15.06
27.0	24.08	24.68	24.58	18.36	20.62	12.74	15.38
32.1	23.59	24.00	24.00	17.72	20.13	12.54	14.82
38.4	23.01	23.59	23.76	17.22	19.58	12.12	14.69
47.3	22.49	22.79	22.92	16.70	19.01	11.66	14.19
Average coefficient for cooling half-cycle (-20°C - +15°C):							
	22.93	23.24	23.25	17.22	19.59	11.73	14.15
Average coefficient for heating half-cycle (+15°C - +50°C):							
	23.38	23.67	23.61	17.30	19.69	12.17	14.66

Composition (%)			Coefficient of Expansion (microstrain per°C)	
Aluminum (wrought)			Published*	Measured
(+20 - +100°C)	Al	99.5	23.5	
	Al	99.0	23.5	
	Mg	2.25	23.5	
	Mg	3.50	23.5	
(Cu 4.0; Mg 0.6; Si 0.4; Mn 0.6)			22.5	
(Cu 4.5; Mg 0.5; Si 0.75; Mn 0.75)			22.5	
(-20 - +65°C) (Cu 2.5; Mg 1.0; Si 0.6; Mn 0.15; Fe 0.70; Zn 0.25; Cr 0.37; Ti 0.15)				22.7
Steel (1020)				
(+20 - +100°C) (C 0.23; Mn 0.6)			12.2	
(-20 - +65°C) (C 0.25)				12.1
Copper				
(+25 - +300°C) (Cu 99.9)			17.7	
(-20 - +65°C)				17.5
Brass				
(+25 - +300°C) (Cu 63; Zn 37)			20.5	
(Cu 60; Zn 40)			20.8	
(-20 - +65°C) (Cu 61.5; Zn 35.3; Pb 3.2)				20.0
Quartz				
(+20 - +100°C) (perp. to C-axis)			14.0	
(-20 - +65°C) (perp . to C-axis)				14.5

*From: *Smithells Metals Reference Book* (1983), 6th Edition, Ed. E. A. Brandes, and *Handbook of Physical Constants* (1966), GSA Memoir 97, p.91, Ed. S.P. Clarke Jr.

Figure B1/ Published and Measured Values for Coefficents of Thermal Expansion